

# Superquantile-Gibbs Relaxation for Minima-selection in Bilevel Optimization

Saeed Masiha<sup>1</sup>, Zebang Shen<sup>2</sup>, Negar Kiyavash<sup>1</sup>, and Niao He<sup>2</sup>

<sup>1</sup>EPFL School of Management of Technology, Station 5, 1015 Lausanne, Switzerland,  
mohammadsaeed.masiha@epfl.ch, negar.kiyavash@epfl.ch

<sup>2</sup>ETH Department of Computer Science, Universitätstrasse 6, 8092 Zürich, Switzerland,  
zebang.shen@inf.ethz.ch, niao.he@inf.ethz.ch

## Abstract

Bilevel optimization (BLO) becomes fundamentally more challenging when the lower-level objective admits multiple minimizers. In contrast to the commonly studied unique-minimizer setting, this regime introduces two additional difficulties: (1) evaluating the hyper-objective  $F_{\max}$  requires a *minima-selection* step, which, in the worst case, amounts to solving an optimization problem over a *topologically disconnected* set; (2)  $F_{\max}$  is in general discontinuous without strong structural assumptions.

In this paper, we show that both difficulties can be circumvented under a local Polyak–Łojasiewicz (PŁ) property, denoted by  $\text{PŁ}^\circ$ , on the lower-level objective. This condition is strictly weaker than the global PŁ property assumed in recent BLO studies, encompassing a broader range of problems, such as hyperparameter tuning in over-parameterized deep learning. The implications of the  $\text{PŁ}^\circ$  condition are two-folded: Under this condition, we first show that  $F_{\max}$  is Lipschitz continuous; Moreover, we identify that, for all upper-level variables, the corresponding set of lower-level minimizers are *topologically connected* and are provably closed embedded submanifolds, all sharing a common intrinsic dimension  $\kappa$ .

Importantly, we show that this intrinsic dimension  $\kappa$ , rather than the ambient dimension, fundamentally governs the complexity of BLO: We propose a method that finds an  $(\epsilon, \rho)$ -Goldstein stationary point of  $F_{\max}$  using at most  $\mathcal{O}(m^{8\kappa+9}(\epsilon\rho)^{-8\kappa-10})$  queries to the gradient oracle of the lower-level function, where  $m$  is the dimension of the upper-level domain. The key ingredient behind this result is a novel construction of an approximate function-evaluation oracle for  $F_{\max}$ : via a *Superquantile–Gibbs relaxation*, we reduce the minima-selection step, an optimization problem over a non-convex set, to a sampling problem that can be efficiently addressed using standard Langevin dynamics. To the best of our knowledge, this is the first work that rigorously tackles minima selection in BLO and explicitly characterizes how its complexity scales with the *intrinsic dimensionality* of the lower-level problem.

**Keywords:** Bilevel optimization, non-convex lower-level problem, and local PŁ condition.

## 1 Introduction

We study the pessimistic/optimistic formulation of Bilevel Optimization (BLO), which is a common paradigm in the literature [Ye et al., 1997, Ye and Ye, 1997, Dempe et al., 2007, Liu et al., 2021b, Xu and Ye, 2014], although alternatives to pessimistic/optimistic formulation for BLO also exist (see e.g., [Arbel and Mairal, 2022, Jiang et al., 2025, Bolte et al., 2025]). The pessimistic formulation of BLO is defined as follows<sup>1</sup>:

$$\min_{\theta \in \Theta \subseteq \mathbb{R}^m} F_{\max}(\theta) := \left\{ \max_{x \in \mathcal{S}(\theta) \subseteq \mathbb{R}^d} f(\theta, x) \right\}, \quad \mathcal{S}(\theta) := \arg \min_{x \in \mathbb{R}^d} g(\theta, x), \quad (1)$$

<sup>1</sup>All results extend to the optimistic setting where minimizing is considered instead of maximizing  $f$  over  $x$ .

where  $\theta$  and  $x$  are the upper- and lower-level variables,  $f$  and  $g$  are the upper- and lower-level objectives, respectively, and  $\Theta$  is a *closed compact convex* subset of  $\mathbb{R}^m$ . We focus on the setting where the lower-level minima set  $\mathcal{S}(\theta)$  is *non-singleton*. We refer to the maximization of  $f$  over  $x \in \mathcal{S}(\theta)$  as *minima-selection* and call  $F_{\max}$  the *hyper-objective*. BLO captures problems with a nested structure, such as hyper-parameter optimization [Feurer and Hutter, 2019], meta-learning [Bertinetto et al., 2018], and reinforcement learning [Hong et al., 2023, Liu et al., 2021a]. In particular, when the lower-level problem pertains to deep learning, the set  $\mathcal{S}(\theta)$  is typically nonconvex and non-singleton [Lin et al., 2024, Kuditipudi et al., 2019, Nguyen, 2019, Garipov et al., 2018, Draxler et al., 2018, Liang et al., 2018, Venturi et al., 2018, Sagun et al., 2017]. Therefore, minima-selection becomes important.

**Relaxing strong convexity to the global PL condition** Recent work on BLO have studied nonconvex lower-level problems under the *global* Polyak-Łojasiewicz (PL) condition [Chen et al., 2024a, Kwon et al., 2023a, Xiao et al., 2023, Huang, 2024, Shen et al., 2025, Liu et al., 2022]. This condition relaxes the classical strong convexity assumption on  $g$ , which implies singleton  $\mathcal{S}(\theta)$ , to cover nonconvex and potentially non-singleton optimal solution sets. Another motivation for adopting the global PL condition is to guarantee the continuity of the hyper-objective function  $F_{\max}$ , which might otherwise become discontinuous and render BLO problems generally intractable [Kwon et al., 2023a, Chen et al., 2024a].

All of the aforementioned work and their results are crucially dependent on the assumption that  $g$  is  $\mathcal{C}^2$  and satisfies the global PL condition. Under these conditions, it can be proved that the lower-level solution set  $\mathcal{S}(\theta)$  would be limited to either a singleton or an unbounded subset of  $\mathbb{R}^d$  [Criscitiello et al., 2025].

More specifically, Huang [2024] assume a nondegenerate Hessian of  $g$  at global minimizers, implicitly enforcing uniqueness; Liu et al. [2022] explicitly assume  $\mathcal{S}(\theta)$  is a singleton; Xiao et al. [2023] and Shen et al. [2025, Sec. 4] assume additional convexity of the lower-level objective, implying that the minimizer set is a linear subspace; and Kwon et al. [2023a] require  $g$  to be coercive which again yields a singleton solution<sup>2</sup>. The above observations hint the necessity of a further relaxation to capture richer landscapes.

**Our setting: Relaxing the global PL condition to a local PL condition** We relax the global PL assumption to the  $\text{PL}^\circ$  condition, which was recently proposed by Gong et al. [2024], to accommodate applications of interest such as those in deep learning. For a fixed  $\theta$ , a  $\text{PL}^\circ$  lower-level objective  $g(\theta, \cdot)$  admits a provably connected optimal set  $\mathcal{S}(\theta)$  and it satisfies the PL inequality *locally* in a neighborhood of  $\mathcal{S}(\theta)$ . Moreover, the  $\text{PL}^\circ$  condition ensures that  $\mathcal{S}(\theta)$  is a  $\mathcal{C}^2$  embedding submanifold of the ambient space  $\mathbb{R}^d$  without boundary [Gong et al., 2024]. We shall define  $\text{PL}^\circ$  condition formally in Definition 2.2. This setting is sufficiently rich as the lower-level problem admits bounded *non-singleton* minimizers. Hence, the minima-selection step remains relevant. One such example is when  $g$  represents the loss function of some deep learning tasks in the over-parameterized regime, where the local minima are observed to be connected [Draxler et al., 2018, Garipov et al., 2018, Nguyen, 2019, Kuditipudi et al., 2019, Lin et al., 2024]. Another advantage of this setting is that, as we prove in Corollary 3.4, the hyper-objective under the  $\text{PL}^\circ$  condition is Lipschitz continuous. However, under the same condition, the hyper-objective function is not necessarily differentiable, and conditions on functions  $f$  and  $g$  that would ensure the differentiability of the hyper-objective are often restrictive and unrealistic in practice (see the discussion in Section 1.4).

**Solution concept for nonsmooth nonconvex optimization.** Solving BLO problems with a *non-singleton* lower-level solution set  $\mathcal{S}(\theta)$  involves two main challenges: 1) As previously emphasized, for a fixed upper-level variable  $\theta$ , the minima selection problem requires maximization over a *nonconvex* set. Consequently, exact evaluations of the hyper-objective  $F_{\max}$  are generally inaccessible. 2) Even when the minima selection

<sup>2</sup>Kwon et al. [2023a] assume the proximal error bound for  $g$  (with  $\sigma = 0$ ), equivalent to the global PL condition for smooth  $g$  [Chen et al., 2024a, Prop. C.1].

subproblem can be solved exactly, the resulting hyper-objective  $F_{\max}$  may still be *non-differentiable* with respect to the upper-level variable  $\theta$ . Addressing this issue requires establishing local optimality guarantees for a nonsmooth nonconvex objective, a widely recognized challenge in the literature [Kornowski et al., 2024, Jordan et al., 2023, Tian et al., 2022, Kornowski and Shamir, 2021, Zhang et al., 2020].

To address these issues, we introduce the superquantile–Gibbs relaxation to approximate the hyper-objective, providing a practical surrogate for  $F_{\max}$ . Using evaluations of this surrogate, we propose a zeroth-order method that seeks a *generalized Goldstein stationary point* of  $F_{\max}$  (see Definition 5.4; cf. [Liu et al., 2024]).

## 1.1 Finding a Goldstein Stationary Point of the Hyper-objective

As we shall see in Theorem 4.5, under the  $\text{P}\mathbb{L}^\circ$  condition the hyper-objective  $F_{\max}$  is Lipschitz continuous. A natural choice for approximate stationarity in this setting is Clarke’s notion of stationarity [Clarke, 1990]. However, Zhang et al. [2020] showed that, for nonsmooth Lipschitz problems, obtaining an  $\epsilon$ -Clark stationary point in polynomial time is generally impossible, motivating more nuanced concepts. We therefore adopt the notion of  $(\epsilon, \rho)$ -Goldstein stationarity [Goldstein, 1977].

For the domain-constrained objective in (1), akin to [Liu et al., 2024], we measure stationarity by a *generalized*  $(\epsilon, \rho)$ -Goldstein criterion which is defined for the gradient mapping<sup>3</sup>, denoted by  $(\epsilon, \rho, \eta)$ -generalized Goldstein stationary point (see Definition 5.4). As  $F_{\max}$  may not be differentiable, we propose a zeroth-order (ZO) method to find such a stationary point of  $F_{\max}$ .

The major obstacle to applying ZO methods to minimize  $F_{\max}$  is that exact function values of this hyper-objective are typically unavailable. To address this, we introduce a tractable surrogate, the superquantile-Gibbs  $\tilde{F}_{\text{SQ-G}}(\theta)$ , which we define next and show that it approximates  $F_{\max}$  well. Consequently, querying  $\tilde{F}_{\text{SQ-G}}$  in place of  $F_{\max}$  provides the finite-difference gradient estimates for our zeroth-order (ZO) method. We prove that the approximation error incurred by replacing  $F_{\max}$  with  $\tilde{F}_{\text{SQ-G}}$  does not adversely affect the convergence guarantees of our ZO algorithm for obtaining an  $(\epsilon, \rho, \eta)$ -Goldstein stationary point.

## 1.2 Superquantile-Gibbs Relaxation (SQ-G)

In this part, we introduce the superquantile of the random variable  $f(\theta, X)$  where  $X$  is sampled according to the the Gibbs measure  $\sim \exp(-g(\theta, x)/\lambda)$ . Our idea is that as  $\lambda \rightarrow 0$ , the Gibbs measure concentrates on the feasible domain  $\mathcal{S}(\theta)$ , and the superquantile at a high confidence level would approach the maximum value of  $f(\theta, \cdot)$  on  $\mathcal{S}(\theta)$ . Formally, we define the Superquantile-Gibbs Relaxation (SQ-G)-loss using the variational formulation of the superquantile by [Rockafellar et al., 2000]:

$$\begin{aligned} (\text{SQ-G-loss}) \quad \tilde{F}_{\text{SQ-G}}(\theta) &:= \min_{\beta \in \mathbb{R}} \phi_{\lambda, \delta}(\theta, \beta) \\ \text{with } \phi_{\lambda, \delta}(\theta, \beta) &:= \beta + \frac{1}{\delta} \mathbb{E}_{X \sim \mu_\theta^\lambda} [\max\{f(\theta, X) - \beta, 0\}]. \end{aligned} \tag{2}$$

Here  $\lambda > 0$  and  $\delta > 0$  are parameters controlling the level of SQ-G relaxation, with  $(1 - \delta)$  known as the confidence level, and  $\mu_\theta^\lambda$  denotes the Gibbs measure:

$$\mu_\theta^\lambda(x) := \frac{\exp(-g(\theta, x)/\lambda)}{Z_\lambda(\theta)}, \tag{3}$$

where  $Z_\lambda(\theta) := \int_{\mathbb{R}^d} \exp(-g(\theta, z)/\lambda) dz$  is a normalizing factor. A key contribution of this project is that we characterize how  $\lambda$  and  $\delta$  impact the accuracy with which  $\tilde{F}_{\text{SQ-G}}(\theta)$  approximates  $F_{\max}$ .

<sup>3</sup>The gradient mapping for  $F : \Theta \rightarrow \mathbb{R}$  at a point  $\theta$  is  $\mathcal{G}_\Theta(\theta, \nabla F; \eta) := \eta^{-1}(\theta - \text{Proj}_\Theta(\theta - \eta \nabla F(\theta)))$ .

### 1.3 Our contributions

Our main contributions are as follows.

- To allow for lower-level optimal sets with rich structures, we relax the global PL condition, commonly imposed on the lower-level objective, to the weaker  $\mathbb{P}\mathcal{E}^\circ$  condition from [Gong et al., 2024]. We show that the  $\mathbb{P}\mathcal{E}^\circ$  condition is sufficient to ensure Lipschitz continuity of the hyper-objective function  $F_{\max}$ .
- We use the Superquantile–Gibbs relaxation (SQ–G) to approximate  $F_{\max}$ . This converts the crucial minima-selection step in BLO—originally a nonconvex optimization over a nonconvex set—into sampling from a Gibbs distribution, which we implement efficiently via Langevin dynamics.
- Building on the manifold structure of the lower-level optimal set, we derive the following results.

**Result 1 (Approximation).** *Assume that  $g$  satisfies the  $\mathbb{P}\mathcal{E}^\circ$  condition (to be stated in Assumption 2.6), along with standard regularity conditions such as continuity of the gradient and Hessian for both  $f$  and  $g$ . As shown in Section 4, this implies the approximation bound  $|F_{\max}(\theta) - \tilde{F}_{\text{SQ-G}}(\theta)| = \mathcal{O}\left(\delta^{\frac{1}{k}} + \delta^{-1}\lambda^{1/2}\right)$ . Here  $k$  is the common<sup>4</sup> dimension of the embedding submanifolds  $\{\mathcal{S}(\theta)\}_{\theta \in \Theta}$ .*

**Result 2 (Optimization).** *Assume that  $g$  satisfies  $\mathbb{P}\mathcal{E}^\circ$  and the regularity conditions for  $f$  and  $g$  (to be stated in Assumption 2.8). As shown in Section 5, by using a Projected Stochastic Zeroth-Order method with minima selection (see Algorithm 2) to optimize  $F_{\max}$ , we obtain an  $(\epsilon, \rho, \eta)$ -generalized Goldstein stationary point of  $F_{\max}$  on average using  $\mathcal{O}(m^{2k+3}(\epsilon\rho)^{-2k-4})$  samples from the distribution  $\mu_\theta^\lambda$  for  $k \geq 1$ . When the samples of  $\mu_\theta^\lambda$  are approximated generated by the Langevin Monte Carlo method, we show in Section 5.3 that the same goal can be achieved with  $\mathcal{O}(m^{8k+9}(\epsilon\rho)^{-8k-10})$  queries to a gradient oracle for  $g$ .*

The precise statements of these results appear in Theorem 4.5, Theorem 5.5 and Theorem 5.7, respectively.

- We evaluate our approach on both synthetic and real-world benchmarks and demonstrate the effect of minima selection. As shown in Section 6, our proposed approach outperforms hyper-gradient and penalty-based baselines.

**Remark 1.1.** *(Exponential dependence on  $k$ ) The  $\epsilon^{-k}$  factor in our results reflects the intrinsic difficulty of the problem. Since evaluating  $F_{\max}(\theta) = \max_{y \in \mathcal{S}(\theta)} f(\theta, y)$  is equivalent to solving a nonconvex optimization problem over a nonconvex set, a single  $\epsilon$ -accurate evaluation of  $F_{\max}(\theta)$  yields an  $\Omega(\epsilon^{-k})$  complexity lower bound. More specifically, consider the instance where  $\mathcal{S}(\theta) = \mathbb{S}^k$  is a hypersphere. Reparameterizing  $y$  in polar coordinates yields  $F_{\max}(\theta) = \max_{x \in \mathbb{B}_k} f(\theta, y(x))$ . Here  $\mathbb{B}_k = [0, \pi]^k$  and the point  $y(x) \in \mathbb{S}^k$  is given by  $y_i(x) = \sin(x_1) \cdots \sin(x_{i-1}) \cos(2x_i)$  for  $i \in [k]$  and  $y_{k+1}(x) = \sin(x_1) \cdots \sin(x_{k-1}) \sin(2x_k)$ . It follows from [Nemirovskij and Yudin, 1983, Section 1.6.2] that the worst-case complexity of finding an  $\epsilon$ -accurate solution to is  $\Omega(\epsilon^{-k})$  for  $f(\theta, \cdot) \in \mathcal{C}^1$ .*

### 1.4 Related work

Bilevel optimization has a long history in mathematical programming; see, e.g., the early bibliographic review by Vicente and Calamai [1994], the monograph Dempe [2002], the survey Colson et al. [2007], the classical text on mathematical programs with equilibrium constraints (MPECs) by Luo et al. [1996], and the recent collection Dempe and Zemkoho [2020]. A large part of this literature treated bilevel problems by transforming them into single-level ones, either through value-function reformulations or by replacing the lower-level problem with its Karush–Kuhn–Tucker (KKT) optimality system. In the latter case, the KKT

<sup>4</sup>In Lemma 3.5, we show that the manifolds  $\{\mathcal{S}(\theta)\}_{\theta \in \Theta}$  admit a common dimension  $k$ .

complementarity relations between multipliers and constraint violations appear explicitly as equilibrium constraints, so the resulting problem is a mathematical program with equilibrium constraints; see, for example, Ye and Zhu [1995, 2010], Dempe and Zemkoho [2012], Zemkoho and Zhou [2021]. In many practical models, these KKT-based formulations were implemented using so-called big- $M$  techniques, where large constants were introduced to linearize complementarity conditions. Choosing suitable big- $M$  constants is delicate: if they are too small, feasible bilevel solutions may be lost, whereas overly large values can lead to weak relaxations and numerical instability. These issues were analyzed in detail by Kleinert et al. [2020].

**Gradient-based bilevel methods with strongly convex lower level.** Modern large-scale machine-learning applications led to gradient-based methods for bilevel empirical risk minimization and hyperparameter optimization. When the lower-level objective is strongly convex in the inner variable and  $f, g$  are smooth, the hyper-objective is differentiable and its gradient can be obtained by implicit differentiation. Representative works in this setting included approximate hyper-gradient methods such as HOAG [Pedregosa, 2016], stochastic bilevel schemes [Ghadimi and Wang, 2018, Yang et al., 2021], and complexity-refined algorithms for empirical risk minimization [Dagr eou et al., 2024, Chen et al., 2024b], as well as more abstract treatments of optimization layers via automatic differentiation [Ablin et al., 2020], amortized implicit differentiation [Arbel and Mairal, 2021], and modular implicit differentiation frameworks [Blondel et al., 2022, Grazi et al., 2020]. In these approaches, computing exact hyper-gradients typically required Hessian or Hessian-inverse information for the lower-level problem, which could be prohibitive in large neural networks. This motivated a substantial line of *Hessian-free* or fully first-order methods that approximated the hyper-gradient using only first-order information, including BOME [Liu et al., 2022], Hessian/Jacobian-free stochastic methods with improved sample complexity [Yang et al., 2023], fully first-order stochastic approximation methods such as F<sup>2</sup>BO [Kwon et al., 2023b], and bilevel stochastic-gradient methods that also accommodate nonlinear lower-level constraints and inexact hyper-gradient computations [Giovannelli et al., 2023]. These developments made bilevel optimization scalable in settings with a unique lower-level solution, so the minima-selection problem that we study did not arise.

**Relaxing strong convexity to global PŁ.** A complementary line of work relaxed lower-level strong convexity to a global Polyak–Łojasiewicz (PŁ) condition and developed bilevel gradient methods under this assumption [Chen et al., 2024a, Kwon et al., 2023a, Xiao et al., 2023, Huang, 2024, Shen et al., 2025, Liu et al., 2022]. To obtain a smooth and well-behaved hyper-objective, these methods typically combined the global PŁ condition with additional regularity assumptions on the lower-level problem (as discussed earlier), so that minima selection was effectively avoided. In contrast, our analysis is based on a local PŁ condition and explicitly exploits the geometry of nontrivial minimizer manifolds. In a complementary direction, Chen et al. [2025] assumes a *set-smoothness* property of the solution mapping (implied by uniform error-bound/PŁ-type conditions) and shows that the induced optimistic/pessimistic hyper-objectives are weakly convex/concave, enabling computation of approximate Clarke hyper-stationary points. In contrast, we work under a *local* PŁ<sup>◦</sup> condition that allows nontrivial minimizer manifolds and does not rely on weak convexity/concavity of the hyper-objective; instead, we handle non-uniqueness via a superquantile–Gibbs surrogate and derive dimension-aware complexity bounds driven by  $\dim(\mathcal{S}(\theta))$ .

**Morse- and correspondence-based formulations.** Beyond such regularity-based assumptions (strong convexity or global PŁ), recent works proposed alternative formulations of BLO that target nonconvex lower-level problems. For instance, Bolte et al. [2025] worked under a (piecewise) Morse-type parametric qualification, showed that the graphs of lower-level critical points and local minima generically decomposed into finitely many smooth manifolds, and used this structure to define branch-wise hyper-objectives and study gradient methods that updated the upper-level variable along individual branches. Arbel and Mairal

[2022] instead introduced bilevel games with *selection maps*, where a selection map chose a specific critical point (for instance, the limit of a gradient flow) for each upper-level parameter, and showed that standard bilevel algorithms based on truncated unrolling and implicit differentiation tended to approximate such selection-based games rather than the classical bilevel formulation. Jiang et al. [2025] further argued that, for general nonconvex lower levels, the classical hyper-objective may be ill-posed when global minimizers are unattainable; they proposed a correspondence-driven hyper-objective that evaluated the upper-level loss at the output of a prescribed lower-level algorithm, applied Gaussian smoothing to this mapping, and developed a projected stochastic-gradient method with convergence and oracle-complexity guarantees for the smoothed problem. In contrast, our work retains the classical (pessimistic or optimistic) hyper-objective, combines it with a local  $\text{PL}^\circ$  condition to obtain a manifold structure for the lower-level minimizers, and uses a superquantile–Gibbs relaxation to define an explicit selection rule together with dimension-aware complexity bounds.

**Pessimistic bilevel optimization.** The approaches discussed above treat lower-level non-uniqueness either by enforcing regularity conditions (strong convexity or global  $\text{PL}$ ) or by embedding explicit selection mechanisms (Morse branches, selection maps, or algorithmic correspondences), and thus remain essentially in an optimistic or selection-based setting. By contrast, the *pessimistic* formulation evaluates each upper-level decision against the worst upper-level value over all lower-level minimizers, which is natural when the follower may act adversarially or unreliably [Beck et al., 2023]. This risk-averse viewpoint was studied in mathematical programming, including structural and complexity results for general pessimistic models [Wiesemann et al., 2013], surveys of modelling and solution schemes [Liu et al., 2018], and necessary optimality conditions based on generalized differentiation and value-function techniques [Dempe et al., 2014]. On the algorithmic side, several works constructed single-level relaxations of the pessimistic problem: Zeng and Ye [2020] designed a tight relaxation and a computation scheme for (mainly linear) pessimistic bilevel problems; Benchouk et al. [2025] analyzed a Scholtes-type relaxation of the KKT system; and Antoniou et al. [2024] proposed a  $\delta$ -perturbed formulation that enforced an *approximate* unique follower response and derived error bounds between the perturbed and original pessimistic problems. Pessimistic ideas also appeared in machine learning: Apaydin Ustun et al. [2024] formulated hyperparameter tuning as a pessimistic bilevel problem over a finite set of tasks, and Jiang et al. [2021] interpreted adversarial training as a bilevel game in which a learned attacker played the role of the follower. All these approaches, however, either (i) resolved non-uniqueness by modifying the lower-level problem (e.g.,  $\delta$ -perturbations, KKT relaxations) or (ii) specialized to finite or discrete follower responses, and gradient-based methods with nonasymptotic guarantees rarely addressed the continuous pessimistic setting with a non-singleton solution set. In contrast, we work directly with the pessimistic hyper-objective  $F_{\max}$  under a local  $\text{PL}^\circ$  condition, model pessimism via a superquantile risk over Gibbs samples on the minimizer manifolds, and obtain dimension-aware complexity bounds that explicitly depend on the intrinsic dimension  $\kappa$  of  $\mathcal{S}(\theta)$  rather than on the ambient dimension.

## 1.5 Organization

The remainder of the paper is organized as follows. Section 2 introduces the  $\text{PL}^\circ$  assumption and additional regularity conditions, and discusses their implications for the structure of the solution set as well as for the convergence of the Gibbs measure to its limit. Building on this, Section 3 develops uniform geometric properties of the minimizer manifolds  $\{\mathcal{S}(\theta)\}_{\theta \in \Theta}$ , showing in particular that the solution mapping is locally Lipschitz and that these manifolds share a common intrinsic dimension. Section 4 shows that, under our assumptions, the SQ–G relaxation provides a sharp approximation of  $F_{\max}$  (see Lemma 4.4). Using this approximation result, in Section 5 we show our main complexity guarantees: Theorem 5.5 and Theorem 5.7 show that the complexity of optimizing  $F_{\max}$  via a zeroth-order algorithm (see Algorithm 2) scales with the common intrinsic dimension of the lower-level solution manifolds. Finally, Section 6 presents our numerical

results: we first study the dependence on the Riemannian dimension in a synthetic example and then compare our method with several competitive baselines on both a toy problem and a data hyper-cleaning task.

## 1.6 Notations

Unless stated otherwise,  $\|\cdot\|$  denotes the Euclidean ( $\ell_2$ ) vector norm and the associated operator norm on matrices and higher-order tensors. For a random variable  $Z$ ,  $\text{supp}(Z)$  denotes its support. For  $d \in \mathbb{N}$ ,  $x \in \mathbb{R}^d$ , and  $r > 0$ , we write  $\mathbb{B}_d(x; r) := \{y \in \mathbb{R}^d : \|y - x\| \leq r\}$  for the closed  $d$ -dimensional Euclidean ball with center  $x$  and radius  $r$ . For  $p \geq 1$  and probability measures  $\mu, \nu$  on  $\mathbb{R}^d$  with finite  $p$ -th moments, the  $p$ -Wasserstein distance is

$$\mathbb{W}_p(\mu, \nu) := \left[ \inf_{\pi \in \Pi(\mu, \nu)} \int_{\mathbb{R}^d \times \mathbb{R}^d} \|x - y\|^p d\pi(x, y) \right]^{1/p},$$

where  $\Pi(\mu, \nu)$  is the set of all couplings of  $\mu$  and  $\nu$ . In particular,  $\mathbb{W}_1$  is the 1-Wasserstein distance. Given a twice differentiable function  $f : \mathbb{R}^m \times \mathbb{R}^d \rightarrow \mathbb{R}$ , we write  $\partial_\theta f(\theta, x)$  and  $\partial_x f(\theta, x)$  for the gradients of  $f$  with respect to its first and second arguments, respectively. The mixed derivative  $\partial_{\theta, x}^2 f(\theta, x) := \partial_\theta(\partial_x f(\theta, x))$  denotes the Jacobian of the vector  $\partial_x f(\theta, x)$  with respect to  $\theta$ , and  $\partial_\theta^2 f(\theta, x)$  denotes the Hessian of  $f$  with respect to  $\theta$ . The diameter of a set  $\Theta \subset \mathbb{R}^d$ , is defined as  $\text{diam}(\Theta) := \sup_{\theta_1, \theta_2 \in \Theta} \|\theta_1 - \theta_2\|$ . The class of continuous real-valued functions on  $\mathbb{R}^d$  is denoted by  $\mathcal{C}(\mathbb{R}^d, \mathbb{R})$ . We write  $f \in \mathcal{C}^k$  if  $f$  has continuous derivatives up to order  $k$ . For a set  $A \subset \mathbb{R}^d$ , we denote its closure by  $\bar{A}$ . For a scalar random variable  $Z$  and  $\delta \in (0, 1)$ , the  $(1 - \delta)$ -quantile is defined as

$$\mathbb{Q}_{1-\delta}(Z) := \inf\{t \in \mathbb{R} : \mathbb{P}[Z > t] \leq \delta\}.$$

For a closed convex set  $\Theta \subset \mathbb{R}^m$  and  $y \in \mathbb{R}^m$ , we denote by  $\text{Proj}_\Theta(y) = \arg \min_{z \in \Theta} \|y - z\|$  the (Euclidean) projection of  $y$  onto  $\Theta$ . We use the notation  $\mathcal{O}$  to hide constants, and the notation  $\tilde{\mathcal{O}}$  to hide both constants and logarithmic factors. We write  $a \lesssim b$  to indicate that  $a \leq cb$  for some universal positive constant  $c > 0$  that is independent of the problem parameters. We write  $\mathbb{R}_\alpha(P\|Q)$  for the Rényi divergence of order  $\alpha \in (0, \infty) \setminus \{1\}$ , defined by

$$\mathbb{R}_\alpha(P\|Q) = \begin{cases} \frac{1}{\alpha - 1} \log \int \left(\frac{dP}{dQ}\right)^\alpha dQ, & P \ll Q, \\ +\infty, & \text{otherwise.} \end{cases}$$

We denote  $\text{Law}(X)$  as the probability distribution (or law) of a random variable  $X$ .

## 2 Summary of Assumptions and Preliminaries

In this work, we focus on the setting where the lower-level objective is coercive and satisfies local Polyak-Łojasiewicz ( $\text{PE}^\circ$ ) condition for all upper-level variable  $\theta$ , formally stated as follows.

**Definition 2.1.** *Let  $\mathcal{M}$  be the collection of all local minima of a function  $g \in \mathcal{C}^1(\mathbb{R}^d, \mathbb{R})$ .  $g$  is locally  $\text{PE}$  if there exists a constant  $\mu > 0$  such that for any connected component  $\mathcal{M}' \subseteq \mathcal{M}$ , there exists an open neighborhood  $\mathcal{N}(\mathcal{M}')$  containing  $\mathcal{M}'$  ( $\mathcal{N}(\mathcal{M}') \supset \mathcal{M}'$ ) such that*

$$\forall x \in \mathcal{N}(\mathcal{M}'), \quad g(x) - \min_{x' \in \mathcal{N}(\mathcal{M}')} g(x') \leq (2\mu)^{-1} \|\nabla g(x)\|^2. \quad (4)$$

**Definition 2.2.** *A function  $g : \mathbb{R}^d \rightarrow \mathbb{R}$  satisfies the  $\text{PE}^\circ$  condition if the following hold.*

- $g$  is a  $\mathcal{C}^2$  and locally  $\mathcal{P}\mathcal{L}$  function, and  $g$  is a  $\mathcal{C}^4$  function in every neighborhood  $\mathcal{N}(\mathcal{M}')$ <sup>5</sup>.
- Let  $\mathcal{N}(\mathcal{M}) := \cup_{\mathcal{M}'} \mathcal{N}(\mathcal{M}')$ . For any  $x \in \mathbb{R}^d \setminus \mathcal{N}(\mathcal{M})$ , if  $\nabla g(x) = 0$ , then  $\nabla^2 g(x) \prec 0$ .
- The collection of all local minima  $\mathcal{M}$  is contained within a compact set.

A fundamental implication of the  $\mathcal{P}\mathcal{L}^\circ$  condition is the connectivity of the optimal set.

**Proposition 2.3** (Connectivity, Proposition 3 in [Gong et al., 2024]). *For a  $\mathcal{P}\mathcal{L}^\circ$  function, its local minima set  $\mathcal{M}$  is path-connected.*

Consequently, all local minima of a  $\mathcal{P}\mathcal{L}^\circ$  function are global minima which are all connected. Further, Rejock and Boumal [2023] proved the local manifold structure for  $\mathcal{M}$ . It is later extend to a global version in [Gong et al., 2024], where they also provide an explicit statement about the boundary.

**Remark 2.4** (No-saddle point property). *The second condition in Definition 2.2 is used solely to establish the connectedness of the local minima set via the mountain pass theorem (see the proof of Proposition 3 in [Gong et al., 2024] for details). Our results remain valid if this condition is replaced with the assumption that  $\mathcal{S}(\theta)$  is connected. Empirically, such connectedness has been widely observed in over-parameterized deep learning settings; see, e.g., [Draxler et al., 2018, Nguyen, 2019, Kuditipudi et al., 2019].*

**Proposition 2.5** (Manifold structure, Corollary 1 in [Gong et al., 2024]). *For a  $\mathcal{P}\mathcal{L}^\circ$  function, its optimal set  $\mathcal{M}$  is a compact  $\mathcal{C}^2$  embedding submanifold of the ambient space  $\mathbb{R}^d$  without boundary.*

**Assumption 2.6.** *For every  $\theta \in \Theta$ , the lower-level objective  $g(\theta, \cdot)$  satisfies the  $\mathcal{P}\mathcal{L}^\circ$  condition.*

Following [Gong et al., 2024], we make the next assumption to exclude the manifolds with ill-conditioned chart. We also use it to establish a nonzero lower bound on the injectivity radius, allowing us to analyze the volume-radius relationship of geodesic balls, which is crucial for our approximation results.

**Assumption 2.7** (Second-order fundamental form). *For every  $\theta \in \Theta$ , the manifold  $\mathcal{S}(\theta)$  has a well-defined second fundamental form in the sense of Definition A.1 in Section A.1, and its operator norm is uniformly bounded by a constant  $C > 0$ .*

We further need the following regularity conditions, which are standard in the BLO literature.

**Assumption 2.8.** *The following statements hold for all  $\theta \in \Theta$ .*

- $f$  is a  $\mathcal{C}^1$  function and  $L_{f,1}$ -Lipschitz, and  $L_{f,2}$ -smooth w.r.t.  $(\theta, x)$ . For all  $x \in \mathbb{R}^d$ ,  $|f(\theta, x)| \leq C_f \|x\|^{n_f} + D_f$  where  $C_f, D_f \geq 0$  are two constant and  $n_f \geq 1$  is an integer constant.
- $g$  is a  $\mathcal{C}^2$  function and  $L_{g,2}$ -smooth w.r.t.  $\theta$  for every  $x \in \mathbb{R}^d$ . For all  $x \in \mathbb{R}^d$ ,  $\|\partial_\theta g(\theta, x)\| \leq C_g \|x\|^{n_g} + D_g$  where  $C_g, D_g \geq 0$  are two constant and  $n_g \geq 1$  is an integer constant.
- The Hessian  $\partial_x^2 g(\theta, x)$  is continuous w.r.t.  $(\theta, x)$ .
- Beyond a compact set,  $g(\theta, \cdot)$  satisfies the quadratic growth, i.e.,  $\exists D > 0$  such that  $\forall |x| \geq D$ ,  $\mu_{\text{qg}} \cdot \text{dist}^2(x, \mathcal{S}(\theta))/2 \leq g(\theta, x) - \min_{z \in \mathbb{R}^d} g(\theta, z)^a$ .

<sup>a</sup>W.L.O.G., we assume that  $D$  is sufficiently large so that  $\mathcal{S}(\theta) \subseteq \mathbb{B}_d(0; D)$  for all  $\theta \in \Theta$ . This assumption implies the coercivity of function  $g(\theta, \cdot)$ .

The regularity conditions in Assumption 2.8, such as Lipschitzness and smoothness, are standard in the literature [Kwon et al., 2023a, Chen et al., 2024a]. However, unlike Kwon et al. [2023a], we do not assume a bounded  $x$ -domain in the lower-level problem. Instead, we impose quadratic growth beyond a compact

<sup>5</sup>Gong et al. [2024] require  $g \in \mathcal{C}^3$ . Here we slightly enhance the assumption to  $\mathcal{C}^4$  to enable Proposition 2.11.

set, ensuring  $\mu_g^\lambda$  is well-defined [Hasenpflug et al., 2024]. Additionally, while Kwon et al. [2023a] assumes boundedness of  $f$ , we relax this to a polynomial bound condition. We also assume a bounded  $\theta$ -domain and polynomial bound on  $\partial_\theta g$ , which we plan to further relax in future work.

**Example 2.9.** *To justify that the assumptions allow for a nontrivial function class, we provide a simple example. Since  $f$  only requires regularity conditions, it can be easily constructed, so we focus on  $g$ . Consider  $g(\theta, x) = \frac{1}{4}(\|x\|^2 - \theta)^2 - \frac{1}{2}\|x\|^2$  for  $0 \leq \theta \leq 1$ , which satisfies all given assumptions. Here, the lower-level minima set  $\mathcal{S}(\theta) = \{x : \|x\| = \theta + 1\}$  is non-singleton and nonconvex.*

Under Assumption 2.8, the mappings  $(\theta, x) \mapsto f(\theta, x)$  and  $(\theta, x) \mapsto \partial_\theta g(\theta, x)$  are continuous on the compact set  $\Theta \times \mathbb{B}_d(0; R)$  with  $R > 0$ . We define the constants

$$L_{f,0}(R) := \sup_{\theta \in \Theta} \sup_{x \in \mathbb{B}_d(0; R)} |f(\theta, x)|, \quad L_{g,1}(R) := \sup_{\theta \in \Theta} \sup_{x \in \mathbb{B}_d(0; R)} \|\partial_\theta g(\theta, x)\|. \quad (5)$$

By compactness and continuity, these suprema are finite.

## 2.1 Implications of the $\mathbf{P}\mathcal{L}^\circ$ Condition

We review implications of Assumption 2.6, in particular how it helps to quantify the convergence of the Gibbs measures  $\mu_\theta^\lambda$  to the limiting measure  $\mu_\theta^0$  under the Wasserstein-1 metric. In this subsection,  $\theta$  is considered fixed, and hence for ease of the notation, we omit it and simply write  $\mu^\lambda$ , and  $\mu^0$ .

### 2.1.1 Implications of the Embedding Submanifold Structure in Proposition 2.5

Following Remark 1 in [Gong et al., 2024], WLOG and for the ease of notation, we assume that the atlas of the manifold  $\mathcal{S}$  consists of a single chart  $(\mathcal{U}, \phi)$ , where  $\mathcal{U} = \mathcal{S}$ . Let  $\Gamma = \phi(\mathcal{U}) \subseteq \mathbb{R}^k$  denote the coordinate domain<sup>6</sup>. The corresponding parametrization (the inverse of the chart) can be represented as  $x = S(u) := [m_1(u), \dots, m_d(u)]^\top$  for all  $u \in \Gamma$ , where  $m_j : \Gamma \rightarrow \mathbb{R}$  for  $j \in [d]$  are  $\mathcal{C}^2$  coordinate functions.

**Tubular Neighborhood.** For  $x \in \mathcal{S}$ , the tangent space at  $x$  is denoted by  $T_x(\mathcal{S})$ . The orthogonal complement of  $T_x(\mathcal{S})$  in  $\mathbb{R}^d$  is denoted by  $T_x(\mathcal{S})^\perp$ . The tubular neighborhood  $\mathcal{N}(\varepsilon)$  of  $\mathcal{S}$  for  $\varepsilon > 0$  is defined as:  $\mathcal{N}(\varepsilon) := \{x + v : x \in \mathcal{S}, v \in T_x(\mathcal{S})^\perp, \|v\| < \varepsilon\}$ . A key property of the  $\mathcal{C}^2$  embedded submanifold is as follows<sup>7</sup> [LEE, 2024, Theorem 6.17]: There exists  $\varepsilon_0 > 0$  such that for all  $0 < \varepsilon \leq \varepsilon_0$ , there is a  $\mathcal{C}^2$  diffeomorphism  $\Phi$ :

$$\Phi : \mathcal{S} \times \mathbb{B}_{d-k}(0; \varepsilon) \rightarrow \mathcal{N}(\varepsilon), \quad (x, t) \mapsto x + \sum_{j=1}^{d-k} t_j e^{(j)}(x), \quad (6)$$

where  $\{e^{(1)}(x), \dots, e^{(d-k)}(x)\}$  forms an orthonormal basis for the normal space  $T_x(\mathcal{S})^\perp$ . Under the local chart  $(\Gamma, \phi)$ , any  $y \in \mathcal{N}(\varepsilon)$  can be written as  $y = x + v$ , where  $x$  is a point on  $\mathcal{S}$  and  $v \perp \mathcal{S}$  at  $x$  with  $\|v\| \leq \varepsilon$ . The map  $y(u, t) := \Phi(S(u), t) \rightarrow (x, v)$  is a  $\mathcal{C}^2$  diffeomorphism.

**Volume measure.** We define the Riemannian (tensor) metric  $g_S$  on  $\mathcal{S}$  as the pullback metric by including map  $i_S : \mathcal{S} \hookrightarrow \mathbb{R}^d$ , i.e.  $g_S = i_S^*(g_E)$ , where  $g_E$  is the standard Riemannian metric on  $\mathbb{R}^d$  and  $i_S^*$  is the pullback map associated with  $i_S$ . Now we can define the standard volume form  $d\mathcal{M}^8$  as  $d\mathcal{M}(u) = \sqrt{\det(g_S)} du$ ,  $u \in \Gamma$ , where  $\det(g_S)$  is the determinant of  $g_S$ .

<sup>6</sup>The standard technique of partition of unity can be used to translate the results to the multi-chart case.

<sup>7</sup>For simplicity, we assume a single chart and omit the dependence on the inclusion  $i_S$ .

<sup>8</sup>Note that  $d\mathcal{M}$  stands for  $d\mathcal{M}_\theta$  in all the following sections.

**Poincaré constant.** A probability measure  $\pi$  over  $\mathbb{R}^d$  is said to satisfy the Poincaré inequality with inverse Poincaré constant  $C_{PI}$  if for all test functions  $\varphi \in \mathbb{H}^1(\mu)$ , the following inequality holds:

$$\int \left( \varphi - \int \varphi d\mu \right)^2 d\mu \leq C_{PI} \int \|\nabla \varphi\|^2 d\mu,$$

where  $\mathbb{H}^1(\mu)$  denotes the Sobolev space weighted by  $\mu$ . Importantly, for all  $\mathbb{P}\mathbb{L}^\circ$  functions  $g : \mathbb{R}^d \rightarrow \mathbb{R}$ , the constant  $C_{PI}$  for the Gibbs probability measure  $\mu^\lambda \propto \exp(-g/\lambda)$  is *independent* of  $\lambda$  for all sufficiently small  $\lambda \leq \lambda_0$ , where both  $\lambda_0$  and an upper bound of  $C_{PI}$  are explicitly given in [Gong et al., 2024].

### 2.1.2 Limiting measure of Gibbs measures

To sample approximately from the optimal set  $\mathcal{S}$ , we select a temperature parameter  $\lambda$  approaching zero, which causes the Gibbs measure (3) to concentrate on  $\mathcal{S}$ . Let  $\mu^0 := \lim_{\lambda \rightarrow 0} \mu^\lambda$  denote the weak limit of the Gibbs measures. By combining the manifold characterization of the optimal set for  $\mathbb{P}\mathbb{L}^\circ$  functions in [Gong et al., 2024] with the asymptotic analysis in [Hwang, 1980, Theorem 3.1], the following lemma establishes that  $\mu^0$  is well-defined, has support restricted to  $\mathcal{S}$ , and admits a closed-form density function with respect to the Riemannian volume measure  $d\mathcal{M}$  on the manifold.

**Proposition 2.10** (Theorem 3.1 in [Hwang, 1980]). *Suppose that Assumption 2.6 holds and let  $k$  be the dimension of the submanifold  $\mathcal{S}$ . Let  $\mu^0 := \lim_{\lambda \rightarrow 0} \mu^\lambda$  be the weak limit of the Gibbs measures, then  $\text{supp}(\mu^0) = \mathcal{S}$  and*

$$\rho(u) := \frac{d\mu^0}{d\mathcal{M}} = \frac{|\partial_t^2 g(y(u, t))|_{t=0}|^{-\frac{1}{2}}}{\int_{\mathcal{S}} |\partial_t^2 g(y(v, t))|_{t=0}|^{-\frac{1}{2}} d\mathcal{M}(v)}. \quad (7)$$

Here  $|\cdot| : \mathbb{R}^{(d-k) \times (d-k)} \rightarrow \mathbb{R}$  denotes the matrix determinant. We write  $\mu^0(du) = \rho(u)d\mathcal{M}(u)$ <sup>9</sup>.

**Wasserstein-1 distance between the Gibbs measure and its limit measure.** The following proposition from [Hasenpflug et al., 2024, Theorem 3.6] proves the non-asymptotic convergence of  $\mu^\lambda$  as  $\lambda \rightarrow 0$  to  $\mu^0$  (defined above) in the Wasserstein-1 sense<sup>10</sup>. Establishing convergence in  $\mathbb{W}_1$  is crucial for our analysis because it directly bounds the approximation error between the superquantile-Gibbs surrogate and the superquantile loss taken over the limiting measure  $\mu^0$  (to be defined in (11)). This bound is established by exploiting the Lipschitz continuity of the upper-level objective (see Lemma 4.4).

**Proposition 2.11** (Theorem 3.6 in [Hasenpflug et al., 2024]). *Under Assumptions 2.6 to 2.8,  $\mathbb{W}_1(\mu^\lambda, \mu^0) \leq K_0 \lambda^{\frac{1}{2}}$  where  $K_0$  is  $\lambda$ -independent.*

## 3 Regularity of the Solution Mapping and Geometric Properties

We first establish that  $\mathcal{S}(\theta)$  varies locally Lipschitz in Hausdorff distance under the local  $\mathbb{P}\mathbb{L}^\circ$  condition, and consequently that the hyper-objective  $F_{\max}$  is Lipschitz continuous (Corollary 3.4). In Section 3.2, we show that the minimizer manifolds  $\{\mathcal{S}(\theta)\}_{\theta \in \Theta}$  share a common intrinsic dimension  $k$  (Lemma 3.5), and then show  $\theta$ -independent geometric bounds such as a uniform diameter, curvature control, and a positive injectivity radius (Proposition 3.6). We also show that the limiting Gibbs density on  $\mathcal{S}(\theta)$  is uniformly bounded from below and above (Proposition 3.7). These uniform geometric properties will play a role later in our approximation analysis (Section 4).

<sup>9</sup>Note that  $\mu^0$  and  $\rho$  stand for  $\mu_\theta^0$  and  $\rho_\theta$  in all the following sections.

<sup>10</sup>We use the assumption on  $g$  in Definition 2.2 to ensure that the conditions in [Hasenpflug et al., 2024, Theorem 3.6] hold. Further discussion on the validity of their conditions can be found in Appendix A.2.

### 3.1 Lipschitz Continuity of the Solution Mapping

In this subsection, our goal (Lemma 3.2) is to show that, under the  $\text{P}\mathbb{L}^\circ$  condition, the set-valued mapping  $\theta \mapsto \mathcal{S}(\theta)$  is locally Lipschitz with respect to the Hausdorff distance. We then combine this regularity with the Lipschitz continuity of  $f(\theta, x)$  to deduce the Lipschitz continuity of  $F_{\max}$  (Corollary 3.4). We begin by recalling the notion of Hausdorff distance.

**Definition 3.1** (Hausdorff distance). *Let  $\mathcal{S}_1$  and  $\mathcal{S}_2$  be two subsets of  $\mathbb{R}^d$ . The Hausdorff distance between  $\mathcal{S}_1$  and  $\mathcal{S}_2$  is defined as*

$$\text{dist}(\mathcal{S}_1, \mathcal{S}_2) := \max \left\{ \sup_{x_1 \in \mathcal{S}_1} \inf_{x_2 \in \mathcal{S}_2} \|x_1 - x_2\|, \sup_{x_2 \in \mathcal{S}_2} \inf_{x_1 \in \mathcal{S}_1} \|x_1 - x_2\| \right\}.$$

Since the  $\text{P}\mathbb{L}^\circ$  condition provides only a *local*  $\text{P}\mathbb{L}$  inequality in a neighborhood of the minimizer set  $\mathcal{S}(\theta)$ , Lipschitz stability of the solution mapping does not follow from standard global error-bound arguments. By contrast, under a *global*  $\text{P}\mathbb{L}$  condition for  $g(\theta, \cdot)$ , one obtains a global error bound and then deduces Lipschitz continuity of  $\theta \mapsto \mathcal{S}(\theta)$  directly from the smoothness of  $g$  on  $\theta$  (see, e.g., [Kwon et al., 2023a, Chen et al., 2024a]). In our local setting, the obstruction is geometric: a local error bound alone still allows the minimizer set to have multiple disconnected components, and minimizers could jump from one component to another under arbitrarily small changes in  $\theta$ , precluding any Hausdorff Lipschitz control. This is why we need that  $\mathcal{S}(\theta)$  is connected under our assumptions (see Proposition 2.3) to prove a quantitative stability result showing that minimizers cannot jump and must move continuously under small perturbations of  $\theta$ . The next lemma makes this precise.

**Lemma 3.2.** *Under Assumption 2.6 and Assumption 2.8, the minimizer mapping  $\theta \mapsto \mathcal{S}(\theta)$  is locally Lipschitz continuous in the Hausdorff distance sense: there exists  $\gamma > 0$  such that for every  $\theta_1$  and  $\theta_2$  with  $\|\theta_1 - \theta_2\| \leq \gamma$ , we have*

$$\text{dist}(\mathcal{S}(\theta_1), \mathcal{S}(\theta_2)) \leq \frac{L_{g,2}}{\mu} \|\theta_1 - \theta_2\|.$$

*Proof.* The proof has two steps. First, the local  $\text{P}\mathbb{L}$  condition and  $\mathcal{C}^2$  regularity imply that there exists a neighborhood  $\mathcal{U}(\theta_1)$  of the minimizer manifold  $\mathcal{S}(\theta_1)$  such that inside  $\mathcal{U}(\theta_1)$ , the distance to  $\mathcal{S}(\theta_1)$  is controlled by  $\|\partial_x g(\theta_1, \cdot)\|$ . Second, we show that for small perturbations  $\theta_2$  of  $\theta_1$ , every minimizer  $x_2 \in \mathcal{S}(\theta_2)$  lies in  $\mathcal{U}(\theta_1)$ , by comparing  $g(\theta_1, x_2)$  and  $g(\theta_1, x_1)$  for  $x_1 \in \mathcal{S}(\theta_1)$  using Lipschitz continuity in  $\theta$ . Once  $x_2 \in \mathcal{U}(\theta_1)$ , the error bound and  $L_{g,2}$ -smoothness in  $\theta$  give

$$\text{dist}(x_2, \mathcal{S}(\theta_1)) \lesssim \|\partial_x g(\theta_1, x_2)\| \lesssim L_{g,2} \|\theta_1 - \theta_2\|,$$

and taking the supremum over  $x_2 \in \mathcal{S}(\theta_2)$  yields the desired local Lipschitz bound in Hausdorff distance.

*Step 1: local error bound around  $\mathcal{S}(\theta)$ .* Fix  $\theta \in \Theta$ . By Proposition 2.3, Assumption 2.6 implies that every local minimizer of  $g(\theta, \cdot)$  is in fact global, so the local  $\text{P}\mathbb{L}$  inequality in Assumption 2.6 holds in a neighborhood of the global minimizer set  $\mathcal{S}(\theta)$ . In particular, there exists an open neighborhood  $\mathcal{N}(\mathcal{S}(\theta))$  of  $\mathcal{S}(\theta)$  such that

$$g(\theta, x) - \min_{z \in \mathbb{R}^d} g(\theta, z) \leq \frac{1}{2\mu} \|\partial_x g(\theta, x)\|^2 \quad \forall x \in \mathcal{N}(\mathcal{S}(\theta)). \quad (8)$$

By the local  $\text{P}\mathbb{L}$  condition and  $\mathcal{C}^2$  regularity,  $g(\theta, \cdot)$  satisfies a local *error bound* in a smaller neighborhood of  $\mathcal{S}(\theta)$  [Rebjock and Boumal, 2023, Proposition 2.2]: there exists an open set  $\mathcal{U}(\theta) \subseteq \mathcal{N}(\mathcal{S}(\theta))$  with  $\mathcal{S}(\theta) \subset \mathcal{U}(\theta)$  such that

$$\text{dist}(x, \mathcal{S}(\theta)) \leq \mu^{-1} \|\partial_x g(\theta, x)\| \quad \forall x \in \mathcal{U}(\theta). \quad (9)$$

Moreover, since  $\mathcal{S}(\theta)$  is compact and  $\mathcal{U}(\theta)$  is open, we can find  $\tilde{\epsilon} > 0$  such that the  $\tilde{\epsilon}$ -sub-level set of  $g(\theta, \cdot)$  lies inside  $\mathcal{U}(\theta)$ :

**Lemma 3.3.** *Under the local error bound for  $g(\theta, \cdot)$  with  $\mathcal{U}(\theta)$  being as above, there exists  $\tilde{\epsilon} > 0$  such that*

$$\left\{ x \in \mathbb{R}^d : g(\theta, x) - \min_{z \in \mathbb{R}^d} g(\theta, z) \leq \tilde{\epsilon} \right\} \subset \mathcal{U}(\theta).$$

The proof of Lemma 3.3 is given in Appendix B.1. Intuitively, since  $\mathcal{U}(\theta)$  is an open neighborhood of  $\mathcal{S}(\theta)$  and  $g(\theta, \cdot)$  is continuous, a small enough sub-level set around  $\mathcal{S}(\theta)$  must be contained in  $\mathcal{U}(\theta)$ .

*Step 2: stability of  $\mathcal{S}(\theta)$  under small perturbations of  $\theta$ .* Let  $\mathcal{U}(\theta_1)$  and  $\tilde{\epsilon} > 0$  be as above. By Assumption 2.8 and using Equation (5),  $g$  is  $L_{g,1}(\mathbb{D})$ -Lipschitz in  $\theta$  on a compact domain  $\mathbb{B}_d(0; \mathbb{D})$  in  $x$ , so for any  $x \in \mathbb{R}^d$  and any  $\theta_1, \theta_2 \in \Theta$ ,

$$|g(\theta_1, x) - g(\theta_2, x)| \leq L_{g,1}(\mathbb{D}) \|\theta_1 - \theta_2\|.$$

Let  $x_1 \in \mathcal{S}(\theta_1)$  and  $x_2 \in \mathcal{S}(\theta_2)$ , where  $\theta_2$  will be taken close to  $\theta_1$ . Using optimality of  $x_1$  for  $g(\theta_1, \cdot)$  and of  $x_2$  for  $g(\theta_2, \cdot)$ , we have

$$\begin{aligned} 0 &\leq g(\theta_1, x_2) - g(\theta_1, x_1) \\ &= [g(\theta_1, x_2) - g(\theta_2, x_2)] + [g(\theta_2, x_2) - g(\theta_2, x_1)] + [g(\theta_2, x_1) - g(\theta_1, x_1)] \\ &\leq |g(\theta_1, x_2) - g(\theta_2, x_2)| + 0 + |g(\theta_2, x_1) - g(\theta_1, x_1)| \\ &\leq 2L_{g,1}(\mathbb{D}) \|\theta_1 - \theta_2\|. \end{aligned} \tag{10}$$

Hence, if we choose  $\gamma \leq \tilde{\epsilon}/(2L_{g,1}(2\mathbb{D}))$  and  $\|\theta_1 - \theta_2\| \leq \gamma$ , then (10) implies

$$g(\theta_1, x_2) - \min_z g(\theta_1, z) = g(\theta_1, x_2) - g(\theta_1, x_1) \leq \tilde{\epsilon},$$

so  $x_2$  belongs to the sub-level set in Lemma 3.3. Therefore  $x_2 \in \mathcal{U}(\theta_1)$  whenever  $\|\theta_1 - \theta_2\| \leq \gamma$ . Then the error bound (9) for  $g(\theta_1, \cdot)$  yields

$$\text{dist}(x_2, \mathcal{S}(\theta_1)) \leq \mu^{-1} \|\partial_x g(\theta_1, x_2)\|.$$

Because  $x_2$  is a minimizer for  $g(\theta_2, \cdot)$ , we have  $\partial_x g(\theta_2, x_2) = 0$ , hence

$$\|\partial_x g(\theta_1, x_2)\| = \|\partial_x g(\theta_1, x_2) - \partial_x g(\theta_2, x_2)\| \leq L_{g,2} \|\theta_1 - \theta_2\|,$$

where we used the  $L_{g,2}$ -smoothness of  $g$  with respect to  $\theta$ . Combining the two last inequalities results in

$$\text{dist}(x_2, \mathcal{S}(\theta_1)) \leq \frac{L_{g,2}}{\mu} \|\theta_1 - \theta_2\|.$$

By symmetry (interchanging the roles of  $\theta_1$  and  $\theta_2$  and repeating the same argument) and recalling the definition of the Hausdorff distance in Definition 3.1, we get

$$\text{dist}(\mathcal{S}(\theta_1), \mathcal{S}(\theta_2)) \leq \frac{L_{g,2}}{\mu} \|\theta_1 - \theta_2\| \quad \text{whenever} \quad \|\theta_1 - \theta_2\| \leq \gamma.$$

□

Having established the local Lipschitz continuity of  $\mathcal{S}(\theta)$  in Lemma 3.2, we now turn to the regularity of the hyper-objective  $F_{\max}$ . The following corollary follows by combining the local Lipschitz continuity of  $\theta \mapsto \mathcal{S}(\theta)$  with the Lipschitz continuity of  $f(\theta, x)$ <sup>11</sup>; see, e.g., [Chen et al., 2024a, Theorem 3.1].

**Corollary 3.4.** *Under Assumptions 2.6 and 2.8,  $F_{\max}(\theta)$  is  $(L_{f,1} + L_{f,1}L_{g,2}/\mu)$ -Lipschitz continuous.*

For completeness, we provide the proof in Section B.

<sup>11</sup>A standard chaining argument shows that if  $|F_{\max}(\theta_1) - F_{\max}(\theta_2)| \leq L\|\theta_1 - \theta_2\|$  whenever  $\|\theta_1 - \theta_2\| \leq \gamma$ , then the same constant works uniformly on  $\Theta$ .

### 3.2 Common Dimension and Geometric Properties of $\{\mathcal{S}(\theta)\}_{\theta \in \Theta}$

For each  $\theta \in \Theta$ , the local PL condition implies that on  $\mathcal{S}(\theta)$  the Hessian  $\partial_x^2 g(\theta, x)$  is positive definite in the normal directions and degenerate in the tangent directions [Rebjoek and Boumal, 2023, Proposition 2.7]. In particular, its rank  $\mathfrak{r}(\theta)$  is constant over  $x \in \mathcal{S}(\theta)$ , and the dimension of the minimizer manifold can be written as  $\dim \mathcal{S}(\theta) = \mathfrak{k}(\theta) = d - \mathfrak{r}(\theta)$ . Moreover, the solution mapping  $\theta \mapsto \mathcal{S}(\theta)$  is continuous (Lemma 3.2), and  $\partial_x^2 g(\theta, x)$  is continuous in  $(\theta, x)$ . Thus, when  $\theta$  is perturbed slightly, points in  $\mathcal{S}(\theta)$  move continuously and the corresponding Hessians remain close, so no eigenvalue can cross zero and the rank  $\mathfrak{r}(\theta)$  cannot change. Hence  $\mathfrak{r}(\theta)$ , and therefore  $\mathfrak{k}(\theta)$ , is locally constant in  $\theta$  and we obtain a single intrinsic dimension shared by all manifolds  $\{\mathcal{S}(\theta)\}_{\theta \in \Theta}$ . We summarize this in the following lemma.

**Lemma 3.5.** *Under Assumptions 2.6 to 2.8, the manifolds  $\{\mathcal{S}(\theta)\}_{\theta \in \Theta}$  admit a common dimension  $\mathfrak{k}$ .*

The proof is given in Section B.3. Lemma 3.5 allows us to work with a single geometric parameter  $\mathfrak{k}$  in all later bounds, rather than letting the dimension depend on  $\theta$ . In particular, when we study the Gibbs relaxation and the superquantile approximation of  $F_{\max}$ , the scaling with accuracy is expressed in terms of this common dimension  $\mathfrak{k}$  (see Theorem 4.5). Throughout the paper, we consider  $\mathfrak{k} \geq 1$ , since when  $\mathfrak{k} = 0$ ,  $\mathcal{S}(\theta)$  is a singleton and minima-selection is redundant. Next, we collect basic geometric properties of  $\{\mathcal{S}(\theta)\}_{\theta \in \Theta}$  that will be used in our approximation analysis (see Section 4). The proofs are based on the uniform compactness of the manifolds.

**Proposition 3.6.** *Under compactness of  $\Theta$  and Assumptions 2.6 and 2.7, the following holds for all  $\theta \in \Theta$ .*

- *There exists a constant  $D$  independent of  $\theta$ , such that  $\text{diam}(\mathcal{S}(\theta)) \leq D$ .*
- *The absolute value of sectional curvature<sup>12</sup> of  $\mathcal{S}(\theta)$  is bounded by some constant  $C_0 > 0$ .*
- *There is a constant  $r_0 > 0$  such that the injectivity radius<sup>13</sup>  $\text{inj}(p) \geq r_0$  for all  $p \in \mathcal{S}(\theta)$ .*

The proof is given in Section B.4. Finally, we show a uniform bound on the limiting density  $\rho_\theta$  defined in eq. (7).

**Proposition 3.7.** *Under Assumptions 2.6 and 2.8, there exists a constant  $\kappa > 0$  such that  $\kappa \leq \rho_\theta(x) \leq 1/\kappa$  for all  $x \in \mathcal{S}(\theta)$  and  $\theta \in \Theta$ .*

The proof is given in Section B.5. This result ensures that integration with respect to the limiting Gibbs measure is uniformly comparable to integration with respect to the volume measure on  $\mathcal{S}(\theta)$ , which is crucial for our approximation analysis in the next section.

**Remark 3.8.** *(On the size of the constant  $\kappa$ ) We chose  $\kappa = \mathfrak{b} \cdot (\mu/M_g)^{\frac{d-\mathfrak{k}}{2}}$  in the proof of Proposition 3.7, where  $\mu > 0$  is a uniform lower bound on the nonzero normal eigenvalues of  $\partial_x^2 g(\theta, x)$ ,  $M_g > 0$  is a uniform upper bound on  $\|\partial_x^2 g(\theta, x)\|$  over  $\mathcal{S}(\theta)$ , and the constant  $\mathfrak{b} > 0$  comes from the volume bounds on  $\mathcal{S}(\theta)$  in Lemma B.5 in Section B.5. In the worst case, the ratio  $\mu/M_g$  can be very small, so  $\kappa$  may be exponentially small. In contrast, in an idealized case where in normal coordinates  $g(\theta, \cdot)$  behaves like a pure squared distance to  $\mathcal{S}(\theta)$ , we have  $\mu = M_g$ , so  $\kappa = \mathfrak{b}$ .*

## 4 Approximation Guarantees with SQ-G Relaxation

In this section, we show that the superquantile-Gibbs relaxation  $\tilde{F}_{\text{SQ-G}}$ , defined in Equation (2), provides a valid approximation to  $F_{\max}$  under Assumptions 2.6 to 2.8, given suitable choices of the parameters  $\delta$  and  $\lambda$ . Our approximation result justifies using  $\tilde{F}_{\text{SQ-G}}$  as a surrogate for  $F_{\max}$  when applying zeroth-order methods to optimize the latter. We establish the result through the following steps:

<sup>12</sup>Refer to Definition A.3 for the definition of sectional curvature.

<sup>13</sup>Refer to Definition A.2 for the definition of injectivity radius.

1. The superquantile loss (SQ-loss), defined as

$$\tilde{F}_{\text{SQ}}(\theta) := \min_{\beta} \left\{ \beta + \frac{1}{\delta} \mathbb{E}_{X \sim \mu_{\theta}^0} [\max\{f(\theta, X) - \beta, 0\}] \right\}, \quad (11)$$

closely approximates the hyper-objective  $F_{\max}(\theta)$  point-wisely.

2. The difference between  $\tilde{F}_{\text{SQ}}$  and  $\tilde{F}_{\text{SQ-G}}$  is bounded by the Wasserstein-1 distance between  $\mu_{\theta}^{\lambda}$  and  $\mu_{\theta}^0$ :  $|\tilde{F}_{\text{SQ}}(\theta) - \tilde{F}_{\text{SQ-G}}(\theta)| \leq \mathcal{O}(\delta^{-1} \mathbb{W}_1(\mu_{\theta}^{\lambda}, \mu_{\theta}^0))$ .

Below we formally present these results.

#### 4.1 Approximation of $F_{\max}$ with $\tilde{F}_{\text{SQ}}$

Recall that the  $(1 - \delta)$ -superquantile of the random variable  $Y = f(\theta, X)$  with  $X \sim \mu_{\theta}^0$  is the average of the values of  $Y$  that lie above its  $(1 - \delta)$ -quantile threshold. Our goal is to show that, for small  $\delta$ , the superquantile  $\tilde{F}_{\text{SQ}}(\theta)$  provides a good approximation of  $F_{\max}(\theta)$ . To build intuition, fix  $\theta$  and suppose that the function  $x \mapsto f(\theta, x)$  attains its maximum over  $\mathcal{S}(\theta)$  at a unique point  $x^*(\theta) \in \mathcal{S}(\theta)$ . Consider the high-value set  $\mathfrak{X}_{\delta}(\theta) := \{x \in \mathcal{S}(\theta) : f(\theta, x) \text{ is above the } (1 - \delta)\text{-quantile threshold}\}$ . This set forms a neighborhood of  $x^*(\theta)$ . Since  $x^*(\theta) \in \mathfrak{X}_{\delta}(\theta)$  and  $f$  is Lipschitz, the approximation error  $|\tilde{F}_{\text{SQ}}(\theta) - F_{\max}(\theta)|$  is controlled by how far one can move away from  $x^*(\theta)$  while staying in  $\mathfrak{X}_{\delta}(\theta)$ . Denoting by  $r$  the minimal geodesic distance from  $x^*(\theta)$  to the boundary of  $\mathfrak{X}_{\delta}(\theta)$ , the Lipschitz continuity of  $f$  then bounds the error in terms of  $r$ .

Thus, to bound the approximation error, it suffices to bound  $r$ . To bound this radius  $r$  given our control over the probability mass  $\delta$ , we proceed in two steps: 1) *Probability to Volume*: We first translate probability mass  $\delta$  into Riemannian volume. This is possible because the density of the limiting measure  $\mu_{\theta}^0$  is strictly lower-bounded (see Proposition 3.7), ensuring that a small probability mass implies a small geometric volume. 2) *Volume to Radius*: We then translate Riemannian volume into the radius  $r$ . By establishing that the Riemannian volume scales similarly to Euclidean volume ( $\propto r^k$ ), we deduce that the radius shrinks at the rate  $r \lesssim \delta^{1/k}$ .

Classical results such as [Gray, 1973] give a pointwise asymptotic expansion of the volume of a small geodesic ball, showing that  $\mathcal{M}(B_{\mathfrak{g}}(p; r))/r^k \rightarrow c(p)$  as  $r \rightarrow 0$  with a coefficient depending on the local curvature at  $p$ . For our purposes, this is not sufficient: we will see that in the proof of Theorem 4.2 we need a *uniform*, non-asymptotic lower bound that holds simultaneously for all centers  $p \in \mathcal{S}(\theta)$  and all radii  $0 < r \leq r_1$ , with  $r_1$  depending only on the global bounds on sectional curvature and injectivity radius from Proposition 3.7. Lemma 4.1 provides exactly this quantitative version by turning the asymptotic comparison into an explicit estimate with controlled radius and constants.

**Lemma 4.1.** *Under Assumptions 2.6 and 2.7, there exist constants  $c_H, c_L > 0$ , and  $c_1 > 0$  such that for every  $\theta \in \Theta$ , for any  $p \in \mathcal{S}(\theta)$ , and any radius  $r$  satisfying  $0 < r < \min\{r_0, c_1/\sqrt{2C_0}\}$ , the Riemannian volume of the geodesic ball  $\mathbb{B}_{\mathfrak{g}}(p; r)$  satisfies*

$$c_L \cdot \text{Leb}_k(\mathbb{B}_k(p; r)) \leq \mathcal{M}(\mathbb{B}_{\mathfrak{g}}(p; r)) \leq c_H \cdot \text{Leb}_k(\mathbb{B}_k(p; r)),$$

where  $r_0$  and  $C_0$  are defined in Proposition 3.6,  $\text{Leb}_k(\mathbb{B}_k(p; r))$  is the standard  $k$ -dimensional Lebesgue volume of a ball of radius  $r$  in  $\mathbb{R}^k$ , and  $\mathcal{M}$  is the Riemannian volume measure on  $(\mathcal{S}(\theta), \mathfrak{g})$ .

The proof of Lemma 4.1 is given in Section C.1. Based on Lemma 4.1, the Riemannian volume of a geodesic ball with radius  $r$ ,  $\mathcal{M}(\mathbb{B}_{\mathfrak{g}}(p; r))$ , scales as  $r^k$ . At a high level, the lemma relies on two geometric ingredients: (i) The injectivity radius bound  $r_0 > 0$  guarantees that, around every  $p \in \mathcal{S}$ , we can introduce normal coordinates on the whole geodesic ball  $\mathbb{B}_{\mathfrak{g}}(p; r)$  for all  $r \leq r_0$ . (ii) The curvature bound  $|\text{Sec}| \leq C_0$  then implies that, in these normal coordinates and for radii  $r$  of order  $1/\sqrt{C_0}$ , at a given point  $v \in \mathbb{B}_{\mathfrak{g}}(p; r)$ ,

the matrix  $(g_{ij}(v))_{i,j=1}^k$  representing the Riemannian metric remains uniformly close to the Euclidean metric  $(\delta_{ij}(v))_{i,j=1}^k$ <sup>14</sup>. Consequently, the Riemannian volume element  $\sqrt{\det(g_S(v))} dv$  is uniformly comparable from below to the Euclidean volume element  $dv$  on such balls. Integrating this comparison over  $\mathbb{B}_k(0; r)$  yields the stated lower bound on the Riemannian volume  $\mathcal{M}(\mathbb{B}_g(p; r))$ . We now state the following key result.

**Theorem 4.2** ( $\tilde{F}_{SQ}$  approximates  $F_{\max}$ ). *Recall  $\tilde{F}_{SQ}(\theta) := \min_{\beta} \phi_{0,\delta}(\theta, \beta)$ . Under Assumptions 2.6 to 2.8, for every  $\theta \in \Theta$  and for*

$$0 < \delta \leq c_L \cdot C_k \cdot \kappa \cdot \left(4^{-1} \min\{c_1/\sqrt{2C_0}, r_0\}\right)^k,$$

we have

$$|F_{\max}(\theta) - \tilde{F}_{SQ}(\theta)| \leq \frac{4L_{f,1}\delta^{\frac{1}{k}}}{(\kappa \cdot c_L \cdot C_k)^{\frac{1}{k}}}.$$

Here  $c_L$  and  $c_1$  are defined in Lemma 4.1,  $\kappa$  in Proposition 3.7,  $k$  is the dimension of  $\mathcal{S}(\theta)$ ,  $C_k = \pi^{k/2}/\Gamma(k/2 + 1)$ , and  $r_0, C_0$  are from Proposition 3.6.

*Proof.* Let  $Z := f(\theta, X)$  where  $X \sim \mu_g^0(\theta)$ . Since  $Z$  takes values in  $\{f(\theta, x) : x \in \mathcal{S}(\theta)\}$ , we have the elementary bounds

$$\max_{x \in \mathcal{S}(\theta)} f(\theta, x) \geq \tilde{F}_{SQ}(\theta) \geq Q_{1-\delta}(Z),$$

hence

$$\begin{aligned} |F_{\max}(\theta) - \tilde{F}_{SQ}(\theta)| &= F_{\max}(\theta) - \tilde{F}_{SQ}(\theta) \\ &\leq F_{\max}(\theta) - Q_{1-\delta}(f(\theta, X)). \end{aligned} \tag{12}$$

Thus it remains to bound  $F_{\max}(\theta) - Q_{1-\delta}(f(\theta, X))$ .

We fix  $\theta$  and drop it from the notation. Write  $\mathcal{S} = \mathcal{S}(\theta)$ ,  $f = f(\theta, \cdot)$ ,  $f^* = \max_{x \in \mathcal{S}} f(x)$ ,  $\mathcal{S}_f = \arg \max f$  (nonempty by compactness), and draw  $Y \sim \mu^0$  as in Proposition 2.10. Denote by  $\text{dist}_g$  the geodesic distance on  $\mathcal{S}$ , and write  $\mathbb{B}_g(x; r) := \{u \in \mathcal{S} : \text{dist}_g(u, x) < r\}$  for the geodesic ball (refer to (35) in Section A.1). While  $\mathcal{S}_f$  may generally consist of multiple connected components, we assume without loss of generality that it is connected, as the extension of our analysis below to the general case is straightforward.

**Proof outline.** (i) Let  $\varepsilon := f^* - Q_{1-\delta}(f(Y))$  and  $A_\varepsilon := \{u \in \mathcal{S} : f(u) \geq f^* - \varepsilon\}$ . Set  $r := \text{dist}_g(\overline{\mathcal{S} \setminus A_\varepsilon}, \mathcal{S}_f)$ . A minimizing geodesic between these sets has a midpoint  $x$  with a geodesic ball  $\mathbb{B}_g(x; r/4) \subset A_\varepsilon \setminus \mathcal{S}_f$ . (ii) By Proposition 3.7,  $\mu^0(\cdot)$  is comparable to  $\mathcal{M}(\cdot)$ ; since  $\mu^0(A_\varepsilon) = \delta$ , we get  $\mathcal{M}(\mathbb{B}_g(x; r/4)) \lesssim \delta$ . Under Proposition 3.6 and by Lemma 4.1,  $\mathcal{M}(\mathbb{B}_g(x; r/4)) \gtrsim (r/4)^k$ . Hence  $r \lesssim \delta^{1/k}$  (for small  $\delta$ ). (iii) Lipschitzness of  $f$  yields  $f^* - Q_{1-\delta}(f(Y)) \leq L_{f,1} r$ . Combining with  $r \lesssim \delta^{1/k}$  and the reduction in (12) gives the claimed rate.

**(i) Near-optimal set contains a geodesic ball.** For any set  $A \subseteq \mathcal{S}$ , we write  $\bar{A}$  for the closure of  $A$  in  $\mathcal{S}$ , i.e., with respect to the topology induced by the Riemannian metric on  $\mathcal{S}$ . We then define the geodesic set-set distance using the closure

$$r := \text{dist}_g(\overline{\mathcal{S} \setminus A_\varepsilon}, \mathcal{S}_f) = \min_{z \in \overline{\mathcal{S} \setminus A_\varepsilon}} \min_{y \in \mathcal{S}_f} \text{dist}_g(z, y).$$

<sup>14</sup>Here  $\delta_{ij}$  denotes the Kronecker delta:  $\delta_{ij} = 1$  if  $i = j$  and  $\delta_{ij} = 0$  otherwise.

Since  $\overline{\mathcal{S} \setminus A_\varepsilon}$  and  $\mathcal{S}_f$  are compact, minimizers  $z \in \overline{\mathcal{S} \setminus A_\varepsilon}$  and  $y \in \mathcal{S}_f$  exist with  $\text{dist}_g(z, y) = r$ . Let  $\gamma$  be a minimizing geodesic from  $y$  to  $z$  and set the geodesic midpoint  $x := \gamma(r/2)$ . We claim

$$\mathbb{B}_g(x; r/4) \subset A_\varepsilon \setminus \mathcal{S}_f.$$

Indeed, for any  $w \in \mathbb{B}_g(x; r/4)$ , using that the map  $x \mapsto \text{dist}_g(x, \mathcal{S}_f)$  is 1-Lipschitz<sup>15</sup> we have

$$\text{dist}_g(w, \mathcal{S}_f) \geq \text{dist}_g(x, \mathcal{S}_f) - \text{dist}_g(w, x) \geq r/2 - r/4 = r/4 > 0,$$

so  $w \notin \mathcal{S}_f$ ; and

$$\text{dist}_g(w, \mathcal{S}_f) \leq \text{dist}_g(w, x) + \text{dist}_g(x, y) \leq r/4 + r/2 = 3r/4 < r.$$

Because  $r = \min_{u \in \overline{\mathcal{S} \setminus A_\varepsilon}} \text{dist}_g(u, \mathcal{S}_f)$ , the inequality  $\text{dist}_g(w, \mathcal{S}_f) < r$  implies  $w \notin \overline{\mathcal{S} \setminus A_\varepsilon}$ , hence  $w \in A_\varepsilon$ .

**(ii) From probability mass to a bound on  $r$ .** By Proposition 3.7, the density  $\rho$  of  $\mu^0$  w.r.t. the Riemannian volume  $\mathcal{M}$  satisfies  $\kappa \leq \rho \leq \kappa^{-1}$  on  $\mathcal{S}$ , hence for any Borel  $A \subset \mathcal{S}$ ,

$$\kappa \mathcal{M}(A) \leq \mu^0(A) \leq \kappa^{-1} \mathcal{M}(A).$$

Using  $\mathbb{B}_g(x; r/4) \subset A_\varepsilon$  and  $\mu^0(A_\varepsilon) = \delta$ , we obtain

$$\mathcal{M}(\mathbb{B}_g(x; r/4)) \leq \mathcal{M}(A_\varepsilon) \leq \kappa^{-1} \mu^0(A_\varepsilon) = \kappa^{-1} \delta.$$

On the other hand, the injectivity-radius and curvature bounds in Proposition 3.6 allow us to apply Lemma 4.1. Hence, for  $r \leq \min\{r_0, 1/\sqrt{2K}\}$ , we have

$$c C_k (r/4)^k = c \text{Leb}_k(\mathbb{B}_k(0; r/4)) \leq \mathcal{M}(\mathbb{B}_g(x; r/4)),$$

where  $C_k = \pi^{k/2}/\Gamma(k/2 + 1)$ . Combining the last two inequalities yields

$$c C_k (r/4)^k \leq \kappa^{-1} \delta \implies r \leq 4 \left( \delta \kappa^{-1} [c C_k]^{-1} \right)^{\frac{1}{k}}, \quad (13)$$

provided  $\delta \leq c C_k \kappa [4^{-1} \min\{r_0, 1/\sqrt{2C_0}\}]^k$  so that the small-radius condition of Lemma 4.1 holds.

**(iii) Lipschitz control of the value gap.** Since  $f$  is  $L_{f,1}$ -Lipschitz (in the ambient norm) and  $\text{dist}_g \geq \|\cdot\|$ <sup>16</sup>,

$$\begin{aligned} f^* - \mathbf{Q}_{1-\delta}(f(Y)) &= \varepsilon \leq f^* - f(z) \leq L_{f,1} \|y - z\| \leq L_{f,1} \text{dist}_g(y, z) \\ &= L_{f,1} r. \end{aligned} \quad (14)$$

Together with the bound on  $r$  in (13), we conclude

$$f^* - \mathbf{Q}_{1-\delta}(f(Y)) \leq 4 L_{f,1} \left( \delta \kappa^{-1} [c C_k]^{-1} \right)^{\frac{1}{k}},$$

completing the proof. □

<sup>15</sup>For any  $a \in \mathcal{S}_f$ , the triangle inequality gives  $\text{dist}_g(w, a) \leq \text{dist}_g(w, x) + \text{dist}_g(x, a)$ . Taking  $\inf_{a \in \mathcal{S}_f}$  yields  $\text{dist}_g(w, \mathcal{S}_f) \leq \text{dist}_g(w, x) + \text{dist}_g(x, \mathcal{S}_f)$ . Swapping  $w$  and  $x$  gives the reverse inequality, hence  $|\text{dist}_g(w, \mathcal{S}_f) - \text{dist}_g(x, \mathcal{S}_f)| \leq \text{dist}_g(w, x)$ .

<sup>16</sup>Here we use the fact that the geodesic distance  $\text{dist}_g(x, y)$  is at least as large as the Euclidean distance  $\|x - y\|$  in the ambient space.

**Remark 4.3.** (Sharpness of the  $\delta^{1/k}$ ) The  $\delta^{1/k}$  dependence in Theorem 4.2 is dictated by the  $k$ -dimensional volume growth of small balls on  $\mathcal{S}(\theta)$  and cannot, in general, be improved. Indeed, fix  $\theta$  and a point  $x^*(\theta) \in \mathcal{S}(\theta)$ , and consider the toy function  $f(\theta, x) := -\text{dist}_{\mathbb{g}}(x, x^*(\theta))$ . Clearly,  $F_{\max}(\theta) = 0$ . For  $r > 0$ , the sublevel set  $A_r(\theta) = \{x \in \mathcal{S}(\theta) : -f(\theta, x) \leq r\}$  is exactly the geodesic ball  $B_{\mathbb{g}}(x^*(\theta); r)$ . Let us pick  $r = -Q_{1-\delta}(f(\theta, Y))$  where  $Y \sim \mu_{\theta}^0$  and  $\delta$  sufficiently small as stated in Theorem 4.2. By Proposition 3.7 and Lemma 4.1, we have

$$\begin{aligned} \delta &= \mu_0(A_r(\theta)) = \mu_0(B_{\mathbb{g}}(x^*(\theta); r)) \leq \kappa^{-1} \cdot \mathcal{M}(B_{\mathbb{g}}(x^*(\theta); r)) \\ &\leq \kappa^{-1} \cdot c_H \cdot \text{Leb}_k(B_{\mathbb{g}}(x^*(\theta); r)) \lesssim r^k. \end{aligned} \quad (15)$$

Then  $\delta^{1/k} \lesssim r = F_{\max}(\theta) - Q_{1-\delta}(f(\theta, Y))$ . Thus one cannot, in general, replace the factor  $\delta^{1/k}$  in Theorem 4.2 by a smaller power of  $\delta$ .

## 4.2 Approximation of SQ-loss with SQ-G-loss

The variational formulations  $\phi_{0,\delta}$  and  $\phi_{\lambda,\delta}$  involve expectations of  $\xi(x) := \max\{f(\theta, x) - \beta, 0\}$  over  $\mu_{\theta}^0$  and  $\mu_{\theta}^{\lambda}$ , respectively. Using this expectation structure, we bound the difference between  $\tilde{F}_{\text{SQ}}(\theta)$  and  $\tilde{F}_{\text{SQ-G}}(\theta)$  by the Wasserstein-1 distance between  $\mu_{\theta}^{\lambda}$  and  $\mu_{\theta}^0$ : We use the Kantorovich–Rubinstein duality for the Wasserstein-1 distance with  $\xi(x)$  as a test function.

**Lemma 4.4.** Under Assumption 2.8, for every  $\theta \in \Theta$ , we have,

$$|\tilde{F}_{\text{SQ-G}}(\theta) - \tilde{F}_{\text{SQ}}(\theta)| \leq \frac{L_{f,1}}{\delta} \cdot \mathbb{W}_1(\mu_{\theta}^{\lambda}, \mu_{\theta}^0). \quad (16)$$

The proof of Lemma 4.4 is given in Section C.2. As a consequence of Theorem 4.2, Lemma 4.4, and Proposition 2.11, we have that  $\tilde{F}_{\text{SQ-G}}(\theta)$  approximates  $F_{\max}(\theta)$  by choosing  $\delta$  and  $\lambda$  properly.

**Theorem 4.5.** Under Assumptions 2.6 to 2.8, for  $\delta < c \cdot C_k \cdot \kappa \cdot (4^{-1} \min\{1/\sqrt{2C_0}, r_0\})^k$ , we have

$$\left| F_{\max}(\theta) - \tilde{F}_{\text{SQ-G}}(\theta) \right| \leq \frac{4L_{f,1}\delta^{\frac{1}{k}}}{(\kappa \cdot c \cdot C_k)^{\frac{1}{k}}} + \frac{L_{f,1}}{\delta} \cdot K_0 \lambda^{\frac{1}{2}}. \quad (17)$$

The bound in (17) makes the role of the manifold dimension  $k$  explicit: the bias term scales as  $\delta^{1/k}$ , so larger  $k$  requires smaller  $\delta$  to reach the same accuracy. This bound also yields a simple rule for choosing the parameters to reach any target accuracy: pick  $\delta = \epsilon_v^k$  and  $\lambda = \epsilon_v^{2(k+1)}$ , where  $0 < \epsilon_v < (c \cdot C_k \cdot \kappa)^{\frac{1}{k}} \cdot 4^{-1} \min\{c_1/\sqrt{2C_0}, r_0\}$ , then

$$\left| F_{\max}(\theta) - \tilde{F}_{\text{SQ-G}}(\theta) \right| = \mathcal{O}(\epsilon_v).$$

This provides a clear, dimension-aware recipe for setting  $(\delta, \lambda)$  that we use in Section 5.

## 5 Oracle complexity of optimizing $F_{\max}$

In this section, we develop a zeroth-order algorithm to find a Goldstein stationary point of the hyper-objective  $F_{\max}$ . Zeroth-order methods require pointwise evaluations of the objective, but direct evaluation of  $F_{\max}$  is intractable because it involves an inner maximization over the lower-level solution set. To obtain a tractable objective oracle, we replace  $F_{\max}$  by its Gibbs–superquantile surrogate  $\tilde{F}_{\text{SQ-G}}$  defined in (2), which can be estimated from Gibbs samples. As shown in Theorem 4.5, suitable choices of  $\lambda$  and  $\delta$  ensure that  $\tilde{F}_{\text{SQ-G}}$  uniformly approximates  $F_{\max}$ . We then query  $\tilde{F}_{\text{SQ-G}}$  at multiple points to construct a finite-difference

estimator of a proxy gradient of  $F_{\max}$ , and use this estimator within a zeroth-order scheme to obtain a Goldstein stationary point of the original hyper-objective.

To evaluate  $\tilde{F}_{\text{SQ-G}}(\theta)$ , we use its variational representation in (2), which involves solving the inner minimization problem  $\min_{\beta \in \mathbb{R}} \phi_{\lambda, \delta}(\theta, \beta)$ . Since  $\phi_{\lambda, \delta}(\theta, \cdot)$  is convex but possibly non-smooth, a natural choice is to apply the subgradient method.<sup>17</sup> To ensure convergence, the non-smooth optimization must be restricted to a *bounded* interval. In Lemma 5.1, we show that the optimal set  $\arg \min_{\beta} \phi_{\lambda, \delta}(\theta, \beta)$  lies within  $[-B, B]$ , so that

$$\tilde{F}_{\text{SQ-G}}(\theta) = \min_{\beta \in [-B, B]} \phi_{\lambda, \delta}(\theta, \beta).$$

Given that (i)  $\phi_{\lambda, \delta}(\theta, \cdot)$  is convex and Lipschitz continuous, (ii) the feasible set is bounded, and (iii) the stochastic subgradient  $\tilde{\partial}_{\beta} \phi_{\lambda, \delta}(\theta, \beta; X)$  satisfies  $|\tilde{\partial}_{\beta} \phi_{\lambda, \delta}(\theta, \beta; X)| \leq \sigma := 1 + \delta^{-1}$ , we invoke the classical convergence guarantees for convex Lipschitz objectives [Nemirovskij and Yudin, 1983, Lan et al., 2012] together with the large-deviation analysis for stochastic approximation [Juditsky and Nemirovski, 2008, Thm. 2.1]. Accordingly, the output  $\hat{\beta}$  of projected stochastic gradient descent (PSGD) (see Algorithm 1) satisfies

$$\phi_{\lambda, \delta}(\theta, \hat{\beta}) - \min_{\beta} \phi_{\lambda, \delta}(\theta, \beta) \leq \hat{\epsilon}, \quad \text{with probability at least } 1 - \Delta, \quad (18)$$

after at most  $\mathcal{O}(B^2 \sigma^2 \hat{\epsilon}^{-2} \log(\Delta^{-1}))$  iterations.

Building on the above discussion, we now use the PSGD output to construct a tractable zeroth-order oracle for  $F_{\max}$ . For any query  $\theta$ , we evaluate the scalar quantity  $\phi_{\lambda, \delta}(\theta, \hat{\beta})$ , where  $\hat{\beta}$  is the approximate minimizer returned by PSGD, and regard this as a noisy evaluation of  $\tilde{F}_{\text{SQ-G}}(\theta)$  and hence of  $F_{\max}(\theta)$ . Querying this oracle at carefully chosen perturbations of  $\theta$  yields a multi-point finite-difference estimator of a proxy gradient, which drives the projected zeroth-order scheme in Algorithm 2.

Below, we analyze in detail the convergence of Algorithm 1 (inner minimization of the Gibbs–superquantile) and Algorithm 2 (outer minimization of the hyper-objective).

## 5.1 Inner minimization of Gibbs-superquantile

In this subsection, we first show that all global minimizers of  $\phi_{\lambda, \delta}(\theta, \cdot)$  lie in a common bounded interval. This boundedness allows us to run PSGD on a compact domain and invoke standard convergence guarantees. We then use this result to justify treating the noisy values  $\phi_{\lambda, \delta}(\theta, \hat{\beta})$ , where  $\hat{\beta}$  is the PSGD output, as approximate evaluations of  $F_{\max}(\theta)$ .

We first briefly introduce the PSGD (Algorithm 1) to solve  $\min_{\beta \in [-B, B]} \phi_{\lambda, \delta}(\theta, \beta)$ . Specifically, for a given  $\theta \in \Theta$ , we have

$$\beta^{l+1} \leftarrow \text{Proj}_{[-B, B]}(\beta^l - \eta_l \tilde{\partial}_{\beta} \phi_{\lambda, \delta}(\theta, \beta^l; \tilde{X}^{(l)})), \quad (19)$$

where  $\tilde{\partial}_{\beta} \phi_{\lambda, \delta}(\theta, \beta; \tilde{X}^{(l)})$  represents a sub-gradient of the noisy sample of  $\phi_{\lambda, \delta}(\theta, \beta)$  as follows:

$$\phi_{\lambda, \delta}(\theta, \beta; \tilde{X}^{(l)}) := \beta + \frac{1}{\delta} \max\{f(\theta, \tilde{X}^{(l)}) - \beta, 0\}, \quad (20)$$

and  $\{\tilde{X}^{(l)}\}_{l=0}^{L-1}$  are independent and identically distributed (i.i.d.) samples drawn from  $\mu_{\theta}^{\lambda}$  and  $B$  is a positive constant. A natural choice for the PSGD output at a fixed  $\theta$  is the empirical average  $L^{-1} \sum_{i=1}^L \beta^i$ .

We next show in Lemma 5.1 that the minimizers  $\beta^*(\theta) \in \arg \min_{\beta} \phi_{\lambda, \delta}(\theta, \beta)$  are uniformly bounded. For the upper bound on  $\beta^*(\theta)$ , recall the definition of  $\tilde{F}_{\text{SQ}}(\theta)$  in (11); then

$$\beta^*(\theta) \leq \beta^*(\theta) + \frac{1}{\delta} \mathbb{E}_{X \sim \mu_{\theta}^{\lambda}}[\max\{f(\theta, X) - \beta^*(\theta), 0\}] = \phi_{\lambda, \delta}(\theta, \beta^*(\theta))$$

<sup>17</sup>Because the problem is one-dimensional, the bisection method is also applicable, provided the domain is bounded.

---

**Algorithm 1** PSGD( $\theta, \beta_0; (\lambda, \delta)$ )

---

**Input:**  $\theta, \beta_0, \lambda, \delta$ , and  $L$ 

- 1:  $l = 0$
  - 2: **while**  $\lambda > 0$  and  $l \leq L$  **do**
  - 3:  $\beta^{l+1} = \text{Proj}_{[-B, B]}(\beta^l - \eta_l \tilde{\partial}_\beta \phi_{\lambda, \delta}(\theta, \beta^l; \tilde{X}^{(l)}))$   
 $[\{\tilde{X}^{(l)}\}_{l=0}^{L-1}$  are i.i.d samples of  $\mu_\theta^\lambda$ .]
  - 4:  $l = l + 1$
  - 5: **end while**
  - 6:  $\hat{\beta} = \frac{1}{L} \sum_{i=1}^L \beta^i$
- 

$$\begin{aligned} &= \tilde{F}_{\text{SQ-G}}(\theta) \leq \tilde{F}_{\text{SQ}}(\theta) + |\tilde{F}_{\text{SQ-G}}(\theta) - \tilde{F}_{\text{SQ}}(\theta)| \\ &\leq \tilde{F}_{\text{SQ}}(\theta) + \frac{L_{f,1}}{\delta} K_0 \lambda^{1/2} \end{aligned} \quad (21)$$

$$\leq L_{f,0}(\text{D}) + \frac{L_{f,1}}{\delta} K_0 \lambda^{1/2}, \quad (22)$$

where (21) applies Proposition 2.11 to Lemma 4.4, and (22) uses

$$\tilde{F}_{\text{SQ}}(\theta) \leq \max_{x \in \mathcal{S}(\theta)} f(\theta, x) \leq \max_{x \in \mathbb{B}_d(0; \text{D})} f(\theta, x) \leq L_{f,0}(\text{D}),$$

with  $L_{f,0}(\cdot)$  defined in (5) and  $\text{D}$  large enough that  $\mathcal{S}(\theta) \subseteq \mathbb{B}_d(0; \text{D})$  (see Proposition 3.6).

A key part of the proof is a uniform lower bound on  $\beta^*(\theta)$ : since  $\beta^*(\theta)$  is a  $(1 - \delta)$ -quantile, we have  $\mathbb{P}\{f(\theta, X) \leq \beta^*(\theta)\} \geq 1 - \delta$  for  $X \sim \mu_\theta^\lambda$ . We then prove a tail bound for the Gibbs measure by using the quadratic growth of  $g$  beyond  $\mathbb{B}_d(0; \text{D})$  in Assumption 2.8, which ensures  $\mu_\theta^\lambda(B(0; 2\text{D})) \geq \delta_0$ . Combining both and taking  $\delta < \delta_0$ , it yields

$$\mu_\theta^\lambda(\{x : f(\theta, x) \leq \beta^*(\theta)\} \cap B(0; 2\text{D})) \geq \delta_0 - \delta > 0,$$

so there exists  $x_0 \in B(0; 2\text{D})$  with  $f(\theta, x_0) \leq \beta^*(\theta)$ . Since  $|f(\theta, x)| \leq L_{f,0}(2\text{D})$  on  $B(0; 2\text{D})$ , we conclude  $\beta^*(\theta) \geq -L_{f,0}(2\text{D})$ . Together with (22), this shows  $\beta^*(\theta) \in [-B, B]$  for a suitable  $B < \infty$ . Now we state the result in the following lemma. The complete proof is deferred to Section D.1.

**Lemma 5.1.** *Suppose that Assumption 2.8 holds and the condition  $\delta \leq 1/2$  hold. For any minimizer  $\beta^*(\theta) \in \arg \min_\beta \phi_{\lambda, \delta}(\theta, \beta)$ , we have*

$$|\beta^*(\theta)| \leq B := \max \left\{ L_{f,0}(2\text{D}), L_{f,0}(\text{D}) + \frac{L_{f,1}}{\delta} \cdot K_0 \lambda^{\frac{1}{2}} \right\}. \quad (23)$$

Combining the existing convergence analysis of PSGD with Lemma 5.1, we can apply the guarantee in (18) to the PSGD output  $\hat{\beta}$ . We then define the following function as an accessible approximation of  $\phi_{\lambda, \delta}(\theta, \hat{\beta})$ :

$$\tilde{\psi}(\theta) := \left\{ \phi_{\lambda, \delta}(\theta, \hat{\beta}; \hat{X}_I) = \hat{\beta} + \frac{1}{\delta |I|} \sum_{i \in I} \max\{f(\theta, \hat{X}^{(i)}) - \hat{\beta}, 0\} \right\}. \quad (24)$$

Here  $\hat{X}_I = \{\hat{X}^{(i)}\}_{i \in I}$  denote  $M$  i.i.d. samples from the sampling oracle of  $\mu_\theta^\lambda$ .

The next lemma shows that the quantity  $\tilde{\psi}(\theta)$  defined in (24) closely approximates  $\tilde{F}_{\text{SQ-G}}(\theta)$ . The proof is deferred to Section D.2. Before stating it, we briefly explain the role of the high-probability guarantee in (18). The convergence analysis of the outer zeroth-order algorithm is often based on an  $L^2$ -type control

---

**Algorithm 2** Projected Stochastic Zeroth-order with minima selection (PSZO-MinSel)

---

**Initialization:**  $\beta_0, \theta_0, \lambda, \delta < 1/2$ , and integers  $M, N$ .

- 1: **for**  $n = 0$  to  $N - 1$  **do**
  - 2: Query  $M$  i.i.d. samples from the sampling oracle of  $\mu_{\theta_n}^\lambda$ , denoted by  $\hat{X}_I = \{\hat{X}^{(i)}\}_{i \in I}$ .
  - 3: Sample  $\{u_{n,t}\}_{t=1}^{b_u}$  independently and uniformly from a unit sphere.
  - 4:  $\beta_{n,t}^+ = \text{PSGD}(\theta_n + \rho u_{n,t}, \beta_0; (\lambda, \delta)), \forall t \in [1 : b_u]$ .
  - 5:  $\beta_{n,t}^- = \text{PSGD}(\theta_n - \rho u_{n,t}, \beta_0; (\lambda, \delta)), \forall t \in [1 : b_u]$ .
  - 6:  $\tilde{\psi}(\theta_n + \rho u_{n,t}) = \phi_{\lambda, \delta}(\theta_n + \rho u_{n,t}, \beta_{n,t}^+; \hat{X}_I)$ .
  - 7:  $\tilde{\psi}(\theta_n - \rho u_{n,t}) = \phi_{\lambda, \delta}(\theta_n - \rho u_{n,t}, \beta_{n,t}^-; \hat{X}_I)$ .
  - 8:  $\tilde{\mathbf{g}}_\rho(\theta_n) = \frac{m}{2\rho} \cdot \frac{1}{b_u} \sum_{t=1}^{b_u} [\tilde{\psi}(\theta_n + \rho u_{n,t}) - \tilde{\psi}(\theta_n - \rho u_{n,t})] u_{n,t}$
  - 9:  $\theta_{n+1} = \text{Proj}_\Theta(\theta_n - \tilde{\eta}_n \tilde{\mathbf{g}}_\rho(\theta_n))$
  - 10: **end for**
- 

of the oracle error, i.e.,  $\mathbb{E}[|\tilde{\psi}(\theta) - F_{\max}(\theta)|^2 \mid \theta]$ , rather than just on its expectation. An in-expectation convergence result for PSGD would only control the mean optimality gap and does not, in general, translate into a sufficiently tight second-moment bound. In contrast, the high-probability estimate in (18) provides a tail bound on the PSGD optimization error; by choosing the target accuracy  $\hat{\epsilon}$  and the failure probability  $\Delta$  appropriately, this tail bound can be converted into the required  $L^2$  control on the oracle error used in Lemma 5.2.

**Lemma 5.2.** *Suppose that Assumption 2.8 holds. Given  $\theta \in \Theta$ , by using Algorithm 1 (PSGD( $\theta, \beta_0; (\lambda, \delta)$ )), with the number of iterations  $L = \mathcal{O}(kB^2\epsilon_v^{-2-2k} \log(\epsilon_v^{-1}))$ , and  $|I| \geq 4\tilde{C}_f\epsilon_v^{-2-2k}$ , we obtain*

$$\mathbb{E}[|\tilde{\psi}(\theta) - \tilde{F}_{\text{SQ-G}}(\theta)|^2 \mid \theta] \leq \epsilon_v^2. \quad (25)$$

Here  $B$  is defined in Lemma 5.1 and  $\tilde{C}_f$  is a constant.

We now simply show that  $\tilde{\psi}(\theta)$  provides a good approximation to  $F_{\max}(\theta)$ . Applying Lemma 5.2 together with Theorem 4.5 yields

$$\begin{aligned} \mathbb{E}[|\tilde{\psi}(\theta) - F_{\max}(\theta)|^2 \mid \theta] &\leq \mathbb{E}[|\tilde{\psi}(\theta) - \tilde{F}_{\text{SQ-G}}(\theta)|^2 \mid \theta] + |\tilde{F}_{\text{SQ-G}}(\theta) - F_{\max}(\theta)|^2 \\ &\leq \mathbb{E}[|\phi_{\lambda, \delta}(\theta, \hat{\beta}; \hat{X}_I) - \tilde{F}_{\text{SQ-G}}(\theta)|^2 \mid \theta] + \mathcal{O}(\delta^{2/k} + \lambda\delta^{-2}) \\ &= \mathcal{O}(\epsilon_v^2), \end{aligned} \quad (26)$$

where, in the final bound, we choose  $\delta = \epsilon_v^k$  and  $\lambda = \epsilon_v^{2(k+1)}$ . The Equation (26) will serve as a key ingredient in our later convergence analysis.

## 5.2 Projected Zeroth-order algorithm with minima selection

In this subsection, we analyze the projected stochastic zeroth-order method with minima selection (PSZO-MinSel) introduced in Algorithm 2. Our goal is to quantify how many oracle calls are needed for PSZO-MinSel to reach an approximate Goldstein stationary point of  $F_{\max}$ . In Algorithm 2, we use the stochastic zeroth-order update

$$\theta_{n+1} \leftarrow \text{Proj}_\Theta(\theta_n - \tilde{\eta}_n \tilde{\mathbf{g}}_\rho(\theta_n)),$$

where  $\tilde{\mathbf{g}}_\rho(\theta_n) := b_u^{-1} \sum_{t=1}^{b_u} \tilde{\mathbf{g}}_\rho(\theta_n, u_{n,t})$ , and  $\tilde{\mathbf{g}}_\rho(\theta_n, u_{n,t}) := \frac{m}{2\rho} [\tilde{\psi}(\theta_n + \rho u_{n,t}) - \tilde{\psi}(\theta_n - \rho u_{n,t})] u_{n,t}$ . Here  $\tilde{\psi}$  is defined in (24), and  $\{u_{n,t}\}_{t=1}^{b_u}$  are i.i.d. draws from the uniform distribution on the unit sphere  $\mathbb{S}^{m-1}$ .

The complete procedure is summarized in Algorithm 2. Concretely, lines 4–5 invoke PSGD to approximate the minimisers of the perturbed sub-problems  $\min_{\beta} \phi_{\lambda, \delta}(\theta_n + \rho u, \beta)$  and  $\min_{\beta} \phi_{\lambda, \delta}(\theta_n - \rho u, \beta)$ . These two inner solutions are combined in line 8 to form the standard two-point stochastic gradient estimator of  $\tilde{F}_{\text{SQ-G}}$ , which then drives the projected descent update for  $\theta$  in line 9.

To state our main result, we first recall the definitions of the Goldstein  $\rho$ -subdifferential set and the generalized Goldstein stationary point, as these will be used to formulate the convergence result in Goldstein stationary sense.

**Definition 5.3** (Goldstein [1977]). *Denote  $\mathbb{B}_m(\theta; \rho) = \{v \in \mathbb{R}^m : \|v - \theta\| \leq \rho\}$ . Given a Lipschitz function  $f : \mathbb{R}^m \rightarrow \mathbb{R}$ , a point  $\theta \in \mathbb{R}^m$  and  $\rho \geq 0$ , the Goldstein  $\rho$ -subdifferential of  $f$  at  $\theta$  is defined as*

$$\partial_{\rho} f(\theta) := \text{conv} \left( \bigcup_{v \in \mathbb{B}_d(\theta; \rho)} \partial f(v) \right).$$

**Definition 5.4** (Liu et al. [2024]). *We say the point  $\theta \in \Theta$  is a  $(\epsilon, \rho, \eta)$ -generalized Goldstein stationary point (GGSP) of the problem (1) if it satisfies*

$$\min_{g \in \partial_{\rho} f(x)} \|\mathcal{G}_{\Theta}(x, g; \eta)\| \leq \epsilon.$$

Here the gradient mapping for a vector  $g \in \partial_{\rho} f(x)$  at a point  $\theta$  is  $\mathcal{G}_{\Theta}(\theta, g; \nu) := \nu^{-1}(\theta - \text{Proj}_{\Theta}(\theta - \nu g))$ .

Our main result in this section is summarized in the following theorem; we show that Algorithm 2 converges to a generalized Goldstein stationary point of  $F_{\max}$ . More specifically, using the error bound in (26), we show that the error incurred by approximating  $F_{\max}$  with  $\tilde{\psi}$  in Algorithm 2 can be efficiently controlled. The proof of Theorem 5.5 is deferred to Section D.3.

**Theorem 5.5.** *Let  $\{\theta_i\}_{i=1}^N$  be the sequence generated by Algorithm 2. Under Assumptions 2.6 to 2.8, we obtain*

$$\min_{i \in [1:N]} \mathbb{E} \left[ \min_{g \in \partial_{\rho} F_{\max}(\theta_i)} \|\mathcal{G}_{\Theta}(\theta_i, g; \eta)\| \right] = \mathcal{O}(\epsilon), \quad (27)$$

with  $N \geq \mathcal{O}(m\epsilon^{-2}\rho^{-2})$ ,  $b_u \geq 1$ ,  $|I| \geq \tilde{C}_f m^{2k+2}(\rho\epsilon)^{-2k-2}$ ,  $\eta \leq \mathcal{O}(m^{-1/2}\rho)$ , and

$$L \geq \mathcal{O} \left( \frac{km^{2k+2}B^2}{(\rho\epsilon)^{2k+2}} \cdot \log(m(\rho\epsilon)^{-1}) \right).$$

Based on Theorem 5.5, to obtain (27), the total number of samples from  $\{\mu_{\theta_i}^{\lambda}\}_{i=1}^N$  can be computed as follows:

$$N \times (b_u L + b_u |I|) = \mathcal{O} \left( \frac{m^{3+2k} \cdot (kB^2 + \tilde{C}_f) \cdot \log(m\epsilon^{-1}\rho^{-1})}{\epsilon^{2k+4} \rho^{2k+4}} \right). \quad (28)$$

### 5.3 Gradient Oracle Complexity under LMC-based Implementation

In the previous subsections, we analyze the sampling oracle complexity to identify an  $(\epsilon, \rho, \eta)$ -GGSP. To have a more concrete complexity result, we analyze the lower-level gradient oracle complexity when using Langevin Monte Carlo (LMC) to implement the Gibbs sampling oracle: To sample from the Gibbs measure in Equation (3), a common choice is the Langevin dynamics

$$dX(t) = -\partial_x g(\theta, X(t))dt + \sqrt{2\lambda}dW(t), \quad (29)$$

where  $W(t)$  denotes a  $d$ -dimensional Brownian motion. Note that the Gibbs measure in Equation (3) is the unique invariant distribution of the above dynamics under mild conditions [Chiang et al., 1987]. In practice, one uses the Euler-Maruyama discretization of the above dynamics, which is also known as the unadjusted LMC method:

$$\hat{X}^{k+1} = \hat{X}^k - h_k \partial_x g(\theta, \hat{X}^k) + \sqrt{2\lambda h_k} \xi_k, \quad (30)$$

where  $\{\xi_k\}_{k=0}^\infty$  is a sequence of i.i.d. standard Gaussian random vectors in  $\mathbb{R}^d$  and  $\{h_k\}_{k=0}^\infty$  is a sequence of step-sizes. We denote by  $\hat{\mu}_n$  the law of the  $n$ -th iterate, i.e.,  $\text{Law}(\hat{X}^n) := \hat{\mu}_n$ .

Our idea is to replace the ideal Gibbs oracle in Algorithms 1 and 2 by the output of LMC algorithm. While the analyses of this more concrete implementation closely follow the ones in the previous two subsections, we further need to ensure two points:

- When  $n$  sufficiently large,  $\hat{\mu}_n$  is close to  $\mu_\theta^\lambda$  in Wasserstein-1 distance;
- Conditioned on the first point, make sure that replacing Gibbs samples with LMC samples introduces only a controlled bias in the Gibbs–superquantile estimator.

To fulfill the first point, we first use a general inequality relating  $\mathbb{W}_1$ ,  $\mathbb{W}_2$ , and the Rényi divergence. By Liu [2020, Theorem 1.1],

$$\mathbb{W}_1(\hat{\mu}_n, \mu_\theta^\lambda) \leq \mathbb{W}_2(\hat{\mu}_n, \mu_\theta^\lambda) \leq 2C_{PI}^{1/2} (e^{\mathbb{R}_2(\hat{\mu}_n, \mu_\theta^\lambda)} - 1)^{1/2},$$

where  $\mathbb{R}_2$  is the order-2 Rényi divergence and  $C_{PI}$  is the Poincaré constant of  $\mu_\theta^\lambda$ . To bound  $\mathbb{R}_2(\hat{\mu}_n, \mu_\theta^\lambda)$  for the LMC iterates, we invoke the following result.

**Proposition 5.6.** [Chewi, 2024, Theorem 6.2.9] *Consider the LMC iteration*

$$X^{k+1} = X^k - h \nabla G(X^k) + \sqrt{2h} \xi_k.$$

*Assume that  $\nabla G$  is  $L_{G,2}$ -Lipschitz and  $\pi \propto \exp(-G)$  satisfies a  $C_{PI}$ -Poincaré inequality. Then for a sufficiently small target accuracy  $\varepsilon$  and an appropriate choice of  $h$ , we obtain  $\mathbb{R}_2(\hat{\mu}_n \parallel \pi) \leq \varepsilon^2$ , with*

$$n = \Theta \left( \frac{C_{PI}^2 L_{G,2}^2 d}{\varepsilon^2} \left( \mathbb{R}_3(\hat{\mu}_0 \parallel \pi)^2 + \log^2 \frac{1}{\varepsilon} \right) \right) \quad \textit{iterations},$$

where  $\mathbb{R}_3$  denotes the order-3 Rényi divergence.

For the update (30), we pick  $G(x) := g(\theta, x)/\lambda$  and  $h_k = h/\lambda$ . Then one has  $\mathbb{R}_2(\hat{\mu}_n, \mu_\theta^\lambda) \leq \varepsilon^2$  with  $n = \tilde{\mathcal{O}}(dC_{PI}^2 \lambda^{-2} \varepsilon^{-2})$ . Combining this with the preceding Wasserstein bound shows that  $\mathbb{W}_1(\hat{\mu}_n, \mu_\theta^\lambda) \leq 2C_{PI}^{1/2} C^{1/2} \varepsilon$ , where  $C = 2(e^{1/2} - 1)$ . Moreover, as discussed in the end of Section 2.1.1, the inverse Poincaré constant  $C_{PI}$  in our context is  $\mathcal{O}(1)$ , independent of  $\lambda$  [Gong et al., 2024].

To establish the second point, we show in Section E that replacing the ideal Gibbs oracle in Algorithms 1 and 2 by the output of LMC algorithm after  $n$  steps only introduces an additional approximation error proportional to  $\delta^{-1} \mathbb{W}_1(\hat{\mu}_n, \mu_\theta^\lambda)$ . Choosing  $n$  so that this error is of the same order as the statistical error controlled in Lemma 5.2 ensures that all bounds in Theorem 5.5 remain valid, up to constants, when using LMC instead of exact Gibbs samples. This yields a concrete lower-level gradient oracle complexity, summarized in the following theorem.

**Theorem 5.7.** Let  $\{\theta_i\}_{i=1}^n$  be the sequence generated by Algorithm 4 (refer to Section E.2). Under Assumptions 2.6 to 2.8, we obtain

$$\min_{i \in [1:N]} \mathbb{E} \left[ \min_{g \in \partial_\rho F_{\max}(\theta_i)} \|\mathcal{G}_\Theta(\theta_i, g; \eta)\| \right] = \mathcal{O}(\epsilon), \quad (31)$$

with  $n \geq \mathcal{O}(m\epsilon^{-2}\rho^{-2})$ ,  $b_u = \mathcal{O}(1)$ ,  $|I| \geq \tilde{C}_f m^{2k+2}(\rho\epsilon)^{-2k-2}$ ,  $\eta \leq \mathcal{O}(m^{-1/2}\rho)$ ,

$$L = \mathcal{O} \left( \frac{m^{2k+2} \mathbf{B}^2}{(\rho\epsilon)^{2k+2}} \log(m\epsilon^{-1}\rho^{-1}) \right),$$

and the number of LMC steps  $N = \tilde{\mathcal{O}}(dm^{6+6k}(\epsilon\rho)^{-6-6k})$ . Moreover, the total number queries from lower-level gradient oracle is

$$n \times N \times (b_u L + b_u |I|) = \mathcal{O} \left( \frac{dm^{9+8k} [k\mathbf{B}^2 + \tilde{C}_f] \log(\epsilon^{-1})}{\epsilon^{8k+10} \rho^{8k+10}} \right).$$

The theorem above shows that Algorithm 2 preserves its intrinsic-dimension complexity guarantees when the ideal Gibbs oracle is replaced by an LMC-based implementation, while making explicit the additional polynomial dependence on the ambient dimension  $d$  and the factors  $m^k$  and  $(\rho\epsilon)^{-k}$ .

## 6 Experiments

Before detailing the experiments, we outline our adaptation of Algorithm 2 to the *optimistic* formulation (see footnote 1), the standard in hyperparameter optimization. We will compare this optimistic variant against existing baselines in both synthetic and data hyper-cleaning setups. To approximate  $F_{\min}(\theta) := \min_{x \in \mathcal{S}(\theta)} f(\theta, x)$ , we use the lower-tail superquantile

$$\tilde{F}_{\text{LSQ}}(\theta) := \max_{\beta} \left\{ \beta - \delta^{-1} \mathbb{E}[\max\{\beta - f(\theta, X), 0\}] \right\}.$$

In our implementation of Algorithm 2, we replace  $\phi_{\lambda, \delta}(\theta, \beta)$  with the surrogate

$$\psi_{\lambda, \delta}(\theta, \beta) := \beta - \delta^{-1} \mathbb{E}_{\mu_{\delta}^{\lambda}(\theta)}[\max\{\beta - f(\theta, X), 0\}].$$

Additionally, in Algorithm 1 we change the projected gradient *descent* step in line 2 to a projected gradient *ascent* step.

### 6.1 Toy Example

**Optimistic formulation:** We evaluate our algorithm along with three more algorithms in the literature on the optimistic BLO problem as follows

$$\min_{\theta \in [-\pi, \pi]} \min_{x \in \mathcal{S}(\theta)} f(\theta, x),$$

where  $f(\theta, x) = 2\|x\| + \langle x, u(\theta) \rangle$  and

$$g_k(\theta, x) = \frac{1}{4} \left( \sum_{i=1}^{k+1} x_i^2 - \theta^2 \right)^2 - \frac{1}{2} \|x\|^2. \quad (32)$$

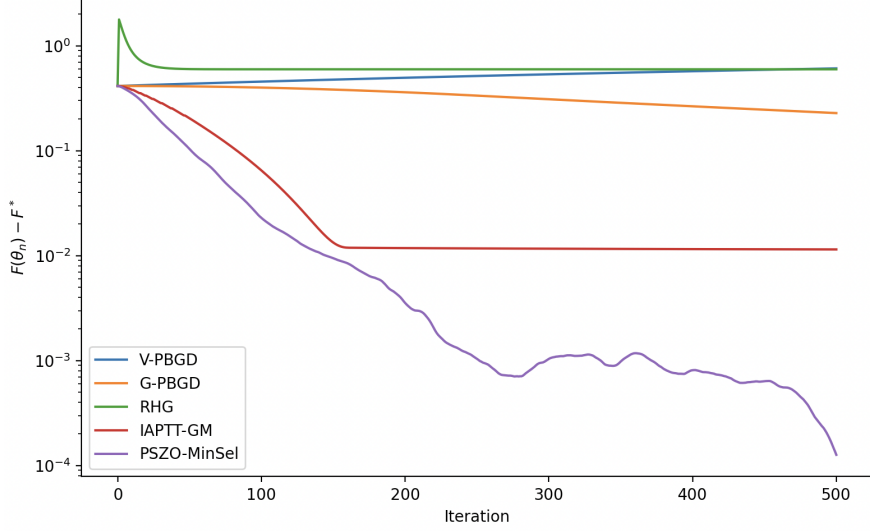


Figure 1: Comparison of  $F(\theta_n) - F^*$  versus iteration for  $d = 2$ . Our algorithm converges faster with the chosen hyperparameters  $\delta = 0.1$  and  $\lambda = 0.01$  in optimistic formulation, while V-PBGD, G-PBGD, RHG, and IAPTT-GM obtain higher values.

and  $u(\theta) = [\cos \theta, \sin \theta, 0, \dots, 0]^\top \in \mathbb{R}^d$ . The solution set is the  $(k - 1)$ -dimensional sphere of radius  $\sqrt{1 + \theta^2}$  embedded in  $\mathbb{R}^d$  along the first  $k$  coordinates:

$$\mathcal{S}(\theta) = \left\{ x \in \mathbb{R}^d : \sum_{i=1}^{k+1} x_i^2 = 1 + \theta^2, x_{k+2} = \dots = x_d = 0 \right\}.$$

So the induced hyper-objective

$$F_{\min}(\theta) = \sqrt{1 + \theta^2}$$

has the unique global minimizer  $\theta^* = 0$ .

Throughout the experiments, we compare the following algorithms:

- **PSZO-MinSel (Algorithm 2)** adapted to  $\min_{x \in \mathcal{S}(\theta)} f(\theta, x)$  instead of pessimistic formulation.
- **V-PBGD** [Shen et al., 2025]: joint gradient descent on the penalized objective  $\Phi(\theta, x) = f(\theta, x) + \gamma(g(\theta, x) - g^*(\theta))$ ,
- **G-PBGD** [Shen et al., 2025]: joint gradient descent on the penalized objective  $\Phi(\theta, x) = f(\theta, x) + \frac{\gamma}{2} \|\nabla_x g(\theta, x)\|^2$ ,
- **RHG** [Franceschi et al., 2017]: truncated reverse-mode hypergradient with re-initialization of  $\theta$  every outer step,
- **IAPTT-GM** [Liu et al., 2021b]: unroll  $T$  inner steps  $x_{k+1} = x_k - \beta \nabla_x g(\theta, x_k)$  from  $x_0 = z$ , pick the pessimistic truncation  $k_\star = \arg \max_k F(\theta, x_k)$ , and update  $\theta, z$  by gradient descent on the truncated objective  $F(\theta, x_{k_\star})$ .

All methods are implemented in JAX with identical initialization  $\theta_0 = 1.0$ ,  $x_0 \sim \mathcal{N}(0, I_d)$ , and random seed. We sweep dimension  $d \in \{2, 5, 10, 20\}$ .

Figure 1 plots  $F(\theta_n) - F^*$  over iterations for  $d = 2$ . The zeroth-order method rapidly converges toward zero, while the other methods tend to plateau or oscillate around suboptimal objective values, primarily due to the absence of a minima selection phase.

$d$	V-PBGD	G-PBGD	RHG	IAPTT-GM	<b>PSZO-MinSel</b>
2	0.297	0.160	0.304	0.152	<b>0.009 ± 0.001</b>
5	0.273	0.160	0.302	0.151	<b>0.015 ± 0.001</b>
10	0.169	0.153	0.303	0.152	<b>0.023 ± 0.001</b>
20	0.113	0.174	0.302	0.154	<b>0.043 ± 0.002</b>

Table 1: Final absolute error  $|\theta_N - \theta^*|$  after  $N = 500$  iterations, evaluated across different dimensions  $d$ . The manifold dimension  $\dim(\mathcal{S}(\theta))$  is  $d - 1$ .

$d$	V-PBGD	G-PBGD	RHG	IAPTT-GM	<b>PSZO-MinSel</b>
5	0.495	0.313	0.302	0.119	<b>0.015 ± 0.001</b>
10	0.499	0.313	0.316	0.114	<b>0.018 ± 0.001</b>
20	0.511	0.315	0.307	0.121	<b>0.018 ± 0.002</b>
30	0.532	0.313	0.311	0.121	<b>0.02 ± 0.002</b>

Table 2: Final absolute error  $|\theta_N - \theta^*|$  after  $N = 500$  iterations, evaluated across different dimensions  $d$ . The manifold dimension  $\dim(\mathcal{S}(\theta)) = 1$  remains constant. Additionally, Algorithm 2 achieves improved accuracy when using a fixed batch size of  $M = 400$ .

### 6.1.1 Dimension sweep and minima-selection

In this experiment, we examine the setting where the intrinsic dimension scales with the ambient dimension, specifically setting  $\kappa = d - 1$ . This simplifies the lower-level objective to  $g(\theta, x) = \frac{1}{4}(\|x\|^2 - \theta^2)^2 - \frac{1}{2}\|x\|^2$ . Table 1 reports the final absolute error  $|\theta_N - \theta^*|$  after  $N = 500$  iterations across varying dimensions  $d$ . The influence of the manifold dimension  $\dim(\mathcal{S}(\theta)) = d - 1$  on the absolute error is also evident. Despite this scaling, our algorithm consistently outperforms the three baseline methods, achieving a significantly closer approximation to the global minimizer  $\theta^* = 0$ . For robustness, we report the mean and confidence intervals over 10 independent runs for our randomized method, compared to single runs for the deterministic baselines.

### 6.1.2 Constant manifold dimension

We next investigate the distinction between intrinsic and ambient dimensionality by fixing the manifold dimension at  $\kappa = 2$  while varying the ambient dimension  $d$ . To align the implementation with our theoretical bounds, we chose the number of Langevin Monte Carlo (LMC) iterations and the batch size  $M$  to closely approximate the target Gibbs distribution. As demonstrated in Table 2, the final error of Algorithm 2 remains nearly constant as  $d$  increases, confirming that the complexity is almost independent of the ambient dimension.

This outcome, when combined with the finding that error increases with  $\kappa$ , validates our central theoretical prediction that the final optimization error is governed solely by the intrinsic dimensionality of the solution set.

**Pessimistic formulation.** To show that our method is able to handle both the optimistic and pessimistic settings, we solve the previous synthetic problem also in the latter setup. To our knowledge, existing hypergradient and penalty-based methods do not model the minimizer-selection step. They either (i) assume the lower-level solution set is a singleton or (ii) return points satisfying KKT conditions, without guaranteeing that these correspond to a selected minimizer of the original bilevel objective. Thus, the connection between their outputs and the true BLO solution is unclear. We also observe that their algorithms are *identical* under the optimistic and pessimistic formulations; when the lower-level solution is non-unique, comparing them in both settings is hence not meaningful. Because these methods are designed for the optimistic case, we

$d$	LL: $g_{d-1}(\theta, x)$ (32)	LL: $g_1(\theta, x)$ (32)
5	<b>0.011 ± 0.001</b>	<b>0.021 ± 0.001</b>
10	<b>0.025 ± 0.002</b>	<b>0.023 ± 0.002</b>
20	<b>0.030 ± 0.002</b>	<b>0.026 ± 0.002</b>
30	<b>0.035 ± 0.003</b>	<b>0.027 ± 0.002</b>

Table 3: Final absolute error  $|\theta_N - \theta^*|$  after  $N = 500$  iterations, evaluated over lower-level dimension  $\delta$  using Algorithm 2 in the pessimistic setting. The first column corresponds to the pessimistic formulation (33) with lower-level  $g_{d-1}$  from (32); the second uses the same problem with lower-level  $g_1$  from (32).

benchmark against them only in the optimistic setting. For the pessimistic formulation, we report results only for our method.

We now study the following pessimistic toy problem

$$\min_{\theta \in [-\pi, \pi]} \max_{x \in \mathcal{S}(\theta)} f(\theta, x), \quad (33)$$

with  $f$  and  $g_k$  identical to the previous setup. The induced hyper-objective  $F_{\max}(\theta) = 3\sqrt{1 + \theta^2}$  admits the unique global minimizer  $\theta^* = 0$ .

We also repeat the experiment under a fixed manifold dimension  $k$ , using the function instance in (32) as the lower-level objective. In Table 3 we replicate the last set of experiments exclusively for Algorithm 2 in the pessimistic setting. In both choices of the lower-level function, we observe a clear dependence on the manifold dimension of the solution set.

## 6.2 Data hyper-cleaning

In this section, we evaluate our method on the data hyper-cleaning benchmark [Franceschi et al., 2017, Shaban et al., 2019], a canonical BLO task widely used in the machine learning community. Given a set of corrupted<sup>18</sup> training samples  $\mathcal{D}_{\text{tr}} = \{(d_i^{\text{tr}}, \ell_i^{\text{tr}})\}_{i=1}^N$ , a *small* clean validation set  $\mathcal{D}_{\text{val}} = \{(d_i^{\text{val}}, \ell_i^{\text{val}})\}_{i=1}^M$ , and a clean test set, the goal is to learn a data cleaner that down-weights mislabeled training points so as to improve generalization on unseen data. Let  $\theta$  denote the data-cleaner parameters (producing per-example weights) and  $x$  the model parameters. We use a sigmoid parameterization for the weights,  $\omega_i(\theta) = (1 + \exp(-x\theta_i))^{-1}$ , ( $i = 1, \dots, N$ ), and constrain  $\|\theta\| \leq B$  to avoid exploding weights. The task is cast as the optimistic bilevel problem in the following:

$$\begin{aligned} \min_{\theta, x} \quad & -\frac{1}{M} \sum_{i=1}^M \log P(\ell_i^{\text{val}} | d_i^{\text{val}}; x) \\ \text{s.t.} \quad & \|\theta\| \leq B, \quad x \in \arg \min_{x' \in \mathbb{R}^{d_y}} \left[ -\frac{1}{N} \sum_{i=1}^N \omega_i(\theta) \log P(\ell_i^{\text{tr}} | d_i^{\text{tr}}; x') + \frac{\eta}{2} \|x'\|^2 \right]. \end{aligned} \quad (34)$$

**Setup.** We use MNIST with  $N = 5,000$  training,  $M = 50$  validation, and 10,000 test examples, and uniformly corrupt a fraction  $\rho \in \{0.4, 0.6, 0.8\}$  of the training labels. In practice, the corrupted/imprecise data are widely available, but clean/precise data are scarce. Thus we intentionally adopt a very small validation set. Much of the literature uses roughly equal training/validation splits, in which case the effect of the corruption rate in the uncleaned training data during training is often not apparent. We compare our

<sup>18</sup>A sample is *clean* if its label equals the true class; otherwise it is *corrupted*. In MNIST, we corrupt by flipping the label of a fraction  $p$  of training points uniformly to a different (incorrect) class.  $p$  is the pollute-rate.

zeroth-order method (Algorithm 2) against V-PBGD and G-PBGD [Shen et al., 2025], RHG [Franceschi et al., 2017], and IAPTT-GM [Liu et al., 2021b], using both a linear model and a two-layer MLP which are standard Neural network models in data hyper-cleaning tasks.

**Results.** Table 4 reports solution quality (test accuracy and F1 score<sup>19</sup>, averaged over 10 runs with 95% confidence intervals). Our zeroth-order method (see Algorithm 2) adapted to the optimistic formulation attains higher accuracy and F1-score in three different pollute-rates ( $p = 40\%, 60\%, 80\%$ ). Our method’s high performance stems from the *minima-selection* step: by choosing the iterate with the lowest validation loss along the trajectory, it produces higher-quality cleaner parameters  $\theta$ , yields better model parameters  $x$ , and ultimately improves generalization on the held-out test set.

Table 4: Data hyper-cleaning on MNIST across three noise phases (pollute rate  $p \in \{40, 60, 80\}\%$ ): test accuracy (%) and F1 score (%) over 10 runs ( $\pm 95\%$  CI). F1 reflects data-cleaner quality.

$p$	Method	Linear model		2-layer MLP	
		Test acc.	F1	Test acc.	F1
40	RHG	55.64 $\pm$ 0.15	26.5 $\pm$ 0.1	54.64 $\pm$ 0.19	16.5 $\pm$ 0.1
	IAPTT-GM	60.4 $\pm$ 0.12	42.3 $\pm$ 0.1	59.37 $\pm$ 0.15	26.5 $\pm$ 0.1
	G-PBGD	73.89 $\pm$ 0.13	50.9 $\pm$ 0.1	72.54 $\pm$ 0.12	65.8 $\pm$ 0.1
	V-PBGD	65.34 $\pm$ 0.13	53.2 $\pm$ 0.1	64.77 $\pm$ 0.1	55.2 $\pm$ 0.1
	<b>PSZO-MinSel</b>	<b>82.85 <math>\pm</math> 0.12</b>	<b>70.1 <math>\pm</math> 0.1</b>	<b>85.31 <math>\pm</math> 0.24</b>	<b>69.1 <math>\pm</math> 0.1</b>
60	RHG	51.24 $\pm$ 0.19	23.8 $\pm$ 0.1	52.94 $\pm$ 0.12	13.5 $\pm$ 0.1
	IAPTT-GM	59.52 $\pm$ 0.18	23.1 $\pm$ 0.1	58.72 $\pm$ 0.15	24.5 $\pm$ 0.1
	G-PBGD	64.56 $\pm$ 0.12	50.2 $\pm$ 0.1	62.65 $\pm$ 0.12	51.7 $\pm$ 0.1
	V-PBGD	63.14 $\pm$ 0.15	48.7 $\pm$ 0.1	62.63 $\pm$ 0.13	50.4 $\pm$ 0.1
	<b>PSZO-MinSel</b>	<b>79.50 <math>\pm</math> 0.18</b>	<b>55.2 <math>\pm</math> 0.1</b>	<b>80.70 <math>\pm</math> 0.18</b>	<b>55.9 <math>\pm</math> 0.1</b>
80	RHG	48.14 $\pm$ 0.12	21.5 $\pm$ 0.1	50.32 $\pm$ 0.14	11.9 $\pm$ 0.1
	IAPTT-GM	56.94 $\pm$ 0.14	18.1 $\pm$ 0.1	58.24 $\pm$ 0.16	17.9 $\pm$ 0.1
	G-PBGD	46.84 $\pm$ 0.12	28.9 $\pm$ 0.1	47.70 $\pm$ 0.14	27.3 $\pm$ 0.1
	V-PBGD	61.23 $\pm$ 0.12	33.5 $\pm$ 0.1	60.42 $\pm$ 0.13	34.9 $\pm$ 0.1
	<b>PSZO-MinSel</b>	<b>69.45 <math>\pm</math> 0.15</b>	<b>35.2 <math>\pm</math> 0.1</b>	<b>70.27 <math>\pm</math> 0.18</b>	<b>44.1 <math>\pm</math> 0.1</b>

## 7 Conclusion and Future Work

This work makes minima selection in bilevel optimization mathematically principled and algorithmically implementable. By working under the  $\mathbb{P}^{\mathcal{L}^\circ}$  condition and exploiting the manifold structure of the lower-level solution set, we introduced a dimension-aware viewpoint: the difficulty of BLO with minima selection is governed by the intrinsic dimension of the minimizer manifold, rather than the ambient dimension of the lower-level variable. The superquantile–Gibbs (SQ–G) relaxation makes this viewpoint concrete, turning minima selection into a controlled sampling-and-selection procedure. More broadly, our analysis shows

<sup>19</sup>F1-score is defined as follows: We take *clean* samples as the positive class and *corrupted* samples as the negative class. Each sample  $i$  is assigned a score  $s_i = \sigma(\theta_i)$ . We predict “clean” for the top  $(1 - p)$ -fraction by  $s_i$ . We compute Precision =  $\frac{TP}{TP+FP}$ , Recall =  $\frac{TP}{TP+FN}$ , where TP, FP, and FN denote true positives, false positives, and false negatives, respectively. The F1 score is the harmonic mean of Precision and Recall,  $F1 = \frac{2 \text{Precision} \cdot \text{Recall}}{\text{Precision} + \text{Recall}}$ . Note that this F1 measures the *cleaner’s* quality, not the classifier’s accuracy.

that minima selection need not be treated as a black box: geometry (via the structure of the minimizer manifold), stochastic approximation (via Gibbs measures), and risk-type functionals (via superquantiles) can be combined to design BLO methods that are both principled and systematically adjustable.

Looking ahead, several directions appear particularly promising. On the algorithmic side, a natural next step is to move from zeroth-order schemes to *hyper-gradient methods*, in which one first selects a point on the minimizer manifold (using ideas similar to the Gibbs-based selection studied here) to maximize<sup>20</sup> the upper-level objective, and then differentiates through this choice via implicit differentiation. In parallel, it is important to improve the efficiency of the Gibbs sampling oracle. Our current framework relies on a standard Langevin Monte Carlo implementation; geometry-aware Langevin samplers tailored to the identified manifold structure could sharpen the dependence on both the intrinsic dimension  $k$  and the ambient dimension  $d$ . Such developments would make the proposed PSZO-MinSel algorithm more practical for large-scale applications.

## References

- P. Ablin, G. Peyré, and T. Moreau. Super-efficiency of automatic differentiation for functions defined as a minimum. In *International Conference on Machine Learning*, pages 32–41. PMLR, 2020.
- M. Antoniou, A. Sinha, and G. Papa.  $\delta$ -perturbation of bilevel optimization problems: An error bound analysis. *Operations Research Perspectives*, 13:100315, 2024. doi: 10.1016/j.orp.2024.100315.
- M. Apaydin Ustun, L. Xu, B. Zeng, and X. Qian. Hyperparameter tuning through pessimistic bilevel optimization. *CoRR*, abs/2412.03666, 2024.
- M. Arbel and J. Mairal. Amortized implicit differentiation for stochastic bilevel optimization. *arXiv preprint arXiv:2111.14580*, 2021.
- M. Arbel and J. Mairal. Non-convex bilevel games with critical point selection maps. *Advances in Neural Information Processing Systems*, 35:8013–8026, 2022.
- Y. Beck, I. Ljubić, and M. Schmidt. A survey on bilevel optimization under uncertainty. *European Journal of Operational Research*, 311(2):401–426, 2023.
- I. Benchouk, L. O. Jolaoso, K. Nachi, and A. B. Zemkoho. Scholtes relaxation method for pessimistic bilevel optimization. *Set-Valued and Variational Analysis*, 33(2):10, 2025. doi: 10.1007/s11228-025-00747-5.
- L. Bertinetto, J. F. Henriques, P. H. Torr, and A. Vedaldi. Meta-learning with differentiable closed-form solvers. *arXiv preprint arXiv:1805.08136*, 2018.
- R. L. Bishop and R. J. Crittenden. *Geometry of Manifolds: Geometry of Manifolds*. Academic press, 2011.
- M. Blondel, Q. Berthet, M. Cuturi, R. Frostig, S. Hoyer, F. Llinares-López, F. Pedregosa, and J.-P. Vert. Efficient and modular implicit differentiation. *Advances in neural information processing systems*, 35: 5230–5242, 2022.
- J. Bolte, Q.-T. Le, E. Pauwels, and S. Vaiter. Bilevel gradient methods and morse parametric qualification. *arXiv preprint arXiv:2502.09074*, 2025.
- H. Chen, J. Li, and A. M.-C. So. Set smoothness unlocks clarke hyper-stationarity in bilevel optimization. *arXiv preprint arXiv:2506.04587*, 2025.

---

<sup>20</sup>For the optimistic formulation, one can also minimize the upper-level function over the lower-level solution manifold.

- L. Chen, J. Xu, and J. Zhang. On finding small hyper-gradients in bilevel optimization: Hardness results and improved analysis. In *The Thirty Seventh Annual Conference on Learning Theory*, pages 947–980. PMLR, 2024a.
- X. Chen, Y. Li, C. Fang, and T. Zhang. Optimal algorithms for stochastic bilevel optimization under minimal assumptions. *Journal of Machine Learning Research*, 25(206):1–64, 2024b.
- S. Chewi. *Log-concave Sampling*. 2024. Draft available at <https://chewisinho.github.io/>.
- T.-S. Chiang, C.-R. Hwang, and S. J. Sheu. Diffusion for global optimization in  $r^n$ . *SIAM Journal on Control and Optimization*, 25(3):737–753, 1987.
- F. H. Clarke. *Optimization and nonsmooth analysis*. SIAM, 1990.
- B. Colson, P. Marcotte, and G. Savard. An overview of bilevel optimization. *Annals of Operations Research*, 153(1):235–256, 2007.
- C. Criscitiello, Q. Rebjock, and N. Boumal. If a smooth function is globally PL and coercive, then it has a unique minimizer, 2025. URL [www.racetothetobottom.xyz/posts/PL-smooth-unique/](http://www.racetothetobottom.xyz/posts/PL-smooth-unique/).
- M. Dagr  ou, T. Moreau, S. Vaiter, and P. Ablin. A lower bound and a near-optimal algorithm for bilevel empirical risk minimization. In *Proceedings of the 27th International Conference on Artificial Intelligence and Statistics*, volume 238 of *Proceedings of Machine Learning Research*, pages 82–90, 2024.
- S. Dempe. *Foundations of Bilevel Programming*, volume 61 of *Nonconvex Optimization and Its Applications*. Springer, New York, 2002.
- S. Dempe and A. B. Zemkoho. On the karush–kuhn–tucker reformulation of the bilevel optimization problem. *Nonlinear Analysis: Theory, Methods & Applications*, 75(3):1202–1218, 2012. doi: 10.1016/j.na.2011.09.018.
- S. Dempe and A. B. Zemkoho, editors. *Bilevel Optimization: Advances and Next Challenges*, volume 161 of *Springer Optimization and Its Applications*. Springer, Cham, 2020.
- S. Dempe, J. Dutta, and B. Mordukhovich. New necessary optimality conditions in optimistic bilevel programming. *Optimization*, 56(5-6):577–604, 2007.
- S. Dempe, B. S. Mordukhovich, and A. B. Zemkoho. Necessary optimality conditions in pessimistic bilevel programming. *Optimization*, 63(4):505–533, 2014. doi: 10.1080/02331934.2012.696641.
- F. Draxler, K. Veschgini, M. Salmhofer, and F. Hamprecht. Essentially no barriers in neural network energy landscape. In *International conference on machine learning*, pages 1309–1318. PMLR, 2018.
- M. Feurer and F. Hutter. Hyperparameter optimization. *Automated machine learning: Methods, systems, challenges*, pages 3–33, 2019.
- L. Franceschi, M. Donini, P. Frasconi, and M. Pontil. Forward and reverse gradient-based hyperparameter optimization. In *International conference on machine learning*, pages 1165–1173. PMLR, 2017.
- T. Garipov, P. Izmailov, D. Podoprikin, D. P. Vetrov, and A. G. Wilson. Loss surfaces, mode connectivity, and fast ensembling of dnns. *Advances in neural information processing systems*, 31, 2018.
- S. Ghadimi and M. Wang. Approximation methods for bilevel programming. *arXiv preprint arXiv:1802.02246*, 2018.

- T. Giovannelli, G. D. Kent, and L. N. Vicente. Inexact bilevel stochastic gradient methods for constrained and unconstrained lower-level problems. *arXiv preprint arXiv:2110.00604*, 2023.
- A. A. Goldstein. Optimization of lipschitz continuous functions. *Mathematical Programming*, 13:14–22, 1977.
- Y. Gong, N. He, and Z. Shen. Poincare inequality for local log-polyak-lojasiewicz measures: Non-asymptotic analysis in low-temperature regime. *arXiv preprint arXiv:2501.00429*, 2024.
- A. Gray. The volume of a small geodesic ball of a Riemannian manifold. *Michigan Mathematical Journal*, 20(4):329–344, 1973. doi: 10.1307/mmj/1029001150. URL <https://projecteuclid.org/euclid.mmj/1029001150>.
- R. Grazi, L. Franceschi, M. Pontil, and S. Salzo. On the iteration complexity of hypergradient computation. In *Proceedings of the 37th International Conference on Machine Learning*, volume 119 of *Proceedings of Machine Learning Research*, pages 3748–3758. PMLR, 2020.
- M. Hasenpflug, D. Rudolf, and B. Sprungk. Wasserstein convergence rates of increasingly concentrating probability measures. *The Annals of Applied Probability*, 34(3):3320–3347, 2024.
- M. Hong, H.-T. Wai, Z. Wang, and Z. Yang. A two-timescale stochastic algorithm framework for bilevel optimization: Complexity analysis and application to actor-critic. *SIAM Journal on Optimization*, 33(1): 147–180, 2023.
- F. Huang. Optimal hessian/jacobian-free nonconvex-pl bilevel optimization. *arXiv preprint arXiv:2407.17823*, 2024.
- C.-R. Hwang. Laplace’s method revisited: weak convergence of probability measures. *The Annals of Probability*, pages 1177–1182, 1980.
- H. Jiang, Z. Chen, Y. Shi, B. Dai, and T. Zhao. Learning to defend by learning to attack. In *Proceedings of the 24th International Conference on Artificial Intelligence and Statistics (AISTATS)*, volume 130 of *Proceedings of Machine Learning Research*, pages 2616–2626, 2021.
- X. Jiang, J. Li, M. Hong, and S. Zhang. A correspondence-driven approach for bilevel decision-making with nonconvex lower-level problems. *CoRR*, abs/2509.01148, 2025.
- M. Jordan, G. Kornowski, T. Lin, O. Shamir, and M. Zampetakis. Deterministic nonsmooth nonconvex optimization. In *The Thirty Sixth Annual Conference on Learning Theory*, pages 4570–4597. PMLR, 2023.
- A. Juditsky and A. Nemirovski. Large deviations of vector-valued martingales and uniform confidence bounds in stochastic approximation problems. *Annals of Statistics*, 36(2):799–841, 2008. doi: 10.1214/009053607000000859.
- T. Kleinert, M. Labbé, F. Plein, and M. Schmidt. Technical note—there’s no free lunch: On the hardness of choosing a correct big-M in bilevel optimization. *Operations Research*, 68(6):1716–1721, 2020.
- G. Kornowski and O. Shamir. Oracle complexity in nonsmooth nonconvex optimization. *Advances in Neural Information Processing Systems*, 34:324–334, 2021.
- G. Kornowski, S. Padmanabhan, and O. Shamir. On the hardness of meaningful local guarantees in nonsmooth nonconvex optimization. *arXiv preprint arXiv:2409.10323*, 2024.

- R. Kuditipudi, X. Wang, H. Lee, Y. Zhang, Z. Li, W. Hu, R. Ge, and S. Arora. Explaining landscape connectivity of low-cost solutions for multilayer nets. *Advances in neural information processing systems*, 32, 2019.
- J. Kwon, D. Kwon, S. Wright, and R. Nowak. On penalty methods for nonconvex bilevel optimization and first-order stochastic approximation. *arXiv preprint arXiv:2309.01753*, 2023a.
- J. Kwon, D. Kwon, S. Wright, and R. D. Nowak. A fully first-order method for stochastic bilevel optimization. In *International Conference on Machine Learning*, pages 18083–18113. PMLR, 2023b.
- G. Lan, A. Nemirovski, and A. Shapiro. Validation analysis of mirror descent stochastic approximation method. *Mathematical Programming*, 134(2):425–458, 2012. doi: 10.1007/s10107-011-0442-6.
- J. M. Lee. *Riemannian manifolds: an introduction to curvature*, volume 176. Springer Science & Business Media, 2006.
- J. M. LEE. Introduction to smooth manifolds. 2024.
- J. Li, L. Zhu, and A. M.-C. So. Nonsmooth composite nonconvex-concave minimax optimization. In *OPT 2022: Optimization for Machine Learning (NeurIPS 2022 Workshop)*, 2022.
- S. Liang, R. Sun, Y. Li, and R. Srikant. Understanding the loss surface of neural networks for binary classification. In *International Conference on Machine Learning*, pages 2835–2843. PMLR, 2018.
- T. Lin, Z. Zheng, and M. Jordan. Gradient-free methods for deterministic and stochastic nonsmooth nonconvex optimization. *Advances in Neural Information Processing Systems*, 35:26160–26175, 2022.
- Z. Lin, P. Li, and L. Wu. Exploring neural network landscapes: Star-shaped and geodesic connectivity. *arXiv preprint arXiv:2404.06391*, 2024.
- B. Liu, M. Ye, S. Wright, P. Stone, and Q. Liu. Bome! bilevel optimization made easy: A simple first-order approach. *Advances in neural information processing systems*, 35:17248–17262, 2022.
- J. Liu, J. Lu, and Y. Gao. Pessimistic bilevel optimization: A survey. *International Journal of Computational Intelligence Systems*, 11(1):560–575, 2018. doi: 10.2991/ijcis.11.1.56.
- R. Liu, J. Gao, J. Zhang, D. Meng, and Z. Lin. Investigating bi-level optimization for learning and vision from a unified perspective: A survey and beyond. *IEEE Transactions on Pattern Analysis and Machine Intelligence*, 44(12):10045–10067, 2021a.
- R. Liu, Y. Liu, S. Zeng, and J. Zhang. Towards gradient-based bilevel optimization with non-convex followers and beyond. *Advances in Neural Information Processing Systems*, 34:8662–8675, 2021b.
- Y. Liu. The poincaré inequality and quadratic transportation-variance inequalities. 2020.
- Z. Liu, C. Chen, L. Luo, and B. K. H. Low. Zeroth-order methods for constrained nonconvex nonsmooth stochastic optimization. In *Forty-first International Conference on Machine Learning*, 2024.
- Z.-Q. Luo, J.-S. Pang, and D. Ralph. *Mathematical Programs with Equilibrium Constraints*. Cambridge University Press, Cambridge, 1996. doi: 10.1017/CBO9780511899003.
- A. S. Nemirovskij and D. B. Yudin. Problem complexity and method efficiency in optimization. 1983.
- Y. Nesterov and V. Spokoiny. Random gradient-free minimization of convex functions. *Foundations of Computational Mathematics*, 17(2):527–566, 2017. doi: 10.1007/s10208-015-9296-2.

- Q. Nguyen. On connected sublevel sets in deep learning. In *International conference on machine learning*, pages 4790–4799. PMLR, 2019.
- F. Pedregosa. Hyperparameter optimization with approximate gradient. In *Proceedings of the 33rd International Conference on Machine Learning*, volume 48 of *Proceedings of Machine Learning Research*, pages 737–746, 2016.
- P. Petersen. Riemannian geometry. *Graduate Texts in Mathematics/Springer-Verlag*, 2006.
- Q. Rebjock and N. Boumal. Fast convergence to non-isolated minima: four equivalent conditions for c2 functions. *arXiv preprint arXiv:2303.00096*, 2023.
- R. T. Rockafellar, S. Uryasev, et al. Optimization of conditional value-at-risk. *Journal of risk*, 2:21–42, 2000.
- L. Sagun, U. Evci, V. U. Guney, Y. Dauphin, and L. Bottou. Empirical analysis of the hessian of over-parametrized neural networks. *arXiv preprint arXiv:1706.04454*, 2017.
- A. Shaban, C.-A. Cheng, N. Hatch, and B. Boots. Truncated back-propagation for bilevel optimization. In *The 22nd international conference on artificial intelligence and statistics*, pages 1723–1732. PMLR, 2019.
- H. Shen, Q. Xiao, and T. Chen. On penalty-based bilevel gradient descent method. *Mathematical Programming*, 2025. doi: 10.1007/s10107-025-02194-4. URL <https://doi.org/10.1007/s10107-025-02194-4>.
- L. Tian, K. Zhou, and A. M.-C. So. On the finite-time complexity and practical computation of approximate stationarity concepts of lipschitz functions. In *International Conference on Machine Learning*, pages 21360–21379. PMLR, 2022.
- L. Venturi, A. S. Bandeira, and J. Bruna. Spurious valleys in two-layer neural network optimization landscapes. *arXiv preprint arXiv:1802.06384*, 2018.
- L. N. Vicente and P. H. Calamai. Bilevel and multilevel programming: A bibliography review. *Journal of Global Optimization*, 5(3):291–306, 1994. doi: 10.1007/BF01096458.
- W. Wiesemann, A. Tsoukalas, P. Kleniati, and B. Rustem. Pessimistic bilevel optimization. *SIAM Journal on Optimization*, 23(1):353–380, 2013. doi: 10.1137/120864015.
- Q. Xiao, S. Lu, and T. Chen. A generalized alternating method for bilevel optimization under the polyak-lojasiewicz condition. *arXiv preprint arXiv:2306.02422*, 2023.
- M. Xu and J. J. Ye. A smoothing augmented lagrangian method for solving simple bilevel programs. *Computational Optimization and Applications*, 59:353–377, 2014.
- J. Yang, K. Ji, and Y. Liang. Provably faster algorithms for bilevel optimization. In *Advances in Neural Information Processing Systems*, volume 34, pages 20719–20731, 2021.
- Y. Yang, P. Xiao, and K. Ji. Achieving  $\mathcal{O}(\varepsilon^{-1.5})$  complexity in hessian/jacobian-free stochastic bilevel optimization. In *Advances in Neural Information Processing Systems*, volume 36, pages 73138–73151, 2023.
- J. Ye, D. Zhu, and Q. J. Zhu. Exact penalization and necessary optimality conditions for generalized bilevel programming problems. *SIAM Journal on optimization*, 7(2):481–507, 1997.

- J. J. Ye and X. Ye. Necessary optimality conditions for optimization problems with variational inequality constraints. *Mathematics of Operations Research*, 22(4):977–997, 1997.
- J. J. Ye and D. Zhu. Optimality conditions for bilevel programming problems. *Optimization*, 33(1):9–27, 1995. doi: 10.1080/02331939508844060.
- J. J. Ye and D. Zhu. New necessary optimality conditions for bilevel programs by combining the MPEC and value function approaches. *SIAM Journal on Optimization*, 20(4):1885–1905, 2010. doi: 10.1137/080725088.
- A. B. Zemkoho and S. Zhou. Theoretical and numerical comparison of the karush–kuhn–tucker and value function reformulations in bilevel optimization. *Computational Optimization and Applications*, 78(2): 625–674, 2021. doi: 10.1007/s10589-020-00250-7.
- S. Zeng and J. J. Ye. A practical scheme to compute the pessimistic bilevel optimization problem. *SIAM Journal on Optimization*, 30(3):2100–2127, 2020.
- J. Zhang, H. Lin, S. Jegelka, S. Sra, and A. Jadbabaie. Complexity of finding stationary points of nonconvex nonsmooth functions. In *International Conference on Machine Learning*, pages 11173–11182. PMLR, 2020.

## A Definitions and technical lemmas

This appendix collects the background components used throughout the paper. We recall the Riemannian notions (distance, second fundamental form, injectivity radius, curvature) needed for the geometric arguments in Section 3. Next, we briefly explain why our standing assumptions imply the technical conditions required to apply [Hasenpflug et al., 2024, Theorem 3.6] in the discussion of Gibbs-measure convergence.

**Additional notations.** We use the notation  $(\cdot)_+$  to denote the positive part of a scalar or vector, defined as  $(\cdot)_+ := \max\{\cdot, 0\}$ .

### A.1 Riemannian notions

In this subsection we fix notation for basic Riemannian objects and record definitions that will be used repeatedly in later proofs. Any compact manifold  $\mathcal{S}$  of class  $\mathcal{C}^3$  (indeed  $\mathcal{C}^1$ ) without boundary admits a Riemannian metric.<sup>21</sup> Given a Riemannian metric  $g$  on  $\mathcal{S}$ , define

$$\text{dist}_g(p, q) := \inf\{\ell(\Gamma) : \Gamma \text{ is a piecewise smooth path in } \mathcal{S} \text{ between } p \text{ and } q.\}. \quad (35)$$

By compactness of  $\mathcal{S}$ , there exists at least one minimizing path  $\Gamma^*$ .

**Definition A.1** (Second fundamental form). *Let  $\mathcal{S} \subset \mathbb{R}^d$  be a  $\mathcal{C}^2$  embedded submanifold endowed with the Riemannian metric induced by the Euclidean inner product. For each  $x \in \mathcal{S}$ , let  $T_x\mathcal{S}$  and  $T_x\mathcal{S}^\perp$  denote the tangent space and its orthogonal complement, respectively. The second fundamental form of  $\mathcal{S}$  at  $x$  is the bilinear map*

$$\mathbb{I}_{\mathcal{S}}(x) : T_x\mathcal{S} \times T_x\mathcal{S} \rightarrow T_x\mathcal{S}^\perp, \quad \mathbb{I}_{\mathcal{S}}(x)[u, v] := (\nabla_u^{\mathbb{R}^d} v)^\perp,$$

where  $\nabla^{\mathbb{R}^d}$  is the Euclidean (Levi–Civita) connection, i.e., the usual directional derivative on  $\mathbb{R}^d$ : for a smooth vector field  $v$  defined near  $x$ ,  $\nabla_u^{\mathbb{R}^d} v = Dv(x)[u]$ , and  $(\cdot)^\perp$  denotes orthogonal projection onto  $T_x\mathcal{S}^\perp$ .

<sup>21</sup>A fundamental theorem in differential geometry states that every paracompact manifold  $M$  of class  $\mathcal{C}^k$  with  $k \geq 1$  can be endowed with a Riemannian metric.

We measure its size by the operator norm

$$\|\mathbb{I}_{\mathcal{S}}(x)\|_{\text{op}} := \sup\{\|\mathbb{I}_{\mathcal{S}}(x)[u, u]\| : u \in T_x\mathcal{S}, \|u\| = 1\},$$

where  $\|\cdot\|_{\text{op}}$  denotes the operator norm induced by the Euclidean norm  $\|\cdot\|$ . This quantity coincides with the maximal normal curvature of  $\mathcal{S}$  at  $x$ . In particular, if  $\gamma$  is a unit-speed geodesic in  $\mathcal{S}$ , then

$$\|\ddot{\gamma}(t)\| = \|\mathbb{I}_{\mathcal{S}}(\gamma(t))[\dot{\gamma}(t), \dot{\gamma}(t)]\| \leq \|\mathbb{I}_{\mathcal{S}}(\gamma(t))\|_{\text{op}}.$$

Assumption 2.7 requires that, for each  $\theta \in \Theta$ , the second fundamental form  $\mathbb{I}_{\mathcal{S}(\theta)}$  is uniformly bounded in this sense, with a constant  $C > 0$  independent of  $\theta$ . For further background, see also [Gong et al., 2024, Appendix D].

**Definition A.2** (Injectivity radius). *Injectivity radius at a point  $p \in \mathcal{S}$  is defined as*

$$\text{inj}(p) = \sup\{r > 0 \mid \exp_p: \mathbb{B}_{d-k}(p; r) \subset T_p\mathcal{S} \rightarrow \mathbb{B}_{\mathbf{g}}(p; r) \subset \mathcal{S} \text{ is a diffeomorphism}\},$$

where  $\mathbb{B}_{d-k}(p; r) \subset T_p\mathcal{S}$  is the open ball of radius  $r$  in the tangent space at  $p$ ,  $\exp_p$  is the Riemannian exponential map at  $p$ ,  $\mathbb{B}_{\mathbf{g}}(p; r) \subset \mathcal{S}$  is the geodesic ball of radius  $r$  in  $\mathcal{S}$ . Equivalently,  $\text{inj}(p)$  is the distance from  $p$  to the first place where the exponential map fails to be one-to-one. The injectivity radius of the whole manifold is the infimum of the pointwise injectivity radii:

$$\text{inj}(\mathcal{S}) = \inf_{p \in \mathcal{S}} \text{inj}(p).$$

In words,  $\text{inj}(\mathcal{S})$  is the largest radius  $r$  such that every point in  $\mathcal{S}$  has a geodesic ball of radius  $r$  on which the exponential map at that point is a diffeomorphism.

**Definition A.3** (Sectional Curvature). *In a Riemannian manifold  $(\mathcal{S}, \mathbf{g})$ , the sectional curvature measures how curved the manifold is in each two-dimensional “slice” (or “plane”) of the tangent space at a point. Concretely 1) Pick a point  $p \in \mathcal{S}$ . 2) Pick a 2-dimensional subspace  $A_p \subset T_p\mathcal{S}$ . (In other words,  $A_p$  is a plane in the tangent space at  $p$ .) The sectional curvature  $K(p, A_p)$  is defined using the Riemann curvature tensor<sup>22</sup>  $R$ . If  $X$  and  $Y$  are any two linearly independent vectors spanning  $A_p$ , then*

$$K(p, A_p) = \frac{\mathbf{g}(R(X, Y)Y, X)}{\mathbf{g}(X, X)\mathbf{g}(Y, Y) - \mathbf{g}(X, Y)^2}.$$

Equivalently, if you choose an orthonormal basis  $\{e_1, e_2\}$  of  $A_p$  with respect to  $\mathbf{g}$  (so  $\mathbf{g}(e_i, e_j) = \delta_{ij}$ ), then the denominator becomes 1, and one obtains the simpler formula

$$K(p, A_p) = \mathbf{g}(R(e_1, e_2)e_2, e_1).$$

## A.2 Discussion on the validity of assumptions in [Hasenpflug et al., 2024, Theorem 3.6]

The assumptions required by Hasenpflug et al. [2024, Theorem 3.6] follow from our standing conditions. First, their *positive definiteness* requirement for  $g(\theta, \cdot)$  holds because the  $\mathbb{P}\mathbb{E}^\circ$  condition implies that  $g(\theta, \cdot)$  is locally Morse–Bott [Rejcek and Boumal, 2023, Section 2.3], and hence the Hessian of  $g$  is positive definite in directions normal to the minimizer manifold  $\mathcal{S}(\theta)$ . Second, their *tail condition* [Hasenpflug et al., 2024, Assumption 3.1] is ensured by our coercivity assumption on  $g$ .

Finally, Propositions 2.3 and 2.5 verify the geometric conditions in [Hasenpflug et al., 2024, Assumption 2.2] (smooth, boundaryless, and connected minimizer manifolds). It is worth noting that the orientability of the manifold is not necessary in our setting. We define the volume measure  $\mathcal{M}$  in a coordinate-free manner based on the Riemannian metric  $g_{\mathcal{S}}$ . Orientability, a stronger condition, ensures the existence of a global top-form rather than just a density, which is not required in our framework.

<sup>22</sup>In a Riemannian manifold  $(\mathcal{S}, \mathbf{g})$  with Levi-Civita connection  $\nabla$ , the Riemann curvature tensor is a  $(1, 3)$ -tensor  $R$  that measures how much the covariant derivative  $\nabla$  fails to commute.

## B Proofs of results in Section 3

This appendix contains deferred proofs for results in Section 3 concerning the structure and regularity of the minimizer sets  $\{\mathcal{S}(\theta)\}_{\theta \in \Theta}$ .

### B.1 Proof of Lemma 3.3

*Proof.* Consider the decreasing sublevel sets  $E_\varepsilon := \{x : g(\theta, x) - g_\star \leq \varepsilon\}$ ; if none is contained in  $\mathcal{U}(\theta)$ , compactness yields a limit point in  $\mathcal{S}(\theta) \cap (\mathbb{R}^d \setminus \mathcal{U}(\theta))$ , a contradiction.

We provide a detailed proof here. Fix  $\theta$  and write  $g(x) := g(\theta, x)$ ,  $g_\star := \min_z g(z)$ , and  $\mathcal{S} := \arg \min_z g(z)$ . Let  $\mathcal{U} = \mathcal{U}(\theta)$  be the neighborhood in (9). Consider the nested sublevel sets

$$E_j := \{x : g(x) \leq g_\star + 1/j\}, \quad j \in \mathbb{N}.$$

By continuity of  $g$ , each  $E_j$  is closed and  $E_{j+1} \subseteq E_j$ , and clearly  $\bigcap_{j \geq 1} E_j = \mathcal{S}$ .

By coercivity of  $g$  (from Assumption 2.8),  $E_1$  is compact, hence the family  $\{E_j\}$  is a nested sequence of nonempty compact sets. If the claim were false, then for every  $j$  we could pick  $x_j \in E_j \setminus \mathcal{U}$ . By compactness of  $E_1$ , there exists a subsequence  $x_{j_k} \rightarrow \bar{x} \in E_1$ . Since the sets are nested,  $\bar{x} \in E_\ell$  for every fixed  $\ell$ , so  $\bar{x} \in \bigcap_\ell E_\ell = \mathcal{S}$ . On the other hand,  $\mathbb{R}^d \setminus \mathcal{U}$  is closed, hence  $\bar{x} \notin \mathcal{U}$ , contradicting  $\mathcal{S} \subset \mathcal{U}$ .

Therefore, there exists  $j_0$  such that  $E_{j_0} \subset \mathcal{U}$ . Setting  $\tilde{\varepsilon} := 1/j_0$  yields  $\{x : g(x) - g_\star \leq \tilde{\varepsilon}\} \subset \mathcal{U}$ , as claimed.  $\square$

### B.2 Proof of Corollary 3.4

The following lemma formalizes a simple but useful observation: if a map is  $L_G$ -Lipschitz on every pair of points that are sufficiently close (i.e., within a fixed radius  $r$ ), then the same Lipschitz constant extends globally. This will be used in the proof of Corollary 3.4.

**Lemma B.1.** *For a given  $r > 0$ , if  $G : \mathbb{R}^{d_1} \rightarrow \mathbb{R}^{d_2}$  is a functional that satisfies  $\|G(x) - G(y)\| \leq L_G \|x - y\|$  for  $x, y \in \mathbb{R}^{d_1}$  with  $\|x - y\| \leq r$ , then  $G$  satisfies  $L_G$ -Lipschitzness over  $\mathbb{R}^{d_1}$ .*

*Proof.* We aim to show that  $\|G(x) - G(y)\| \leq L_G \|x - y\|$  for all  $x, y \in \mathbb{R}^{d_1}$ . If  $\|x - y\| \leq r$ , our proof is complete. Assume  $\|x - y\| = R$  where  $R > r$ . Define  $z_t = (1 - t) \cdot x + t \cdot y$  for  $t \in [0, 1]$ . Let  $w_k := z_{k/(2R/r)}$  for  $k = [1 : 2R/r]$ . Notice that  $\|w_k - w_{k-1}\| = \|x - y\|/2R/r \leq r/2$ . Then

$$\begin{aligned} \|G(x) - G(y)\| &= \left\| \sum_{k=1}^{2R/r} G(w_k) - G(w_{k-1}) \right\| \leq \sum_{k=1}^{2R/r} \|G(w_k) - G(w_{k-1})\| \\ &\leq L_G \sum_{k=1}^{2R/r} \|z_k - z_{k-1}\| = L_G \sum_{k=1}^{2R/r} \frac{k}{2R/r} \cdot \|x - y\| = L_G \|x - y\|. \end{aligned} \quad (36)$$

$\square$

For completeness, we provide a proof of Corollary 3.4:

*Proof.* For any  $\theta_1, \theta_2 \in \Theta$  satisfying  $\|\theta_1 - \theta_2\| \leq \delta$  with  $\delta \leq \tilde{\varepsilon}/(2L_{g,1}(D))$  (where  $\tilde{\varepsilon}$  is defined in Lemma 3.3), we obtain the bound:

$$\text{dist}(\mathcal{S}(\theta_1), \mathcal{S}(\theta_2)) \leq \frac{L_{g,2}}{\mu} \|\theta_1 - \theta_2\|.$$

Selecting  $x_1 \in \arg \max_{x \in \mathcal{S}(\theta_1)} f(\theta_1, x)$  and  $x_2 \in \arg \min_{y \in \mathcal{S}(\theta_2)} \text{dist}(y, x_1)$ , we derive

$$\begin{aligned}
F_{\max}(\theta_1) - F_{\max}(\theta_2) &= f(\theta_1, x_1) - F_{\max}(\theta_2) \leq f(\theta_1, x_1) - f(\theta_2, x_2) \\
&\leq |f(\theta_1, x_1) - f(\theta_2, x_1)| + |f(\theta_2, x_1) - f(\theta_2, x_2)| \\
&\stackrel{(a)}{\leq} L_{f,1} \|\theta_1 - \theta_2\| + L_{f,1} \|x_1 - x_2\| \\
&\stackrel{(b)}{\leq} L_{f,1} \|\theta_1 - \theta_2\| + L_{f,1} \text{dist}(\mathcal{S}(\theta_1), \mathcal{S}(\theta_2)) \\
&\stackrel{(c)}{\leq} L_{f,1} \|\theta_1 - \theta_2\| + L_{f,1} \cdot \frac{L_{g,2}}{\mu} \cdot \|\theta_1 - \theta_2\|. \tag{37}
\end{aligned}$$

Step (a) follows from  $L_{f,1}$ -Lipschitzness of  $f$ . Step (b) follows from

$$\|x_1 - x_2\| = \text{dist}(x_1, \mathcal{S}(\theta_2)) \leq \max_{x \in \mathcal{S}(\theta_1)} \text{dist}(x, \mathcal{S}(\theta_2)) \leq \text{dist}(\mathcal{S}(\theta_1), \mathcal{S}(\theta_2)).$$

Step (c) follows from Lemma 3.2 under the condition  $\delta \leq \tilde{\epsilon}/(2L_{g,1}(\text{D}))$ .

A similar argument shows that  $F_{\max}(\theta_2) - F_{\max}(\theta_1) \leq (L_{f,1} + L_{f,1} \cdot \frac{L_{g,2}}{\mu}) \|\theta_1 - \theta_2\|$ . Thus, for all  $\theta_1, \theta_2 \in \Theta$  with  $\|\theta_1 - \theta_2\| \leq \delta$ ,

$$|F_{\max}(\theta_1) - F_{\max}(\theta_2)| \leq \left( L_{f,1} + L_{f,1} \frac{L_{g,2}}{\mu} \right) \cdot \|\theta_1 - \theta_2\|.$$

In other words,  $F_{\max}$  is *locally* Lipschitz on  $\Theta$  with the same Lipschitz constant and a radius  $\delta$  that do not depend on the base point  $\theta$ . As explained in Lemma B.1, such a uniform local Lipschitz property on  $\Theta$  implies that  $F_{\max}$  is globally (uniformly) Lipschitz on  $\Theta$  with the same constant, which proves the claim.  $\square$

### B.3 Proof of Lemma 3.5

This subsection proves that all minimizer manifolds  $\mathcal{S}(\theta)$  share a common intrinsic dimension. The key step is to show that the Hessian rank (equivalently, the normal-space dimension) cannot change under small perturbations of  $\theta$ , and hence is constant on  $\Theta$ . We provide the proof of Lemma 3.5 in the following.

*Proof.* Fix  $\theta \in \Theta$ . By [Rebjoek and Boumal, 2023, Corollary 2.13] and the path-connectedness of  $\mathcal{S}(\theta)$ , the rank of  $\partial_x^2 g(\theta, x)$  is constant over  $x \in \mathcal{S}(\theta)$ . Denote it by

$$r(\theta) := \text{rank}(\partial_x^2 g(\theta, x)), \quad x \in \mathcal{S}(\theta),$$

so that  $\kappa(\theta) = d - r(\theta)$ .

We show that  $r(\theta)$  is constant on  $\Theta$  by contradiction. Suppose not. Then there exist  $\theta_n \rightarrow \bar{\theta}$  with  $r(\theta_n) \neq r(\bar{\theta})$ . Pick  $x_n \in \mathcal{S}(\theta_n)$ . By the Lipschitz continuity of the solution mapping (Lemma 3.2), there exists  $\bar{x} \in \mathcal{S}(\bar{\theta})$  such that  $\|x_n - \bar{x}\| \rightarrow 0$ . Since  $\partial_x^2 g$  is continuous in  $(\theta, x)$  (Assumption 2.8),

$$\|\partial_x^2 g(\theta_n, x_n) - \partial_x^2 g(\bar{\theta}, \bar{x})\| \rightarrow 0.$$

Moreover,  $\text{PL}^\circ$  implies a local Morse–Bott structure for  $g(\theta, \cdot)$  [Rebjoek and Boumal, 2023, Corollary 2.13], hence the nonzero eigenvalues of  $\partial_x^2 g(\bar{\theta}, x)$  are bounded away from 0 uniformly for  $x$  near  $\mathcal{S}(\bar{\theta})$ . Therefore, for  $n$  large enough, the perturbation above cannot change the number of nonzero eigenvalues, and thus

$$\text{rank}(\partial_x^2 g(\theta_n, x_n)) = \text{rank}(\partial_x^2 g(\bar{\theta}, \bar{x})) = r(\bar{\theta}).$$

Since the rank is constant on each  $\mathcal{S}(\theta_n)$ , the left-hand side equals  $r(\theta_n)$ , contradicting  $r(\theta_n) \neq r(\bar{\theta})$ . Hence  $r(\theta)$  is constant on  $\Theta$ , and so is  $\kappa(\theta) = d - r(\theta)$ .  $\square$

## B.4 Proof of Proposition 3.6

Using the Lipschitz continuity of the solution mapping established in Lemma 3.2, we first show that the family of sets  $\{\mathcal{S}(\theta)\}_{\theta \in \Theta}$  is uniformly bounded.<sup>23</sup> This lemma will be used in the proof of Property 2 in Proposition 3.6 and in the proof of Proposition 3.7.

**Lemma B.2.** *A collection of sets  $\{\mathcal{A}(\theta)\}_{\theta \in \Theta}$  is uniformly bounded if  $\mathcal{A}(\theta)$  is a compact and non-empty set for every  $\theta \in \Theta$ ,  $\Theta$  is a compact set, and  $\mathcal{A}(\theta)$  is continuous in Hausdorff distance.*

*Proof.* We aim to show that  $\sup_{\theta \in \Theta} \sup_{x \in \mathcal{A}(\theta)} \|x\|$  is finite. Let define  $M(\theta) := \sup_{x \in \mathcal{A}(\theta)} \|x\|$ . Since  $\mathcal{A}(\theta)$  is compact and non-empty,  $M(\theta)$  is finite for each  $\theta \in \Theta$ . We will show that  $M(\theta)$  is continuous and since  $\Theta$  is compact,  $M(\theta)$  attains its maximum value on  $\Theta$ .

The mapping  $\theta \mapsto \mathcal{A}(\theta)$  is continuous in the Hausdorff metric. Hence given  $\|\theta_1 - \theta_2\| \leq \delta$ , for any  $x \in \mathcal{A}(\theta_2)$ , there exists  $y \in \mathcal{A}(\theta_1)$  such that  $\|x - y\| < \epsilon$ . Then

$$\|x\| = \|y + (x - y)\| \leq \|y\| + \|x - y\| < \|y\| + \epsilon.$$

Taking the supremum over all  $y \in \mathcal{A}(\theta_1)$ :

$$\|x\| < M(\theta_1) + \epsilon.$$

Since this holds for all  $x \in \mathcal{A}(\theta_2)$ , we have:

$$M(\theta_2) = \sup_{x \in \mathcal{A}(\theta_2)} \|x\| \leq M(\theta_1) + \epsilon.$$

By similar argument,  $M(\theta_1) \leq M(\theta_2) + \epsilon$ . Then

$$|M(\theta_2) - M(\theta_1)| \leq \epsilon.$$

□

We then provide a proof for Proposition 3.6 in the following:

*Proof. Property 1.* Since we know that  $g(\theta, \cdot)$  is coercive, it follows that for each  $\theta \in \Theta$ , the diameter of  $\mathcal{S}(\theta)$  is finite. We aim to prove that  $\sup_{\theta \in \Theta} \text{diam}(\mathcal{S}(\theta))$  is also bounded. Given Assumption 2.6, from Lemma 3.2, we deduce that  $\mathcal{S}(\theta)$  is continuous with respect to  $\theta$  in the Hausdorff distance. Using this property, we will further establish that the diameter of  $\mathcal{S}(\theta)$  is a continuous function of  $\theta$ . We aim to show that for every  $\epsilon > 0$ , there exists  $\delta \in \mathbb{R}_+^m$  such that  $|\text{diam}(\mathcal{S}(\theta + \delta)) - \text{diam}(\mathcal{S}(\theta))| \leq \epsilon$ .

For a given pair  $(x, y) \in \mathcal{S}(\theta) \times \mathcal{S}(\theta)$ , we define their projections onto  $\mathcal{S}(\theta + \delta)$  as  $(\tilde{x}, \tilde{y})$ , where  $\tilde{x}$  is a projection of  $x$  onto  $\mathcal{S}(\theta + \delta)$  and  $\tilde{y}$  is a projection of  $y$  onto  $\mathcal{S}(\theta + \delta)$ . The difference in diameters between  $\mathcal{S}(\theta)$  and  $\mathcal{S}(\theta + \delta)$  can be expressed as:

$$\begin{aligned} \text{diam}(\mathcal{S}(\theta)) - \text{diam}(\mathcal{S}(\theta + \delta)) &= \sup_{x, y \in \mathcal{S}(\theta)} \|x - y\| - \sup_{x', y' \in \mathcal{S}(\theta + \delta)} \|x' - y'\| \\ &\stackrel{(a)}{\leq} \sup_{x, y \in \mathcal{S}(\theta)} \{\|x - y\| - \|\tilde{x} - \tilde{y}\|\} \\ &\stackrel{(b)}{\leq} \sup_{x, y \in \mathcal{S}(\theta)} \{\|x - \tilde{x}\| + \|\tilde{y} - y\|\} \end{aligned}$$

<sup>23</sup>A collection of sets  $\{\mathcal{B}(\theta)\}_{\theta \in \Theta}$  is uniformly bounded if there exists a ball  $\mathbb{B}_d(0; R) \subset \mathbb{R}^d$  such that  $\mathcal{B}(\theta) \subset \mathbb{B}_d(0; R)$  for all  $\theta \in \Theta$ .

$$\leq \sup_{x,y \in \mathcal{S}(\theta)} \text{dist}(\mathcal{S}(\theta), \mathcal{S}(\theta + \delta)) \leq \epsilon, \quad (38)$$

where (a) comes from  $(\tilde{x}, \tilde{y}) \in \mathcal{S}(\theta + \delta) \times \mathcal{S}(\theta + \delta)$ . (b) follows by  $\|x - y\| - \|\tilde{x} - \tilde{y}\| \leq \|x - y - \tilde{x} + \tilde{y}\| \leq \|x - \tilde{x}\| + \|\tilde{y} - y\|$ . The last inequality holds based on the continuity of the solution sets in Hausdorff distance with respect to  $\theta$ , i.e., there exist  $\delta \in \mathbb{R}_+^m$  such that  $\text{dist}(\mathcal{S}(\theta + \delta), \mathcal{S}(\theta)) \leq \epsilon$ .

Similarly, for the reverse case, we have

$$\text{diam}(\mathcal{S}(\theta + \delta)) - \text{diam}(\mathcal{S}(\theta)) \leq \epsilon$$

Therefore, for every  $\epsilon > 0$  there exists  $\delta \in \mathbb{R}_+^m$  such that

$$|\text{diam}(\mathcal{S}(\theta + \delta)) - \text{diam}(\mathcal{S}(\theta))| \leq \epsilon.$$

According to Weierstrass's extreme value theorem, for the continuous function  $\text{diam}(\mathcal{S}(\theta))$ , there exists a  $\theta_0 \in \Theta$  such that  $\text{diam}(\mathcal{S}(\theta_0))$  equals the supremum of  $\text{diam}(\mathcal{S}(\theta))$  over all  $\theta \in \Theta$ . We denote  $\text{diam}(\mathcal{S}(\theta_0))$  by  $D$ .

**Property 2.** We will show that there exists a constant  $C_0 > 0$  such that  $|\text{Sec}(\mathcal{S}(\theta))| \leq C_0$  for all  $\theta \in \Theta$ . In general, for every  $\theta \in \Theta$ , the sectional curvature of a compact manifold is bounded both above and below as stated in the following result.

**Lemma B.3** ([Bishop and Crittenden, 2011], Section 9.3). *If  $\mathcal{M}$  is a compact Riemannian manifold, then there exist  $k, K \in \mathbb{R}$  such that for any plane section  $A_p$  at any point  $p \in \mathcal{M}$ ,  $k \leq K(A_p) \leq K$ .*

For any fixed  $\theta \in \Theta$ , the manifold  $\mathcal{S}(\theta)$  is a compact, boundaryless  $C^2$  submanifold (by Proposition 2.5). As a consequence of general Riemannian geometry (see Lemma B.3), the sectional curvature  $\text{Sec}(\mathcal{S}(\theta))$  is bounded on  $\mathcal{S}(\theta)$ . The sectional curvature  $K_{\mathcal{S}(\theta)}(x, A_x)$  is a continuous function of both the position  $x \in \mathcal{S}(\theta)$  and the upper-level parameter  $\theta \in \Theta$ . This continuity holds because the manifold metrics, coordinate functions, and tangent spaces depend continuously and smoothly on  $\theta$  (stemming from the regularity assumptions on  $g$  in Definition 2.2).

Since the parameter domain  $\Theta$  is compact, the entire collection of manifolds  $\{\mathcal{S}(\theta)\}_{\theta \in \Theta}$  is uniformly bounded (Lemma B.2) and varies continuously, implying that the space of all possible geometric configurations (i.e., all points  $x$  and all planes  $A_x$ ) forms a compact set in the corresponding product space  $\Theta \times \mathcal{S}(\theta)$ . By the Weierstrass Extreme Value Theorem, a continuous function on a compact set attains its maximum. Therefore, the absolute value of the sectional curvature attains a global maximum,  $C_0$ , establishing the uniform bound  $|\text{Sec}(\mathcal{S}(\theta))| \leq C_0$  for every  $\theta \in \Theta$ .

**Property 3.** Given the boundaryless and compactness properties of  $\mathcal{S}$  as well as the  $C^2$  property (see Proposition 2.3), we can apply the following result to establish Property 3.

**Proposition B.4** ([Petersen, 2006], Lemma 6.4.7). *Let  $\mathcal{S}$  be a compact, boundaryless Riemannian manifold of dimension  $k$  with a  $C^2$  metric. Then if  $\text{Sec}(\mathcal{S}) \leq C_0$  for  $C_0 > 0$ ,*

$$\text{inj}(\mathcal{S}) \geq \min \left\{ \frac{\pi}{C_0}, \frac{1}{2} \ell(\mathcal{S}) \right\},$$

where  $\ell(\mathcal{S})$  is the infimum of lengths of closed geodesics in  $\mathcal{S}$ .

In order to give a lower bound on  $\ell(\mathcal{S})$ , we know that for any unit-speed closed geodesic  $\gamma \in \mathcal{S}$ , the extrinsic curvature of  $\gamma$  is given by  $|g(\dot{\gamma}, \dot{\gamma})| \leq C$  where  $C$  is the uniform bound on second fundamental form in Assumption 2.7, then

$$\ell(\gamma) \geq \frac{2\pi}{C}.$$

Thus  $\ell(\mathcal{S}) \geq \frac{2\pi}{C}$ .

From Property 2, we have  $|\text{Sec}(\mathcal{S}(\theta))| \leq C_0$  for every  $\theta \in \Theta$ . Additionally, since  $C$  uniformly bounds the second fundamental form of  $\{\mathcal{S}(\theta)\}_{\theta \in \Theta}$ , the injectivity radius satisfies  $\text{inj}(\mathcal{S}(\theta)) \geq \min\left\{\frac{\pi}{C_0}, \frac{\pi}{C}\right\}$ .  $\square$

### B.5 Proof of Proposition 3.7

To establish the uniform bounds on the limiting density  $\rho_\theta$  in (7), it is necessary to control the  $\theta$ -dependent normalizing factor, which involves the Riemannian volume  $\mathcal{M}(\mathcal{S}(\theta))$ . We therefore first show that the volumes of the minimizer manifolds are uniformly bounded away from 0 and  $\infty$  over  $\theta \in \Theta$ .

**Lemma B.5.** *Under Assumption 2.6, there exists a constant  $0 < b < 1$  such that*

$$b \leq \mathcal{M}(\mathcal{S}(\theta)) \leq b^{-1}, \quad \forall \theta \in \Theta,$$

where  $\mathcal{M}$  denotes the Riemannian volume measure on  $(\mathcal{S}(\theta), g)$ .

*Proof.* For each fixed  $\theta$ ,  $\mathcal{S}(\theta)$  is a compact  $k$ -dimensional Riemannian manifold, hence  $0 < \mathcal{M}(\mathcal{S}(\theta)) < \infty$  by the standard coordinate formula for the Riemannian volume element; see [Lee, 2006, Section ‘‘Riemannian volume’’].

It remains to make the bounds uniform over  $\Theta$ . Define  $V(\theta) := \mathcal{M}(\mathcal{S}(\theta))$ . By Lemma B.2, the family  $\{\mathcal{S}(\theta)\}_{\theta \in \Theta}$  is uniformly bounded, i.e., there exists  $D < \infty$  such that  $\mathcal{S}(\theta) \subset \mathbb{B}_d(0; D)$  for all  $\theta \in \Theta$ . Since  $\theta \mapsto \mathcal{S}(\theta)$  is continuous in Hausdorff distance and the manifolds are  $\mathcal{C}^1$  (indeed  $\mathcal{C}^2$ ) with the induced metric varying continuously in  $(\theta, x)$  on  $\Theta \times \mathbb{B}_d(0; D)$ , the volume functional  $V(\theta)$  depends continuously on  $\theta$ .

Because  $\Theta$  is compact and  $V(\theta) > 0$  for all  $\theta$ , the extreme value theorem yields

$$0 < V_{\min} := \min_{\theta \in \Theta} V(\theta) \quad \text{and} \quad V_{\max} := \max_{\theta \in \Theta} V(\theta) < \infty.$$

Setting  $b := \min\{V_{\min}, V_{\max}^{-1}\}$  gives  $b \leq V(\theta) \leq b^{-1}$  for all  $\theta \in \Theta$ .  $\square$

Now we provide the proof of Proposition 3.7:

*Proof.* To establish the boundedness of the density  $\rho_\theta$ , it suffices to show that  $|\partial_r^2 g(\theta, y(u, r))|$  is bounded. Since the  $\mathbb{P}\mathbb{L}^\circ$  condition ensures that  $g(\theta, \cdot)$  is locally Morse-Bott (see [Rebjock and Boumal, 2023, section 2.3]), we have  $\partial_r^2 g(\theta, y(u, r))|_{r=0} \succeq \mu \cdot I_{(d-k) \times (d-k)}$ .

Note that  $y(u, r)$  is linear in  $r$  and we have

$$\partial_r g(\theta, y(u, r)) = \partial_r y(u, r) \partial_x g(\theta, y(u, r)) = \mathbf{N} \partial_x g(\theta, y(u, r)),$$

where  $\mathbf{N} := [v_{k+1}(u), \dots, v_d(u)]^T$ . Then

$$\partial_r^2 g(\theta, y(u, r)) = \mathbf{N} \partial_x^2 g(\theta, y(u, r)) \mathbf{N}^T.$$

When  $r = 0$ ,  $y(u, r) = u$ , then for every  $u \in \mathcal{S}(\theta)$ ,  $\partial_r^2 g(\theta, y(u, r))|_{r=0} = \mathbf{N} \partial_x^2 g(\theta, u) \mathbf{N}^T$ .

From Assumption 2.8,  $\partial_x^2 g(\theta, x)$  is continuous with respect to  $(\theta, x)$ . Since  $\Theta$  is a compact set, the collection  $\{\mathcal{S}(\theta)\}_{\theta \in \Theta}$  is uniformly bounded (see Lemma B.2). By Weierstrass’s extreme value theorem,  $\|\partial_x^2 g(\theta, u)\|$  achieves its supremum at some  $(\theta_0, u_0) \in \Theta \times \mathcal{S}(\theta_0)$ , denoted by  $\|\partial_x^2 g(\theta_0, u_0)\| = M_g$ . Then  $\partial_r^2 g(\theta, y(u, r))|_{r=0} \preceq M_g I_{(d-k) \times (d-k)}$

Now, recall the definition of the density  $\rho_\theta(u)$ :

$$\rho_\theta(u) = \frac{d\mu_\theta^0}{d\mathcal{M}_\theta} = \frac{|\partial_r^2 g(\theta, y(u, r))|_{r=0}|^{-\frac{1}{2}}}{\int_{\mathcal{S}(\theta)} |\partial_r^2 g(\theta, y(v, r))|_{r=0}|^{-\frac{1}{2}} d\mathcal{M}_\theta(v)}.$$

Using the lower and upper bounds on  $\partial_r^2 g(\theta, y(u, r))|_{r=0}$ , we obtain:

$$\frac{M_g^{-\frac{d-k}{2}}}{\mu^{-\frac{d-k}{2}} \mathcal{M}_\theta(\mathcal{S}(\theta))} \leq |\rho_\theta(u)| \leq \frac{\mu^{-\frac{d-k}{2}}}{M_g^{-\frac{d-k}{2}} \mathcal{M}_\theta(\mathcal{S}(\theta))}.$$

From Lemma B.5, we have  $b \leq \mathcal{M}_\theta(\mathcal{S}(\theta)) \leq b^{-1}$ . Finally, we define  $\kappa := b \cdot \left(\frac{\mu}{M_g}\right)^{\frac{d-k}{2}}$ .  $\square$

## C Proofs of results in Section 4

This appendix provides proofs for the geometric and measure-approximation results in Section 3. We first establish a uniform comparison between the volume of small geodesic balls on  $\mathcal{S}(\theta)$  and Euclidean balls, and then use Wasserstein stability to control the superquantile functional under perturbations of the underlying measure.

### C.1 Proof of Lemma 4.1

We begin by showing that, for a  $k$ -dimensional ( $\mathcal{C}^2$ ) embedded Riemannian manifold, the Riemannian volume of a sufficiently small geodesic ball is comparable to the  $k$ -dimensional Lebesgue measure of an Euclidean ball of the same radius. We already used this result to prove Theorem 4.2.

*Proof.* Let  $(\mathcal{S}, g)$  be a  $k$ -dimensional compact Riemannian manifold. By compactness,  $\mathcal{S}$  is geodesically complete. Assume:

1.  $\text{inj}(\mathcal{S}) \geq r_0 > 0$  (uniform lower bound on the injectivity radius),
2.  $|\text{Sec}(x)| \leq C_0$  for all  $x \in \mathcal{S}$  (uniform bound on sectional curvature).

*Step 1: Expressing the volume of a geodesic ball in normal coordinates.* For a Riemannian manifold  $(\mathcal{S}, g)$ , the volume measure  $\mathcal{M}$  is locally given by the *Riemannian volume form*. In a coordinate chart  $\{x^i\}$ , one has

$$d\mathcal{M}(x) = \sqrt{\det(g_{ij}(x))} dx^1 \cdots dx^k,$$

so that, for any measurable  $U$ ,

$$\int_U f(x) d\mathcal{M}(x) = \int_U f(x) \sqrt{\det(g_{ij}(x))} dx^1 \cdots dx^k,$$

where  $g_{ij}(x)$  is the coordinate matrix of the metric  $g$ .

Fix a point  $p \in \mathcal{S}$  and  $0 < r < r_0$ . By [Petersen, 2006, Theorem 5.4.2], the exponential map

$$\exp_p : \mathbb{B}_k(0; r) \subset T_p \mathcal{S} \rightarrow \mathbb{B}_g(p; r) \subset \mathcal{S}$$

is a diffeomorphism, where we identify  $T_p \mathcal{S} \cong \mathbb{R}^k$  via an orthonormal basis and  $\mathbb{B}_k(0; r)$  is the Euclidean ball of radius  $r$ .

Using  $\exp_p$  as a change of variables, we write the volume of the geodesic ball as

$$\mathcal{M}(\mathbb{B}_g(p; r)) = \int_{\mathbb{B}_g(p; r)} d\mathcal{M}(x) = \int_{\mathbb{B}_k(0; r)} (\exp_p^* d\mathcal{M})(v), \quad (39)$$

where  $v = (v^1, \dots, v^k)$  are coordinates on  $T_p \mathcal{S} \cong \mathbb{R}^k$  and  $dv$  is the standard Lebesgue measure on  $\mathbb{R}^k$ .

In *normal coordinates* at  $p$ , the exponential map  $\exp_p$  is precisely the coordinate map, so  $\exp_p^* d\mathcal{M}$  has the expression

$$(\exp_p^* d\mathcal{M})(v) = \sqrt{\det(\mathbf{g}_{ij}(v))} dv^1 \cdots dv^k,$$

where  $\mathbf{g}_{ij}(v)$  is the metric tensor in these normal coordinates. Thus (39) becomes

$$\mathcal{M}(\mathbb{B}_{\mathbf{g}}(p; r)) = \int_{\mathbb{B}_k(0; r)} \sqrt{\det(\mathbf{g}_{ij}(v))} dv. \quad (40)$$

*Step 2: Quadratic control of the metric in normal coordinates, uniformly in  $p$ .* In a normal coordinate neighborhood of  $p$ , the metric admits the expansion (see, e.g., [Petersen, 2006, Section 5.4])

$$\mathbf{g}_{ij}(v) = \delta_{ij} - \frac{1}{3} R_{ikjl}(p) v^k v^l + \mathcal{O}(\|v\|^3), \quad (41)$$

where  $R_{ikjl}(p)$  are the components of the Riemann curvature tensor at  $p$ , and  $\delta_{ij}$  is the Kronecker delta.

The sectional curvature bound  $|\text{Sec}| \leq C_0$  implies that the curvature tensor is uniformly bounded on  $\mathcal{S}$ : there exists a constant  $\tilde{C} > 0$ , depending only on  $C_0$  and  $k$ , such that

$$|R_{ikjl}(x)| \leq \tilde{C} \quad \text{for all } x \in \mathcal{S} \text{ and all indices } i, k, j, l.$$

(For example, this follows from norm equivalence on the finite-dimensional space of algebraic curvature tensors.) After possibly increasing the constant, we may (and do) assume  $\tilde{C} = C_0$  for notational simplicity, so that  $|R_{ikjl}(x)| \leq C_0$  for all  $x \in \mathcal{S}$ .

Since  $\mathcal{S}$  is compact, higher-order derivatives of the metric are also bounded, and the  $\mathcal{O}(\|v\|^3)$  term in (41) can be dominated uniformly in  $p$ . Hence there exist constants  $r_1 \in (0, r_0]$  and  $C > 0$ , depending only on  $(k, C_0, r_0)$ , such that for all  $p \in \mathcal{S}$  and all  $\|v\| \leq r_1$ ,

$$|\mathbf{g}_{ij}(v) - \delta_{ij}| \leq C C_0 \|v\|^2 \quad \text{for all } i, j. \quad (42)$$

Let  $\|\cdot\|_{\text{op}}$  denote the operator norm on matrices with respect to the Euclidean norm. Using the elementary bound  $\|\mathbf{g}(v) - I\|_{\text{op}} \leq k \max_{i,j} |\mathbf{g}_{ij}(v) - \delta_{ij}|$ , we obtain from (42) that

$$\|\mathbf{g}(v) - I\|_{\text{op}} \leq C' C_0 \|v\|^2, \quad \|v\| \leq r_1, \quad (43)$$

for some constant  $C' > 0$  depending only on  $(k, C_0, r_0)$ .

*Step 3: Explicit small-radius condition in terms of  $r_0$  and  $C_0$ .* Define

$$r_* := \min\left\{r_1, \frac{1}{2\sqrt{C' C_0}}\right\}.$$

Then for every  $v$  with  $\|v\| \leq r_*$ , (43) yields  $\|\mathbf{g}(v) - I\|_{\text{op}} \leq C' C_0 r_*^2 \leq 1/4$ . Thus all eigenvalues of the symmetric matrix  $\mathbf{g}(v)$  lie in the interval  $[3/4, 5/4]$ . In particular,

$$\frac{3}{4} I \preceq \mathbf{g}(v) \preceq \frac{5}{4} I \implies \left(\frac{3}{4}\right)^{k/2} \leq \sqrt{\det(\mathbf{g}_{ij}(v))} \leq \left(\frac{5}{4}\right)^{k/2}, \quad \text{for all } \|v\| \leq r_*. \quad (44)$$

Observe that  $r_*$  depends only on  $(k, C_0, r_0)$ . In particular, there exists a numerical constant  $c_k > 0$ , such that

$$r_* \geq \min\left\{r_0, \frac{c_k}{\sqrt{C_0}}\right\}.$$

Thus, up to adjusting the constant, we may think of the admissible radius as

$$0 < r \leq \min\left\{r_0, \frac{c_k}{\sqrt{C_0}}\right\},$$

which makes the dependence on the injectivity radius and sectional curvature bound explicit.

*Step 4: Volume comparison.* Combining (40) and (44), for any  $0 < r \leq r_*$  we get

$$\left(\frac{3}{4}\right)^{k/2} \text{Leb}_k(\mathbb{B}_k(p; r)) \leq \mathcal{M}(\mathbb{B}_g(p; r)) = \int_{\mathbb{B}_k(0; r)} \sqrt{\det(\mathbf{g}_{ij}(v))} dv \leq \left(\frac{5}{4}\right)^{k/2} \text{Leb}_k(\mathbb{B}_k(p; r)).$$

where  $\text{Leb}_k$  denotes Lebesgue measure on  $\mathbb{R}^k$ . This is the desired comparison, with constants  $c_L := (3/4)^{k/2}$  and  $c_H := (5/4)^{k/2}$  valid for all radii

$$0 < r \leq r_* \text{ and hence for all } 0 < r \leq \min\left\{r_0, \frac{c_k}{\sqrt{C_0}}\right\}.$$

□

## C.2 Proof of Lemma 4.4

We next provide the proof of Lemma 4.4 which is essential for our approximation result in Theorem 4.5.

*Proof.* Recall

$$\phi_{\lambda, \delta}(\theta, \beta) = \beta + \frac{1}{\delta} \mathbb{E}_{X \sim \mu_\theta^\lambda}[(f(\theta, X) - \beta)_+].$$

By Assumption 2.8,  $f(\theta, \cdot)$  is  $L_{f,1}$ -Lipschitz. Since  $t \mapsto (t - \beta)_+$  is 1-Lipschitz, the map

$$G_\beta(x) := (f(\theta, x) - \beta)_+$$

is  $L_{f,1}$ -Lipschitz in  $x$ . Hence, by the Kantorovich–Rubinstein duality for  $\mathbb{W}_1$ ,

$$|\phi_{\lambda, \delta}(\theta, \beta) - \phi_{0, \delta}(\theta, \beta)| = \frac{1}{\delta} \left| \mathbb{E}_{\mu_\theta^\lambda}[G_\beta(X)] - \mathbb{E}_{\mu_\theta^0}[G_\beta(X)] \right| \leq \frac{L_{f,1}}{\delta} \mathbb{W}_1(\mu_\theta^\lambda, \mu_\theta^0). \quad (45)$$

Finally, to prove the statement of Lemma 4.4, we have

$$\begin{aligned} \min_{\beta'} \phi_{0, \delta}(\theta, \beta') &\leq \phi_{0, \delta}(\theta, \beta) \\ &\leq \phi_{\lambda, \delta}(\theta, \beta) + |\phi_{0, \delta}(\theta, \beta) - \phi_{\lambda, \delta}(\theta, \beta)| \\ &\stackrel{(a)}{\leq} \phi_{\lambda, \delta}(\theta, \beta) + \frac{L_{f,1}}{\delta} \cdot \mathbb{W}_1(\mu_g^\lambda(\theta), \mu_g^0(\theta)), \end{aligned} \quad (46)$$

where (a) follow by (45). Then, taking the minimum over  $\beta$  at the r.h.s. of (46), we get  $\min_{\beta'} \phi_{0, \delta}(\theta, \beta') - \min_{\beta} \phi_{\lambda, \delta}(\theta, \beta) \leq \frac{L_{f,1}}{\delta} (\mu_g^\lambda(\theta), \mu_g^0(\theta))$ . Interchanging  $\min_{\beta} \phi_{\lambda, \delta}(\theta, \beta)$  and  $\min_{\beta'} \phi_{0, \delta}(\theta, \beta')$ , one obtains

$$\left| \min_{\beta} \phi_{\lambda, \delta}(\theta, \beta) - \min_{\beta'} \phi_{0, \delta}(\theta, \beta') \right| \leq L_{f,1} \delta^{-1} \mathbb{W}_1(\mu_g^\lambda(\theta), \mu_g^0(\theta)). \quad (47)$$

□

## D Proofs of results in Section 5

This appendix collects technical results for the oracle analysis in Section 5. We begin by deriving moment and tail bounds for the Gibbs measure; these bounds are then used to prove Lemma 5.1. Next, we establish accuracy guarantees for the PSGD-based inner estimator. Finally, we present the complete proof of Theorem 5.5, separating the standard zeroth-order argument from our new control of the minima-selection error.

### D.1 Proof of Lemma 5.1

We start by presenting the following technical lemma, which is an essential prerequisite for the proof of Lemma 5.1. It establishes a technical result ensuring the finiteness of the moments of the Gibbs measure  $\mu_\theta^\lambda$ .

**Lemma D.1.** *Under Assumption 2.6, for*

$$\lambda \leq \min \left\{ \frac{(2\pi)^{d/2} M_g^{-\frac{d}{2}}}{2c}, \frac{2D^2}{n+d} \right\},$$

we have for every  $n \in \mathbb{N} \cup \{0\}$

$$\mathbb{E}_{X \sim \mu_\theta^\lambda} [\|X\|^n \cdot \mathbf{1}[X \notin \mathbb{B}_d(0; 2D)]] \leq W_n \cdot \lambda^{-\frac{d}{2}+1} e^{-\frac{D^2}{\lambda}}.$$

Here,

$$W_n := M_g^{\frac{d}{2}} \cdot 2^{-d/2+2} \pi^{d/2+n-1} \cdot 2\mu_{\text{qg}}^{-1} \cdot \max\{(d+n)/2, 1\} \cdot D^{d+n-1}$$

with  $M_g$  is defined in Proposition 3.7 and  $c > 0$  is a constant.

*Proof.* Assume without loss of generality that  $g$  does not depend on  $\theta$ ,  $\min_x g(x) = 0$ , and  $0 \in \mathcal{S} = \arg \min_x g(x)$ . We first note that by switching to spherical coordinates, one obtains for any  $n \geq 0$  the bound

$$\begin{aligned} & \int_{x: \|x\| > R} \|x\|^n e^{-c\|x\|^2} dx \\ &= \int_0^\pi \cdots \int_0^\pi \int_0^{2\pi} \int_{r>R} e^{-cr^2} r^{d+n-1} \sin^{d-2}(\phi_1) \sin^{d-3}(\phi_2) \cdots \sin(\phi_{d-2}) dr d\phi_1 \cdots d\phi_{d-1} \\ &\leq \int_0^\pi \cdots \int_0^\pi \int_0^{2\pi} \int_{r>R} e^{-cr^2} r^{d+n-1} dr d\phi_1 \cdots d\phi_{d-1} \leq 2\pi^{d-1} \int_R^{+\infty} e^{-cr^2} r^{d+n-1} dr \\ &\leq 2\pi^{d+n-1} c^{-\frac{d+n}{2}} \cdot \Gamma\left(\frac{d+n}{2}, cR^2\right), \end{aligned} \tag{48}$$

where in the last inequality we use the definition of the upper incomplete Gamma function, i.e.,  $\Gamma(s, x) := \int_x^{+\infty} t^{s-1} e^{-t} dt$ . By Gautschi's inequality<sup>24</sup>, for  $cR^2 > (d+n)/2$  and  $d+n \geq 2$ ,

$$\begin{aligned} & \int_{x: \|x\| > R} \|x\|^n e^{-c\|x\|^2} dx \leq 2\pi^{d+n-1} \cdot c^{-\frac{d+n}{2}} \max\{(d+n)/2, 1\} (cR^2)^{\frac{d+n}{2}-1} e^{-cR^2} \\ &\leq 2\pi^{d+n-1} \cdot c^{-1} \max\{(d+n)/2, 1\} R^{d+n-2} e^{-cR^2}. \end{aligned} \tag{49}$$

Since

$$\mathbb{E}_{X \sim \mu_\theta^\lambda} [\|X\|^n \cdot \mathbf{1}[X \notin \mathbb{B}_d(0; 2D)]] = \frac{1}{Z_\lambda} \int_{\|x\| \geq 2D} \|x\|^n e^{-g(x)/\lambda} dx,$$

<sup>24</sup>By Gautschi-type's inequality,  $\Gamma(x, s) \leq sx^{s-1} e^{-x}$  for  $x > s$  and  $s \geq 1$ . Note that for  $s = 1$ ,  $\Gamma(s, x) = e^{-x}$ .

and noting that, if  $\mathcal{S} \subseteq \mathbb{B}_d(0; D)$ , then for  $x \notin \mathbb{B}_d(0; 2D)$  we have

$$\|x\| - D \leq \text{dist}(x, \mathcal{S}),$$

the quadratic growth of  $g$  outside  $\mathbb{B}_d(0; 2D)$  implies

$$\frac{\mu_{\text{qg}}}{2} (\|x\| - D)^2 \leq g(x), \quad \forall \|x\| \geq 2D. \quad (50)$$

Hence,

$$\mathbb{E}_{X \sim \mu_\theta^\lambda} [\|X\|^n \cdot \mathbf{1}[X \notin \mathbb{B}_d(0; 2D)]] \leq \frac{1}{Z_\lambda} \int_{\|x\| \geq 2D} \|x\|^n e^{-\frac{\mu_{\text{qg}}(\|x\| - D)^2}{2\lambda}} dx.$$

Applying (49) gives for  $\lambda < 2D^2/(n + d)$ ,

$$\mathbb{E}_{X \sim \mu_\theta^\lambda} [\|X\|^n \cdot \mathbf{1}[X \notin \mathbb{B}_d(0; 2D)]] \leq \frac{1}{Z_\lambda} \cdot 2\pi^{d+n-1} \cdot \left( \frac{2\lambda}{\mu_{\text{qg}}} \right) \cdot \max\{(d+n)/2, 1\} \cdot D^{d+n-2} e^{-\frac{D^2}{\lambda}}. \quad (51)$$

For a lower bound on  $Z_\lambda$ , we use the estimate (see [Hasenpflug et al., 2024, Remark A.21]): for a compact set  $U \subset \mathbb{R}^d$  and  $x_0 \in \mathcal{S}$ ,

$$\int_U e^{-g(x)/\lambda} dx \geq \lambda^{\frac{d}{2}} \left[ (2\pi)^{d/2} \det \left( \frac{\partial^2 g(x_0)}{\partial x^2} \right)^{-\frac{1}{2}} - c\lambda \right].$$

Since  $\det \left( \frac{\partial^2 g(x_0)}{\partial x^2} \right) \leq M_g^d$  (by Proposition 3.7), it follows that

$$Z_\lambda \geq \lambda^{\frac{d}{2}} \left[ (2\pi)^{d/2} M_g^{-\frac{d}{2}} - c\lambda \right].$$

Thus, if

$$\lambda \leq \min \left\{ \frac{(2\pi)^{d/2} M_g^{-\frac{d}{2}}}{2c}, \frac{2D^2}{n+d} \right\},$$

we have

$$Z_\lambda \geq \lambda^{\frac{d}{2}} \cdot (2\pi)^{d/2} M_g^{-\frac{d}{2}} / 2.$$

Substituting this into (51) completes the proof.  $\square$

We then prove Lemma 5.1 which states that every global minimizer of  $\phi_{\lambda, \delta}(\theta, \cdot)$  lies in a bounded interval.

*Proof. Upper bound on  $\beta^*(\theta)$ :* Pick a  $\beta^*(\theta) \in \arg \min_\beta \phi_{\lambda, \delta}(\theta, \beta)$ . It follows that

$$\begin{aligned} \beta^*(\theta) &\leq \beta^*(\theta) + \delta^{-1} \mathbb{E}[\max\{0, f(\theta, X) - \beta^*(\theta)\}] \\ &= \min_\beta \phi_{\lambda, \delta}(\theta, \beta) \end{aligned} \quad (52)$$

In the following, we give an upper bound on  $\min_\beta \phi_{\lambda, \delta}(\theta, \beta)$ . First, note that similar to the proof of Lemma 4.4, we have

$$\left| \min_\beta \phi_{0, \delta}(\theta, \beta) - \min_\beta \phi_{\lambda, \delta}(\theta, \beta) \right| \leq \frac{L_{f,1}}{\delta} \cdot \mathbb{W}_1(\mu_\theta^\lambda, \mu_\theta^0).$$

Using this bound along with the result of Proposition 2.11, we obtain

$$\begin{aligned}\beta^*(\theta) &\leq \min_{\beta} \phi_{\lambda,\delta}(\theta, \beta) \leq \min_{\beta} \phi_{0,\delta}(\theta, \beta) + |\min_{\beta} \phi_{0,\delta}(\theta, \beta) - \min_{\beta} \phi_{\lambda,\delta}(\theta, \beta)| \\ &\leq \min_{\beta} \phi_{0,\delta}(\theta, \beta) + \frac{L_{f,1}}{\delta} \cdot K_0 \lambda^{\frac{1}{2}}.\end{aligned}\tag{53}$$

Then we have for  $Y \sim \mu_{\theta}^0$ ,

$$\min_{\beta} \phi_{0,\delta}(\theta, \beta) = \text{SQ}_{1-\delta}(f(\theta, Y)) \leq \max_{x \in \mathcal{S}(\theta)} f(\theta, x),$$

where the last inequality comes from the definition of superquantile and the fact that  $\text{supp}(\mu_{\theta}^0) = \mathcal{S}(\theta)$ . By Equation (5),  $\max_{x \in \mathcal{S}(\theta)} f(\theta, x) \leq L_{f,0}(D)$ . Hence, we have  $\min_{\beta} \phi_{0,\delta}(\theta, \beta) \leq L_{f,0}(D)$  and then from (53), we obtain

$$\beta^*(\theta) \leq L_{f,0}(D) + \frac{L_{f,1}}{\delta} \cdot K_0 \lambda^{1/2}\tag{54}$$

**Lower bound on  $\beta^*(\theta)$ :** By the definition of the  $(1 - \delta)$ -quantile of the random variable  $f(\theta, X)$  under  $X \sim \mu_{\theta}^{\lambda}$ , it holds that

$$\mathbb{P}_{X \sim \mu_{\theta}^{\lambda}}[f(\theta, X) < \beta^*(\theta)] > 1 - \delta.$$

Because  $\delta \leq 1/2$ , we in particular have

$$\mathbb{P}_{X \sim \mu_{\theta}^{\lambda}}[f(\theta, X) < \beta^*(\theta)] > \frac{1}{2}.$$

W.L.O.G., we assume that  $\mathcal{S}(\theta) \subseteq \mathbb{B}_d(0; D)$  with sufficiently large  $D$ . Then

$$\begin{aligned}\frac{1}{2} &< \mathbb{P}_{X \sim \mu_{\theta}^{\lambda}}[f(\theta, X) < \beta^*(\theta)] \\ &\leq \mathbb{P}[f(\theta, X) < \beta^*(\theta), X \in \mathbb{B}_d(0; 2D)] + \mathbb{P}[f(\theta, X) < \beta^*(\theta), X \notin \mathbb{B}_d(0; 2D)] \\ &\leq \mathbb{P}[f(\theta, X) < \beta^*(\theta), X \in \mathbb{B}_d(0; 2D)] + \mathbb{P}[X \notin \mathbb{B}_d(0; 2D)],\end{aligned}$$

Next, we use the result in Lemma D.1 for  $n = 0$ , to give the following bound:

$$\mathbb{P}_{X \sim \mu_{\theta}^{\lambda}}[X \notin \mathbb{B}_d(0; 2D)] \leq W_0 \cdot \lambda^{-\frac{d}{2}+1} e^{-\frac{D^2}{\lambda}}.$$

Then

$$\begin{aligned}\mathbb{P}[f(\theta, X) < \beta^*(\theta), X \in \mathbb{B}_d(0; 2D)] &\geq \\ &\frac{1}{2} - W_0 \cdot \lambda^{-\frac{d}{2}+1} e^{-\frac{D^2}{\lambda}}.\end{aligned}\tag{55}$$

For the case  $d \leq 2$ , when  $\lambda \leq \frac{D^2}{\log(4W_0)}$ , we have  $\mathbb{P}[f(\theta, X) < \beta^*(\theta), X \in \mathbb{B}_d(0; 2D)] \geq \frac{1}{4}$ . For the case  $d > 2$ , when

$$\lambda \leq \frac{2D^2}{(d-2) \cdot W_{\text{Lam}} \left( \frac{2}{d-2} \left( \frac{4W_0}{D} \right)^{\frac{2}{d-2}} \right)},$$

where  $W_{\text{Lam}}$  is the Lambert function, we have

$$\mathbb{P}[f(\theta, X) < \beta^*(\theta), X \in \mathbb{B}_d(0; 2D)] \geq \frac{1}{4}.$$

Thus, there exists some  $x_0 \in \mathbb{B}_d(0; 2D)$  such that  $f(\theta, x_0) \leq \beta^*(\theta)$ . We conclude from Equation (5),  $-L_{f,0}(2D) \leq \min_{x \in \mathbb{B}_d(0; D)} f(\theta, x) \leq \beta^*(\theta)$ . This completes the proof.  $\square$

## D.2 Proof of Lemma 5.2

This subsection proves the mean-square accuracy bound for the PSGD estimator of  $\tilde{F}_{\text{SQ-G}}(\theta)$ . This estimate is the key input in the zeroth-order convergence proof.

For completeness, we state the following bounds, which are used in the convergence analysis of PSGD (see Algorithm 1). The function  $\phi_{\lambda,\delta}(\theta, \beta)$  is  $(1 + \delta^{-1})$ -Lipschitz on  $\beta$  since, given  $\theta \in \Theta$ , for every  $\beta_1, \beta_2 \in \mathbb{R}$ ,

$$\begin{aligned} |\phi_{\lambda,\delta}(\theta, \beta_1) - \phi_{\lambda,\delta}(\theta, \beta_2)| &\leq |\beta_1 - \beta_2| + \frac{1}{\delta} \cdot \mathbb{E}[|h(f(\theta, X) - \beta_1) - h(f(\theta, X) - \beta_2)|] \\ &\leq \left[1 + \frac{1}{\delta}\right] \cdot |\beta_1 - \beta_2|. \end{aligned} \quad (56)$$

Here the last inequality comes from  $h(t) := \max\{t, 0\}$  is 1-Lipschitz. Moreover,

$$|\tilde{\partial}_\beta \phi_{\lambda,\delta}(\theta, \beta; X)| = \left|1 + \frac{1}{\delta} \hat{\partial}_\beta [\max\{f(\theta, X) - \beta, 0\}]\right|^2 \leq |1 + \delta^{-1}| := \sigma.$$

Here  $\hat{\partial}_\beta [\max\{f(\theta, X) - \beta, 0\}]$  is the sub-gradient of  $\max\{f(\theta, X) - \beta, 0\}$  and is bounded uniformly by 1. We then provide the proof of Lemma 5.2 in the following:

*Proof.* To give an upper bound on  $\mathbb{E}[|\tilde{\psi}(\theta) - \tilde{F}_{\text{SQ-G}}(\theta)|^2 | \theta]$ , by the triangle inequality, we have

$$\begin{aligned} \mathbb{E}[|\phi_{\lambda,\delta}(\theta, \hat{\beta}; \tilde{X}_I) - \tilde{F}_{\text{SQ-G}}(\theta)|^2 | \theta] &\leq \\ &2\mathbb{E}[|\phi_{\lambda,\delta}(\theta, \hat{\beta}; \tilde{X}_I) - \phi_{\lambda,\delta}(\theta, \hat{\beta})|^2 | \theta] + 2\mathbb{E}[|\phi_{\lambda,\delta}(\theta, \hat{\beta}) - \tilde{F}_{\text{SQ-G}}(\theta)|^2 | \theta] \\ &= 2\underbrace{\mathbb{E}[|\phi_{\lambda,\delta}(\theta, \hat{\beta}; \tilde{X}_I) - \phi_{\lambda,\delta}(\theta, \hat{\beta})|^2 | \theta]}_{(i)} + 2\underbrace{\mathbb{E}[|\phi_{\lambda,\delta}(\theta, \hat{\beta}) - \min_\beta \phi_{\lambda,\delta}(\theta, \beta)|^2 | \theta]}_{(ii)}, \end{aligned} \quad (57)$$

where the last equation follows from  $\tilde{F}_{\text{SQ-G}}(\theta) = \min_\beta \phi_{\lambda,\delta}(\theta, \beta)$ . We will give the upper bounds on the terms (i) and (ii) in the following.

**Upper bound on (i) in (57):** We use the following chain of inequalities:

$$\begin{aligned} \mathbb{E}[|\phi_{\lambda,\delta}(\theta, \hat{\beta}; \tilde{X}_I) - \phi_{\lambda,\delta}(\theta, \hat{\beta})|^2 | \theta] &= \mathbb{E}\left[\mathbb{E}\left[|\phi_{\lambda,\delta}(\theta, \hat{\beta}; \tilde{X}_I) - \phi_{\lambda,\delta}(\theta, \hat{\beta})|^2 | \theta, \hat{\beta}\right]\right] \\ &= \frac{1}{\delta^2} \cdot \mathbb{E}\left[\mathbb{E}\left[\left(\frac{1}{|I|} \sum_{i \in I} h(f(\theta, \tilde{X}^{(i)}) - \hat{\beta}) - \mathbb{E}[h(f(\theta, X) - \hat{\beta}) | \theta, \hat{\beta}]\right)^2 | \theta, \hat{\beta}\right]\right] \\ &= \frac{1}{\delta^2} \cdot \mathbb{E}\left[\left(\frac{1}{|I|^2} \sum_{i \in I} \mathbb{E}\left[\left(h(f(\theta, \tilde{X}^{(i)}) - \hat{\beta}) - \mathbb{E}[h(f(\theta, X) - \hat{\beta}) | \theta, \hat{\beta}]\right)^2 | \theta, \hat{\beta}\right]\right)\right], \end{aligned} \quad (58)$$

where the last inequality comes from the fact that  $\{h(f(\theta, \tilde{X}^{(i)}) - \hat{\beta})\}_{i \in I}$  are independent random variables given  $\theta$  and  $\hat{\beta}$ .

Now we give a constant upper bound on (58) in the following:

$$\begin{aligned} &\mathbb{E}\left[\left(h(f(\theta, \tilde{X}^{(i)}) - \hat{\beta}) - \mathbb{E}[h(f(\theta, X) - \hat{\beta}) | \theta, \hat{\beta}]\right)^2 | \theta, \hat{\beta}\right] \\ &\leq \mathbb{E}\left[\left(h(f(\theta, \tilde{X}^{(i)}) - \hat{\beta}) - h(f(\theta, X) - \hat{\beta})\right)^2 | \theta, \hat{\beta}\right] \end{aligned}$$

$$\begin{aligned}
&\leq \mathbb{E} \left[ \left( f(\theta, \tilde{X}^{(i)}) - f(\theta, X) \right)^2 \mid \theta, \hat{\beta} \right] \\
&\leq 4\mathbb{E} \left[ (f(\theta, X))^2 \mid \theta, \hat{\beta} \right] \\
&\stackrel{(a)}{\leq} 4\mathbb{E} \left[ (C_f \|X\|^{n_f} + D_f)^2 \mid \theta, \hat{\beta} \right] \\
&\leq 8C_f^2 \mathbb{E}[\|X\|^{2n_f}] + 8D_f^2 \\
&\stackrel{(b)}{\leq} \tilde{C}_f := 8C_f^2 \cdot \left( (2D)^{2n_f} + W_{2n_f} \cdot \lambda^{-\frac{d}{2}} e^{-\frac{D^2}{\lambda}} \right) + 8D_f^2,
\end{aligned} \tag{59}$$

where step (a) follows from Assumption 2.8, and step (b) uses Lemma D.1.

Then from (58), we get

$$\mathbb{E}[|\phi_{\lambda,\delta}(\theta, \hat{\beta}; \tilde{X}_I) - \phi_{\lambda,\delta}(\theta, \hat{\beta})|^2 \mid \theta] \leq \frac{\tilde{C}_f}{\delta^2 |I|}. \tag{60}$$

**Upper bound on (ii) in (57):** Because  $\phi_{\lambda,\delta}(\theta, \cdot)$  is  $\sigma$ -Lipschitz in  $\beta$  and the feasible interval for  $\beta$  is  $[-B, B]$ , we have the deterministic range bound

$$0 \leq \phi_{\lambda,\delta}(\theta, \hat{\beta}) - \min_{\beta} \phi_{\lambda,\delta}(\theta, \beta) \leq R := 2\sigma B.$$

Given that (i)  $\phi_{\lambda,\delta}(\theta, \cdot)$  is convex and Lipschitz continuous, (ii) the feasible set is bounded, and (iii) the stochastic subgradient  $\tilde{\partial}_{\beta} \phi_{\lambda,\delta}(\theta, \beta; X)$  satisfies  $|\tilde{\partial}_{\beta} \phi_{\lambda,\delta}(\theta, \beta; X)| \leq \sigma := 1 + \delta^{-1}$ , we invoke the convergence guarantees for convex Lipschitz objectives [Nemirovskij and Yudin, 1983, Lan et al., 2012] together with the large-deviation analysis for stochastic approximation [Juditsky and Nemirovski, 2008, Thm. 2.1]. Accordingly, the output  $\hat{\beta}$  of PSGD (see Algorithm 1) satisfies

$$\mathbb{P} \left( \phi_{\lambda,\delta}(\theta, \hat{\beta}) - \min_{\beta} \phi_{\lambda,\delta}(\theta, \beta) \leq \epsilon_v \mid \theta \right) \geq 1 - \Delta.$$

after at most  $\mathcal{O}(B^2 \sigma^2 \epsilon_v^{-2} \log(\Delta^{-1}))$  iterations.

From  $0 \leq \phi_{\lambda,\delta}(\theta, \hat{\beta}) - \min_{\beta} \phi_{\lambda,\delta}(\theta, \beta) \leq R$  and the tail bound we get

$$\mathbb{E} \left[ \left( \phi_{\lambda,\delta}(\theta, \hat{\beta}) - \min_{\beta} \phi_{\lambda,\delta}(\theta, \beta) \right)^2 \mid \theta \right] \leq \epsilon_v^2 (1 - \Delta) + R^2 \Delta \leq \epsilon_v^2 + R^2 \Delta.$$

Choosing  $\Delta := \min\{1, \epsilon_v^2/R^2\}$  yields

$$\mathbb{E} \left[ \left( \phi_{\lambda,\delta}(\theta, \hat{\beta}) - \min_{\beta} \phi_{\lambda,\delta}(\theta, \beta) \right)^2 \mid \theta \right] \leq 2\epsilon_v^2, \tag{61}$$

at the cost of

$$L \geq C \cdot \frac{B^2}{\delta^2 \epsilon_v^2} \cdot \log \left( \frac{1}{\epsilon_v \delta} \right).$$

Thus, by substituting (61) and (60) into (57), we obtain

$$\mathbb{E}[|\tilde{\psi}(\theta) - \tilde{F}_{\text{SQ-G}}(\theta)|^2 \mid \theta] \leq 2\epsilon_v^2 + \frac{2\tilde{C}_f}{\delta^2 |I|}. \tag{62}$$

By picking  $\delta = \epsilon_v^k$  and  $|I| \geq 4\tilde{C}_f \epsilon_v^{-2k}$  and

$$L \geq \mathcal{O} \left( k \cdot \frac{B^2}{\epsilon_v^{2(k+1)}} \cdot \log \left( \frac{1}{\epsilon_v} \right) \right),$$

we get  $\mathbb{E}[|\tilde{\psi}(\theta) - \tilde{F}_{\text{SQ-G}}(\theta)|^2 \mid \theta] \leq \epsilon_v^2$ . □

### D.3 Proof of Theorem 5.5

We now prove Theorem 5.5. The argument follows the standard projected zeroth-order analysis for the smoothed objective, and the only additional step is to bound the error introduced by replacing  $F_{\max}$  with  $\tilde{\psi}$  using Equation (26) and Lemma 5.2.

*Proof.* The proof has two parts. We first follow the standard convergence analysis for projected zeroth-order methods applied to the smoothed objective of  $F_{\max}$ . The only nonstandard step is then to control the additional error induced by replacing  $F_{\max}$  with  $\tilde{\psi}$  in the gradient estimator, where we invoke Lemma 5.2.

*Step 1: Standard zeroth-order analysis for the smoothed problem.* We define the smoothed objective  $\psi_\rho(\theta) := \mathbb{E}_{u \sim \text{uniform}(\mathbb{S}^{m-1})}[F_{\max}(\theta + \rho u)]$ , where  $u$  is uniformly distributed on the unit sphere  $\mathbb{S}^{m-1}$ . As shown in [Nesterov and Spokoiny, 2017, Theorem 1 and Lemma 2], for any  $L_{f,1}$ -Lipschitz function  $f : \mathbb{R}^m \rightarrow \mathbb{R}$ , the smoothed version  $f_\rho(\theta) := \mathbb{E}_{u \sim \text{uniform}(\mathbb{S}^{m-1})}[f(\theta + \rho u)]$  satisfies:

- $f_\rho$  is a  $\rho\sqrt{m}L_{f,1}$ -approximation of  $f$ ,  $f_\rho$  is a  $L_{f,1}$ -Lipschitz function,
- $f_\rho$  is differentiable with gradient Lipschitz constant  $L_{f,2} = \sqrt{m}L_{f,1}\rho^{-1}$ ,
- $\nabla f_\rho(\theta) \in \partial_\rho f(\theta)$ , the  $\rho$ -subdifferential of  $f$ , as shown in [Lin et al., 2022, Theorem 3.1].

In our scenario, by using Corollary 3.4,  $F_{\max}$  is Lipschitz continuous with the constant  $L_{F_{\max},1} := L_{f,1}(1 + L_{g,2}/\mu)$ . By applying the aforementioned findings on  $F_{\max}$ , it follows that  $\psi_\rho$  is  $L_{\psi,2} = \sqrt{m}L_{F_{\max},1}\rho^{-1}$ -smooth. Furthermore, the gradient  $\nabla\psi_\rho(\theta)$  is contained in the  $\rho$ -subdifferential set of  $F_{\max}$  at the point  $\theta$ . Therefore, if a point  $\theta$  satisfies  $\|\mathcal{G}_\Theta(\theta, \nabla\psi_\rho; \eta)\| \leq \epsilon$ , then  $\theta$  is an  $(\epsilon, \rho, \eta)$ -generalized Goldstein stationary point of  $F_{\max}$  (see Definition 5.4). In what follows, we analyze the convergence of Algorithm 2 to a critical point of  $\psi_\rho$  in terms of the gradient mapping.

Given the  $(L_{\psi,2} = \sqrt{m}L_{F_{\max},1}\rho^{-1})$ -smoothness of  $\psi_\rho(\theta)$ , we have

$$\psi_\rho(\theta_{i+1}) \leq \psi_\rho(\theta_i) + \langle \nabla\psi_\rho(\theta_i), \theta_{i+1} - \theta_i \rangle + \frac{L_{\psi,2}}{2} \|\theta_{i+1} - \theta_i\|^2 \quad (63)$$

Substituting  $\theta_{i+1} - \theta_i = -\tilde{\eta}_i \mathcal{G}_\Theta(\theta_i, \tilde{\mathbf{g}}_\rho(\theta_i); \tilde{\eta}_i)$ , we have

$$\psi_\rho(\theta_{i+1}) \leq \psi_\rho(\theta_i) - \tilde{\eta}_i \langle \nabla\psi_\rho(\theta_i), \mathcal{G}_\Theta(\theta_i, \tilde{\mathbf{g}}_\rho(\theta_i); \tilde{\eta}_i) \rangle + \frac{L_{\psi,2}}{2} \tilde{\eta}_i^2 \|\mathcal{G}_\Theta(\theta_i, \tilde{\mathbf{g}}_\rho(\theta_i); \tilde{\eta}_i)\|^2 \quad (64)$$

Expanding the inner product and rearranging terms

$$\begin{aligned} \psi_\rho(\theta_{i+1}) &\leq \psi_\rho(\theta_i) - \tilde{\eta}_i \langle \tilde{\mathbf{g}}_\rho(\theta_i), \mathcal{G}_\Theta(\theta_i, \tilde{\mathbf{g}}_\rho(\theta_i); \tilde{\eta}_i) \rangle + \frac{L_{\psi,2}}{2} \tilde{\eta}_i^2 \|\mathcal{G}_\Theta(\theta_i, \tilde{\mathbf{g}}_\rho(\theta_i); \tilde{\eta}_i)\|^2 \\ &\quad - \tilde{\eta}_i \langle \nabla\psi_\rho(\theta_i) - \tilde{\mathbf{g}}_\rho(\theta_i), \mathcal{G}_\Theta(\theta_i, \tilde{\mathbf{g}}_\rho(\theta_i); \tilde{\eta}_i) \rangle \end{aligned} \quad (65)$$

Further simplifying and using the fact that  $\|\mathcal{G}_\Theta(\theta, v; \eta)\|^2 \leq \langle \mathcal{G}_\Theta(\theta, v; \eta), v \rangle$  for every  $v \in \Theta$ , we have

$$\psi_\rho(\theta_{i+1}) \leq$$

$$\begin{aligned}
& \psi_\rho(\theta_i) - \left[ \tilde{\eta}_i - \frac{L_{\psi,2} \tilde{\eta}_i^2}{2} \right] \cdot \|\mathcal{G}_\Theta(\theta_i, \tilde{\mathbf{g}}_\rho(\theta_i); \tilde{\eta}_i)\|^2 - \tilde{\eta}_i \langle \nabla \psi_\rho(\theta_i) - \tilde{\mathbf{g}}_\rho(\theta_i), \mathcal{G}_\Theta(\theta_i, \nabla \psi_\rho(\theta_i); \tilde{\eta}_i) \rangle \\
& \quad - \tilde{\eta}_i \langle \nabla \psi_\rho(\theta_i) - \tilde{\mathbf{g}}_\rho(\theta_i), \mathcal{G}_\Theta(\theta_i, \nabla \psi_\rho(\theta_i); \tilde{\eta}_i) - \mathcal{G}_\Theta(\theta_i, \tilde{\mathbf{g}}_\rho(\theta_i); \tilde{\eta}_i) \rangle \\
& \leq \psi_\rho(\theta_i) - \left[ \tilde{\eta}_i - \frac{L_{\psi,2} \tilde{\eta}_i^2}{2} \right] \cdot \|\mathcal{G}_\Theta(\theta_i, \tilde{\mathbf{g}}_\rho(\theta_i); \tilde{\eta}_i)\|^2 - \tilde{\eta}_i \langle \nabla \psi_\rho(\theta_i) - \tilde{\mathbf{g}}_\rho(\theta_i), \mathcal{G}_\Theta(\theta_i, \nabla \psi_\rho(\theta_i); \tilde{\eta}_i) \rangle \\
& \quad + \tilde{\eta}_i \|\nabla \psi_\rho(\theta_i) - \tilde{\mathbf{g}}_\rho(\theta_i)\|^2, \tag{66}
\end{aligned}$$

where the last inequality comes from the Cauchy-Schwartz inequality and  $\|\mathcal{G}_\Theta(\theta, v_1; \eta) - \mathcal{G}_\Theta(\theta, v_2; \eta)\| \leq \|v_1 - v_2\|$ . Let us define  $\mathbf{g}_\rho(\theta) := \frac{1}{b_u} \sum_{t=1}^{b_u} \mathbf{g}_\rho(\theta, u_t)$  where  $\mathbf{g}_\rho(\theta, u_t) := \frac{m}{2\rho} \cdot [F_{\max}(\theta + \rho u_t) - F_{\max}(\theta - \rho u_t)] u_t$ . Then

$$\begin{aligned}
& \psi_\rho(\theta_{i+1}) \leq \\
& \psi_\rho(\theta_i) - \left[ \tilde{\eta}_i - \frac{L_{\psi,2} \tilde{\eta}_i^2}{2} \right] \cdot \|\mathcal{G}_\Theta(\theta_i, \tilde{\mathbf{g}}_\rho(\theta_i); \tilde{\eta}_i)\|^2 - \tilde{\eta}_i \langle \nabla \psi_\rho(\theta_i) - \mathbf{g}_\rho(\theta_i), \mathcal{G}_\Theta(\theta_i, \nabla \psi_\rho(\theta_i); \tilde{\eta}_i) \rangle \\
& \quad - \tilde{\eta}_i \langle \mathbf{g}_\rho(\theta_i) - \tilde{\mathbf{g}}_\rho(\theta_i), \mathcal{G}_\Theta(\theta_i, \nabla \psi_\rho(\theta_i); \tilde{\eta}_i) \rangle + \tilde{\eta}_i \|\nabla \psi_\rho(\theta_i) - \tilde{\mathbf{g}}_\rho(\theta_i)\|^2, \tag{67}
\end{aligned}$$

By picking  $\tilde{\eta}_i \leq 1/L_{\psi,2}$ , we have

$$\begin{aligned}
\|\mathcal{G}_\Theta(\theta_i, \tilde{\mathbf{g}}_\rho(\theta_i); \tilde{\eta}_i)\|^2 & \leq \frac{2[\psi_\rho(\theta_i) - \psi_\rho(\theta_{i+1})]}{\tilde{\eta}_i} - 2\langle \nabla \psi_\rho(\theta_i) - \mathbf{g}_\rho(\theta_i), \mathcal{G}_\Theta(\theta_i, \nabla \psi_\rho(\theta_i); \tilde{\eta}_i) \rangle \\
& \quad - 2\langle \mathbf{g}_\rho(\theta_i) - \tilde{\mathbf{g}}_\rho(\theta_i), \mathcal{G}_\Theta(\theta_i, \nabla \psi_\rho(\theta_i); \tilde{\eta}_i) \rangle + 2\|\nabla \psi_\rho(\theta_i) - \tilde{\mathbf{g}}_\rho(\theta_i)\|^2. \tag{68}
\end{aligned}$$

Then by using Young's inequality ( $\langle \mathbf{a}, \mathbf{b} \rangle \leq c\|\mathbf{a}\|^2/2 + \|\mathbf{b}\|^2/(2c)$  for the vectors  $\mathbf{a}, \mathbf{b}$  and positive constant  $c$ ), we have

$$\begin{aligned}
\|\mathcal{G}_\Theta(\theta_i, \tilde{\mathbf{g}}_\rho(\theta_i); \tilde{\eta}_i)\|^2 & \leq \frac{2[\psi_\rho(\theta_i) - \psi_\rho(\theta_{i+1})]}{\tilde{\eta}_i} - 2\langle \nabla \psi_\rho(\theta_i) - \mathbf{g}_\rho(\theta_i), \mathcal{G}_\Theta(\theta_i, \nabla \psi_\rho(\theta_i); \tilde{\eta}_i) \rangle \\
& \quad + 4\|\mathbf{g}_\rho(\theta_i) - \tilde{\mathbf{g}}_\rho(\theta_i)\|^2 + 4^{-1}\|\mathcal{G}_\Theta(\theta_i, \nabla \psi_\rho(\theta_i); \tilde{\eta}_i)\|^2 + 2\|\nabla \psi_\rho(\theta_i) - \tilde{\mathbf{g}}_\rho(\theta_i)\|^2. \tag{69}
\end{aligned}$$

Using [Li et al., 2022, Lemma D1],  $\mathbb{E}_{u_t}[\mathbf{g}_\rho(\theta_i) \mid \theta_i] = \nabla \psi_\rho(\theta_i)$ . Taking expectation given  $\theta_i$

$$\begin{aligned}
\mathbb{E}[\|\mathcal{G}_\Theta(\theta_i, \tilde{\mathbf{g}}_\rho(\theta_i); \tilde{\eta}_i)\|^2 \mid \theta_i] & \leq \frac{2[\psi_\rho(\theta_i) - \mathbb{E}[\psi_\rho(\theta_{i+1}) \mid \theta_i]]}{\tilde{\eta}_i} + 4\mathbb{E}[\|\mathbf{g}_\rho(\theta_i) - \tilde{\mathbf{g}}_\rho(\theta_i)\|^2 \mid \theta_i] + \\
& \quad + 4^{-1}\mathbb{E}[\|\mathcal{G}_\Theta(\theta_i, \nabla \psi_\rho(\theta_i); \tilde{\eta}_i)\|^2 \mid \theta_i] + 2\mathbb{E}[\|\nabla \psi_\rho(\theta_i) - \tilde{\mathbf{g}}_\rho(\theta_i)\|^2 \mid \theta_i] \\
& \leq \frac{2[\psi_\rho(\theta_i) - \mathbb{E}[\psi_\rho(\theta_{i+1}) \mid \theta_i]]}{\tilde{\eta}_i} + 6\mathbb{E}[\|\mathbf{g}_\rho(\theta_i) - \tilde{\mathbf{g}}_\rho(\theta_i)\|^2 \mid \theta_i] + \\
& \quad + 4^{-1}\mathbb{E}[\|\mathcal{G}_\Theta(\theta_i, \nabla \psi_\rho(\theta_i); \tilde{\eta}_i)\|^2 \mid \theta_i], \tag{70}
\end{aligned}$$

where the last inequality comes from Jensen's inequality and  $\mathbb{E}_{u_t}[\mathbf{g}_\rho(\theta_i) \mid \theta_i] = \nabla \psi_\rho(\theta_i)$ ;  $\mathbb{E}[\|\nabla \psi_\rho(\theta_i) - \tilde{\mathbf{g}}_\rho(\theta_i)\|^2 \mid \theta_i] = \mathbb{E}[\|\mathbb{E}_{u_t}[\mathbf{g}_\rho(\theta_i) \mid \theta_i] - \tilde{\mathbf{g}}_\rho(\theta_i)\|^2 \mid \theta_i] \leq \mathbb{E}[\|\mathbf{g}_\rho(\theta_i) - \tilde{\mathbf{g}}_\rho(\theta_i)\|^2 \mid \theta_i]$ .

In order to give a bound on  $\mathbb{E}[\|\mathcal{G}_\Theta(\theta_i, \nabla \psi_\rho(\theta_i); \tilde{\eta}_i)\|^2 \mid \theta_i]$ , we have

$$\begin{aligned}
\mathbb{E}[\|\mathcal{G}_\Theta(\theta_i, \nabla \psi_\rho(\theta_i); \tilde{\eta}_i)\|^2 \mid \theta_i] & \leq 2\mathbb{E}[\|\mathcal{G}_\Theta(\theta_i, \tilde{\mathbf{g}}_\rho(\theta_i); \tilde{\eta}_i)\|^2 \mid \theta_i] \\
& \quad + 2\mathbb{E}[\|\mathcal{G}_\Theta(\theta_i, \tilde{\mathbf{g}}_\rho(\theta_i); \tilde{\eta}_i) - \mathcal{G}_\Theta(\theta_i, \nabla \psi_\rho(\theta_i); \tilde{\eta}_i)\|^2 \mid \theta_i] \\
& \stackrel{(a)}{\leq} 2\mathbb{E}[\|\mathcal{G}_\Theta(\theta_i, \tilde{\mathbf{g}}_\rho(\theta_i); \tilde{\eta}_i)\|^2 \mid \theta_i] + 2\mathbb{E}[\|\tilde{\mathbf{g}}_\rho(\theta_i) - \nabla \psi_\rho(\theta_i)\|^2 \mid \theta_i]
\end{aligned}$$

$$\stackrel{(b)}{\leq} 2\mathbb{E}[\|\mathcal{G}_\Theta(\theta_i, \tilde{\mathbf{g}}_\rho(\theta_i); \tilde{\eta}_i)\|^2 | \theta_i] + 2\mathbb{E}[\|\tilde{\mathbf{g}}_\rho(\theta_i) - \mathbf{g}_\rho(\theta_i)\|^2 | \theta_i]. \quad (71)$$

where (a) follows by  $\|\mathcal{G}_\Theta(\theta, v_1; \eta) - \mathcal{G}_\Theta(\theta, v_2; \eta)\| \leq \|v_1 - v_2\|$  and (b) is followed similarly to the last inequality in (70). Incorporating (70) in (71), we get

$$\begin{aligned} \mathbb{E}[\|\mathcal{G}_\Theta(\theta_i, \nabla\psi_\rho(\theta_i); \tilde{\eta}_i)\|^2 | \theta_i] &\leq \frac{4[\psi_\rho(\theta_i) - \mathbb{E}[\psi_\rho(\theta_{i+1}) | \theta_i]]}{\tilde{\eta}_i} + 14\mathbb{E}[\|\mathbf{g}_\rho(\theta_i) - \tilde{\mathbf{g}}_\rho(\theta_i)\|^2 | \theta_i] + \\ &+ 2^{-1}\mathbb{E}[\|\mathcal{G}_\Theta(\theta_i, \nabla\psi_\rho(\theta_i); \tilde{\eta}_i)\|^2 | \theta_i]. \end{aligned} \quad (72)$$

Finally, we get

$$\mathbb{E}[\|\mathcal{G}_\Theta(\theta_i, \nabla\psi_\rho(\theta_i); \tilde{\eta}_i)\|^2 | \theta_i] \leq \frac{8[\psi_\rho(\theta_i) - \mathbb{E}[\psi_\rho(\theta_{i+1}) | \theta_i]]}{\tilde{\eta}_i} + 28\mathbb{E}[\|\mathbf{g}_\rho(\theta_i) - \tilde{\mathbf{g}}_\rho(\theta_i)\|^2 | \theta_i]. \quad (73)$$

Up to this point, the analysis is standard for constrained zeroth-order methods and does not use the specific structure of  $F_{\max}$ .

*Step 2: Controlling the approximation error via Lemma 5.2.* We now invoke Lemma 5.2 to bound the last term in (73):

$$\begin{aligned} &\mathbb{E}[\|\tilde{\mathbf{g}}_\rho(\theta_i) - \mathbf{g}_\rho(\theta_i)\|^2 | \theta_i] \\ &\leq \frac{m^2}{\rho^2} \cdot \mathbb{E}[|\tilde{\psi}(\theta_i + \rho u_t) - F_{\max}(\theta_i + \rho u_t)|^2 + |\tilde{\psi}(\theta_i - \rho u_t) - F_{\max}(\theta_i - \rho u_t)|^2] \\ &\leq \frac{m^2}{\rho^2} \cdot \mathcal{O}(\epsilon_v^2), \end{aligned} \quad (74)$$

where the last inequality comes from Lemma 5.2 with  $|I| \geq 4\tilde{C}_f\epsilon_v^{-2-2k}$ , and

$$L = \mathcal{O}\left(\frac{k\mathbb{B}^2}{\epsilon_v^{2+2k}} \cdot \log(\epsilon_v^{-1})\right).$$

By choosing  $\tilde{\eta}_i = \eta \leq 1/L_{\psi,2} = m^{-1/2}\rho L_{F_{\max},1}^{-1}$  and integrating (74) into (73), followed by averaging over  $\theta_i$ , we obtain

$$\begin{aligned} \frac{1}{N} \sum_{t=1}^N \mathbb{E}[\|\mathcal{G}_\Theta(\theta_t, \nabla\psi_\rho; \eta)\|^2] &\leq \frac{4\psi_\rho(\theta_0) - 4\mathbb{E}[\psi_\rho(\theta_N)]}{N\eta} + \frac{8m^2}{\rho^2} \cdot \mathcal{O}(\epsilon_v^2) \\ &\leq \mathcal{O}\left(\frac{m^{\frac{1}{2}} \cdot (\psi_\rho(\theta_0) - \mathbb{E}[\psi_\rho(\theta_N)])}{N\rho} + \frac{m^2}{\rho^2} \cdot \epsilon_v^2\right) \\ &\leq \mathcal{O}\left(\frac{m \cdot \text{diam}(\Theta)}{N\rho^2} + \frac{m^2}{\rho^2} \cdot \epsilon_v^2\right), \end{aligned} \quad (75)$$

where the final inequality results from the Lipschitz continuity of  $F_{\max}$  with constant  $(\sqrt{m}\rho^{-1}L_{F_{\max},1})$  and the boundedness of domain  $\Theta$ .

Let  $\hat{\theta} := \arg \min_{i \in [1:N]} \|\mathcal{G}_\Theta(\theta_i, \nabla\psi_\rho; \eta)\|$ . Let us define  $\hat{\theta} = \arg \min_{i \in [1:N]} \mathbb{E}[\|\mathcal{G}_\Theta(\theta_i, \nabla\psi_\rho; \eta)\|^2]$ . Then by Jensen's inequality, we have

$$\mathbb{E}[\|\mathcal{G}_\Theta(\hat{\theta}, \nabla\psi_\rho; \eta)\|] = \mathcal{O}\left(\frac{m^{\frac{1}{2}}(\text{diam}(\Theta))^{\frac{1}{2}}}{\sqrt{N}\rho} + \frac{m}{\rho} \cdot \epsilon_v\right). \quad (76)$$

---

**Algorithm 3** PSGD-LMC( $\theta, \beta_0$ )

---

**Input:**  $\theta, \beta_0$ 

- 1: **for**  $l = 0$  to  $L - 1$  **do**
  - 2:  $\beta^{l+1} = \text{Proj}_{[-B, B]}(\beta^l - \eta_l \tilde{\partial}_\beta \phi_{\lambda, \delta}(\theta, \beta^l; \tilde{X}_i^n))$   
     $[\{\tilde{X}_i^n\}_{i=1}^{L-1}$  are i.i.d samples of  $L$  parallel LMC methods.]
  - 3: **end for**
  - 4:  $\tilde{\beta} = \frac{1}{L} \sum_{i=1}^L \beta^i$
- 

Let us pick  $\epsilon_v = \rho \epsilon m^{-1}$ , and  $N \geq m \cdot \text{diam}(\Theta) \cdot \epsilon^{-2} \rho^{-2}$ . Then  $\mathbb{E}[\|\mathcal{G}_\Theta(\hat{\theta}, \nabla \psi_\rho; \eta)\|] = \mathcal{O}(\epsilon)$ . We also pick  $b_u = \mathcal{O}(1)$ . Then the total number of samples from Gibbs measure is

$$N \times (b_u L + b_u |I|) = \mathcal{O}\left(\frac{m^{3+2k} \cdot \text{diam}(\Theta) \cdot (kB^2 + \tilde{C}_f) \cdot \log(m\epsilon^{-1}\rho^{-1})}{\epsilon^{2k+4} \rho^{2k+4}}\right). \quad (77)$$

□

## E Computational complexity of Gibbs oracle

In this section, we modify the result of Section 5 for the setting where the Gibbs samples are generated approximately by LMC rather than drawn exactly from the Gibbs distribution.

### E.1 Runtime complexity of Algorithm 1 by using LMC

We first replace Algorithm 1 by Algorithm 3, where the only change is that the exact samples  $\{\tilde{X}^l\}_{l=0}^{L-1}$  from the Gibbs distribution  $\mu_\theta^\lambda$  are replaced by approximate samples  $\{\tilde{X}_i^n\}_{i=1}^{L-1}$ , each  $\tilde{X}_i^n$  being produced by running an  $n$ -step Langevin Monte Carlo (LMC) algorithm (see Equation (30)). Our goal is to establish an updated version of Lemma 5.2 tailored to Algorithm 3.

We pick  $\lambda > 0$  and define the following approximate objective:

$$\tilde{\phi}_{\lambda, \delta}(\theta, \beta) := \beta + \frac{1}{\delta} \mathbb{E}_{X \sim \hat{\mu}_n} [\max\{f(\theta, X) - \beta, 0\}], \quad (78)$$

where  $\hat{\mu}_n$  denotes the empirical distribution induced by  $n$ -step LMC output. Since

$$|\tilde{\phi}_{\lambda, \delta}(\theta, \beta) - \phi_{\lambda, \delta}(\theta, \beta)| \leq \frac{L_{f,1}}{\delta} \mathbb{W}_1(\hat{\mu}_n, \mu_\theta^\lambda),$$

we can invoke the LMC Wasserstein bound from Section 5.3 to obtain

$$|\tilde{\phi}_{\lambda, \delta}(\theta, \beta) - \phi_{\lambda, \delta}(\theta, \beta)| \leq \frac{L_{f,1}}{\delta} \cdot 2C_{PI}^{1/2} C^{1/2} \epsilon. \quad (79)$$

Setting  $\epsilon_v := \epsilon/\delta$  with  $\delta = \epsilon_v^k$  and running LMC for  $n = \tilde{\mathcal{O}}(d \epsilon_v^{-6-6k})$  iterations yields

$$|\tilde{\phi}_{\lambda, \delta}(\theta, \beta) - \phi_{\lambda, \delta}(\theta, \beta)| = \mathcal{O}(\epsilon_v).$$

Since (79) holds for every  $\beta$ , the same argument as in Lemma 4.4 implies

$$\left| \min_{\beta} \tilde{\phi}_{\lambda, \delta}(\theta, \beta) - \min_{\beta} \phi_{\lambda, \delta}(\theta, \beta) \right| = \mathcal{O}(\epsilon_v).$$

We then define the LMC-based estimator of  $\tilde{F}_{\text{SQ-G}}(\theta)$  by

$$\hat{\psi}(\theta) := \phi_{\lambda,\delta}(\theta, \tilde{\beta}; \hat{X}_I^n) = \tilde{\beta} + \frac{1}{\delta|I|} \sum_{i \in I} \max\{f(\theta, \hat{X}_i^n) - \tilde{\beta}, 0\}, \quad (80)$$

where  $\hat{X}_I^n := \{\hat{X}_i^n\}_{i \in I}$  are i.i.d.  $n$ -step LMC samples from  $\hat{\mu}_n$ .

We then restate lemma 5.2 by using the updates of algorithm 3 as follows:

**Lemma E.1.** *Given  $\theta \in \Theta$ , by using Algorithm 3 (PSGD-LMC( $\theta, \beta_0$ )), we obtain*

$$\mathbb{E}[|\hat{\psi}(\theta) - \tilde{F}_{\text{SQ-G}}(\theta)|^2 \mid \theta] = \mathcal{O}(\epsilon_v^2), \quad (81)$$

with  $|I| \geq \tilde{C}_f \epsilon_v^{-2k-2}$  and the number of iterations of PSGD as follows

$$L \times n \geq \tilde{\mathcal{O}} \left( \frac{dkB^2 \log(\epsilon_v^{-1})}{\epsilon_v^{8+8k}} \right).$$

Here  $\tilde{C}_f$  is a constant, and  $B$  is defined in Lemma 5.1.

*Proof.* The proof mirrors that of Lemma 5.2; we highlight only the modifications due to the use of LMC samples and the function  $\tilde{\phi}_{\lambda,\delta}$ .

*Step 1: PSGD error for  $\tilde{\phi}_{\lambda,\delta}$ .* Fix  $\theta \in \Theta$ , and let  $\tilde{\beta}$  denote the output of PSGD-LMC( $\theta, \beta_0$ ). As in the proof of Lemma 5.2,  $\tilde{\phi}_{\lambda,\delta}(\theta, \cdot)$  is convex,  $\sigma$ -Lipschitz with  $\sigma = 1 + \delta^{-1}$ , and optimized over the interval  $[-B, B]$ . Therefore, the high-probability PSGD guarantee (18) applies to  $\tilde{\phi}_{\lambda,\delta}$  verbatim: for any  $\epsilon_v > 0$  and  $\Delta \in (0, 1)$ ,

$$\mathbb{P} \left( \tilde{\phi}_{\lambda,\delta}(\theta, \tilde{\beta}) - \min_{\beta \in [-B, B]} \tilde{\phi}_{\lambda,\delta}(\theta, \beta) \leq \epsilon_v \mid \theta \right) \geq 1 - \Delta,$$

after at most

$$L = \mathcal{O}(B^2 \sigma^2 \epsilon_v^{-2} \log(\Delta^{-1})).$$

Choosing  $\delta = \epsilon_v^k$  so that  $\sigma = \mathcal{O}(\epsilon_v^{-k})$  and taking  $\Delta := \min\{1, \epsilon_v^2/R^2\}$  as in the proof of Lemma 5.2, we obtain

$$\mathbb{E} \left[ \left( \tilde{\phi}_{\lambda,\delta}(\theta, \tilde{\beta}) - \min_{\beta} \tilde{\phi}_{\lambda,\delta}(\theta, \beta) \right)^2 \mid \theta \right] \leq C \epsilon_v^2, \quad (82)$$

for some constant  $C > 0$ , using

$$L = \mathcal{O}(k B^2 \epsilon_v^{-2-2k} \log(\epsilon_v^{-1})). \quad (83)$$

*Step 2: From  $\tilde{\phi}_{\lambda,\delta}$  to  $\phi_{\lambda,\delta}$  and  $\tilde{F}_{\text{SQ-G}}$ .* Recall that  $\tilde{F}_{\text{SQ-G}}(\theta) = \min_{\beta} \phi_{\lambda,\delta}(\theta, \beta)$ . For the same  $\tilde{\beta}$  as above,

$$\begin{aligned} \phi_{\lambda,\delta}(\theta, \tilde{\beta}) - \tilde{F}_{\text{SQ-G}}(\theta) &= \phi_{\lambda,\delta}(\theta, \tilde{\beta}) - \min_{\beta} \phi_{\lambda,\delta}(\theta, \beta) \\ &\leq |\phi_{\lambda,\delta}(\theta, \tilde{\beta}) - \tilde{\phi}_{\lambda,\delta}(\theta, \tilde{\beta})| + (\tilde{\phi}_{\lambda,\delta}(\theta, \tilde{\beta}) - \min_{\beta} \tilde{\phi}_{\lambda,\delta}(\theta, \beta)) \\ &\quad + |\min_{\beta} \tilde{\phi}_{\lambda,\delta}(\theta, \beta) - \min_{\beta} \phi_{\lambda,\delta}(\theta, \beta)|. \end{aligned}$$

By the uniform approximation bound (79) and its consequence for minimizers (see the discussion after (79)), both  $|\phi_{\lambda,\delta}(\theta, \beta) - \tilde{\phi}_{\lambda,\delta}(\theta, \beta)|$  and  $|\min_{\beta} \tilde{\phi}_{\lambda,\delta}(\theta, \beta) - \min_{\beta} \phi_{\lambda,\delta}(\theta, \beta)|$  are  $\mathcal{O}(\epsilon_v)$ , uniformly in  $\beta$ , provided  $n$  is chosen as below. Combining these with (82) and using  $(a + b + c)^2 \leq 3(a^2 + b^2 + c^2)$  gives

$$\mathbb{E} \left[ (\phi_{\lambda,\delta}(\theta, \tilde{\beta}) - \tilde{F}_{\text{SQ-G}}(\theta))^2 \mid \theta \right] \leq C_2 \epsilon_v^2, \quad (84)$$

for some constant  $C_2 > 0$ , provided the LMC chain length satisfies

$$n = \tilde{\mathcal{O}}(d \epsilon_v^{-6-6k}),$$

as in the Wasserstein–convergence bound used in Section 5.3.

*Step 3: Bounding the MSE of  $\hat{\psi}(\theta)$ .* By Jensen’s inequality and the triangle inequality,

$$\begin{aligned} \mathbb{E}[|\hat{\psi}(\theta) - \tilde{F}_{\text{SQ-G}}(\theta)|^2 \mid \theta] &\leq 3 \underbrace{\mathbb{E}[|\hat{\psi}(\theta) - \tilde{\psi}(\theta)|^2 \mid \theta]}_{(1)} \\ &\quad + 3 \underbrace{\mathbb{E}[|\tilde{\psi}(\theta) - \phi_{\lambda,\delta}(\theta, \tilde{\beta})|^2 \mid \theta]}_{(2)} + 3 \underbrace{\mathbb{E}[|\phi_{\lambda,\delta}(\theta, \tilde{\beta}) - \tilde{F}_{\text{SQ-G}}(\theta)|^2 \mid \theta]}_{(3)}. \end{aligned} \quad (85)$$

We bound the three terms as follows.

1. Conditioning on  $\theta$  and  $\tilde{\beta}$ , using independence across  $i \in I$ ,

$$\mathbb{E}[|\hat{\psi}(\theta) - \tilde{\psi}(\theta)|^2 \mid \theta] = \mathbb{E}\left[\left|\frac{1}{\delta|I|} \sum_{i \in I} (h(f(\theta, \hat{X}_i^n) - \tilde{\beta}) - h(f(\theta, \tilde{X}^i) - \tilde{\beta}))\right|^2 \mid \theta\right] \quad (86)$$

$$\leq \frac{1}{\delta^2|I|} \sum_{i \in I} \mathbb{E}\left[(h(f(\theta, \hat{X}_i^n) - \tilde{\beta}) - h(f(\theta, \tilde{X}^i) - \tilde{\beta}))^2 \mid \theta\right] \quad (87)$$

$$\leq \frac{L_{f,1}^2}{\delta^2} \mathbb{W}_2^2(\hat{\mu}_n, \mu_{\hat{\theta}}^\lambda), \quad (88)$$

since  $h(f(\theta, \cdot) - \tilde{\beta})$  is  $L_{f,1}$ –Lipschitz. By the LMC convergence bound used in Section 5.3, choosing  $n = \tilde{\mathcal{O}}(d \epsilon_v^{-6-6k})$  ensures  $\mathbb{W}_2^2(\hat{\mu}_n, \mu_{\hat{\theta}}^\lambda) = \mathcal{O}(\epsilon_v^{2+2k})$ , and hence

$$\mathbb{E}[|\hat{\psi}(\theta) - \tilde{\psi}(\theta)|^2 \mid \theta] \leq C_3 \epsilon_v^2 \quad (89)$$

for some constant  $C_3 > 0$ .

2. Exactly as in (59)–(60), we have

$$\mathbb{E}[|\tilde{\psi}(\theta) - \phi_{\lambda,\delta}(\theta, \tilde{\beta})|^2 \mid \theta] \leq \frac{\tilde{C}_f}{\delta^2|I|}, \quad (90)$$

for some constant  $\tilde{C}_f > 0$ . With  $\delta = \epsilon_v^k$  and  $|I| \geq \tilde{C}_f \epsilon_v^{-2k-2}$ , this is  $\mathcal{O}(\epsilon_v^2)$ .

3. This is exactly (84):

$$\mathbb{E}[|\phi_{\lambda,\delta}(\theta, \tilde{\beta}) - \tilde{F}_{\text{SQ-G}}(\theta)|^2 \mid \theta] \leq C_2 \epsilon_v^2. \quad (91)$$

Substituting (89)–(91) into (85), we obtain

$$\mathbb{E}[|\hat{\psi}(\theta) - \tilde{F}_{\text{SQ-G}}(\theta)|^2 \mid \theta] \leq C \epsilon_v^2,$$

for some constant  $C > 0$  independent of  $\theta$  and  $\epsilon_v$ . Finally, combining (83) with  $n = \tilde{\mathcal{O}}(d \epsilon_v^{-6-6k})$  yields

$$L \times n = \tilde{\mathcal{O}}\left(\frac{d k B^2 \log(\epsilon_v^{-1})}{\epsilon_v^{8+8k}}\right),$$

which completes the proof.  $\square$

---

**Algorithm 4** Projected Stochastic Zeroth-order with LMC (PSZO-LMC)

---

**Initialization:**  $\beta_0, \theta_0, \lambda, \delta < 1/2$ , and integers  $N, n$ .

- 1: **for**  $k = 0$  to  $N - 1$  **do**
  - 2:   Query i.i.d. samples of  $|I|$  parallel LMC methods, denoted by  $\hat{X}_I^N = \{\hat{X}_i^N\}_{i \in I}$ .
  - 3:   Sample  $\{u_{k,t}\}_{t=1}^{b_u}$  independently and uniformly from a unit sphere.
  - 4:    $\beta_{k,t}^+ = \text{PSGD-LMC}(\theta_k + \rho u_{k,t}, \beta_0), \forall t \in [1 : b_u]$ .
  - 5:    $\beta_{k,t}^- = \text{PSGD-LMC}(\theta_k - \rho u_{k,t}, \beta_0), \forall t \in [1 : b_u]$ .
  - 6:    $\hat{\psi}(\theta_k + \rho u_{k,t}) = \phi_{\lambda, \delta}(\theta_k + \rho u_{k,t}, \beta_{k,t}^+; \hat{X}_I^N)$ .
  - 7:    $\hat{\psi}(\theta_k - \rho u_{k,t}) = \phi_{\lambda, \delta}(\theta_k - \rho u_{k,t}, \beta_{k,t}^-; \hat{X}_I^N)$
  - 8:    $\hat{\mathbf{g}}_\rho(\theta_k) = \frac{m}{2\rho} \cdot \frac{1}{b_u} \sum_{t=1}^{b_u} [\hat{\psi}(\theta_k + \rho u_{k,t}) - \hat{\psi}(\theta_k - \rho u_{k,t})] u_{k,t}$
  - 9:    $\theta_{k+1} = \text{Proj}_\Theta(\theta_k - \tilde{\eta}_k \hat{\mathbf{g}}_\rho(\theta_k))$
  - 10: **end for**
- 

## E.2 Proof of Theorem 5.7

First, we change Algorithm 2 to algorithm 4 by replacing the samples of Gibbs measure with samples of the output of parallel LMCs and changing PSGD to PSGD-LMC (see Algorithm 3) in lines 4 and 5. To apply LMC for simulating the Gibbs measure, based on the proof of Theorem 5.5, the only part we must change is to bound the last term in (73). What we need is to change the bound in (74) on the last of term of right-hand side in (73) for samples from Gibbs to samples from the outputs of parallel LMCs. We provide the proof of Theorem 5.7 in the following:

*Proof.* The argument mirrors the proof of Theorem 5.5. We briefly recall the zeroth-order part and then highlight the only new ingredient, namely the control of the LMC-induced error via Lemma E.1.

*Step 1: Zeroth-order analysis (same as Theorem 5.5).* As in the proof of Theorem 5.5, we work with the smoothed objective  $\psi_\rho(\theta) := \mathbb{E}_{u \sim \text{Unif}(\mathbb{S}^{m-1})} [F_{\max}(\theta + \rho u)]$ . Using the smoothness of  $\psi_\rho$  and the projected gradient-mapping update, the standard analysis of constrained zeroth-order methods yields (see eq. (73) in Section D.3)

$$\mathbb{E}[\|\mathcal{G}_\Theta(\theta_i, \nabla \psi_\rho(\theta_i); \tilde{\eta}_i)\|^2 \mid \theta_i] \leq \frac{8(\psi_\rho(\theta_i) - \mathbb{E}[\psi_\rho(\theta_{i+1}) \mid \theta_i])}{\tilde{\eta}_i} + 28 \mathbb{E}[\|\mathbf{g}_\rho(\theta_i) - \hat{\mathbf{g}}_\rho(\theta_i)\|^2 \mid \theta_i], \quad (92)$$

where

$$\mathbf{g}_\rho(\theta_i) := \frac{1}{b_u} \sum_{t=1}^{b_u} \mathbf{g}_\rho(\theta_i, u_{i,t}), \quad \mathbf{g}_\rho(\theta, u) := \frac{m}{2\rho} [F_{\max}(\theta + \rho u) - F_{\max}(\theta - \rho u)]u,$$

and  $\hat{\mathbf{g}}_\rho(\theta_i)$  is the stochastic gradient estimator used in Algorithm 4. Up to (92), the analysis is identical to Theorem 5.5; the only new task is to control  $\mathbb{E}[\|\hat{\mathbf{g}}_\rho(\theta) - \mathbf{g}_\rho(\theta)\|^2 \mid \theta]$  when  $\hat{\mathbf{g}}_\rho$  is built from the LMC-based oracle  $\hat{\psi}$ .

*Step 2: Bounding the LMC-induced error via lemma E.1.* In Algorithm 4, the proxy gradient in line 8 is

$$\hat{\mathbf{g}}_\rho(\theta) = \frac{m}{2\rho} \cdot \frac{1}{b_u} \sum_{t=1}^{b_u} [\hat{\psi}(\theta + \rho u_t) - \hat{\psi}(\theta - \rho u_t)]u_t, \quad (93)$$

where  $\hat{\psi}(\cdot)$  is the LMC-based estimator of  $\tilde{F}_{\text{SQ-G}}$  returned by PSGD-LMC (Algorithm 3). We need to bound  $\mathbb{E}[\|\hat{\mathbf{g}}_\rho(\theta) - \mathbf{g}_\rho(\theta)\|^2 \mid \theta]$  in (92) with  $\mathbf{g}_\rho(\theta) := \frac{1}{b_u} \sum_{t=1}^{b_u} \mathbf{g}_\rho(\theta, u_t)$  where  $\mathbf{g}_\rho(\theta, u_t) := \frac{m}{2\rho} \cdot [F_{\max}(\theta + \rho u_t) -$

$F_{\max}(\theta - \rho u_t)]u_t$ . Then

$$\begin{aligned} & \mathbb{E}[\|\hat{\mathbf{g}}_\rho(\theta) - \mathbf{g}_\rho(\theta)\|^2 \mid \theta] \\ & \leq \frac{m^2}{\rho^2} \mathbb{E}\left[|\hat{\psi}(\theta + \rho u_t) - F_{\max}(\theta + \rho u_t)|^2 + |\hat{\psi}(\theta - \rho u_t) - F_{\max}(\theta - \rho u_t)|^2 \mid \theta\right]. \end{aligned} \quad (94)$$

Thus it suffices to bound  $\mathbb{E}[|\hat{\psi}(\theta) - F_{\max}(\theta)|^2 \mid \theta]$ .

By Lemma E.1, for any  $\theta \in \Theta$  we have

$$\mathbb{E}[|\hat{\psi}(\theta) - \tilde{F}_{\text{SQ-G}}(\theta)|^2 \mid \theta] = \mathcal{O}(\epsilon_v^2), \quad (95)$$

provided that

$$|I| \geq \tilde{C}_f \epsilon_v^{-2k-2}, \quad L \times n \geq \tilde{\mathcal{O}}\left(\frac{dk B^2 \log(\epsilon_v^{-1})}{\epsilon_v^{8+8k}}\right),$$

with  $\tilde{C}_f$  a constant and  $B$  as in Lemma 5.1. Moreover, by the uniform approximation result for the superquantile–Gibbs relaxation (see Theorem 4.2), we have

$$|\tilde{F}_{\text{SQ-G}}(\theta) - F_{\max}(\theta)| = \mathcal{O}(\epsilon_v) \quad \text{for all } \theta \in \Theta. \quad (96)$$

Combining (95) and (96) and using  $(a + b)^2 \leq 2(a^2 + b^2)$ , we obtain

$$\begin{aligned} \mathbb{E}[|\hat{\psi}(\theta) - F_{\max}(\theta)|^2 \mid \theta] & \leq 2\mathbb{E}[|\hat{\psi}(\theta) - \tilde{F}_{\text{SQ-G}}(\theta)|^2 \mid \theta] + 2|\tilde{F}_{\text{SQ-G}}(\theta) - F_{\max}(\theta)|^2 \\ & = \mathcal{O}(\epsilon_v^2). \end{aligned} \quad (97)$$

Substituting (97) into (94) yields

$$\mathbb{E}[\|\hat{\mathbf{g}}_\rho(\theta) - \mathbf{g}_\rho(\theta)\|^2 \mid \theta] = \mathcal{O}\left(\frac{m^2}{\rho^2} \epsilon_v^2\right). \quad (98)$$

*Step 3: Convergence rate and choice of parameters.* Plugging (98) into (92), choosing a constant stepsize  $\tilde{\eta}_i = \eta \leq m^{-1/2} \rho L_{F_{\max}, 1}^{-1}$ , and summing  $i = 0, \dots, N - 1$  exactly as in the proof of Theorem 5.5 gives

$$\frac{1}{N} \sum_{i=0}^{N-1} \mathbb{E}[\|\mathcal{G}_\Theta(\theta_i, \nabla \psi_\rho(\theta_i); \eta)\|^2] = \mathcal{O}\left(\frac{m \text{diam}(\Theta)}{N\rho^2} + \frac{m^2}{\rho^2} \epsilon_v^2\right).$$

Let  $\hat{\theta}$  be the best iterate in terms of the gradient-mapping norm. By Jensen's inequality,

$$\mathbb{E}[\|\mathcal{G}_\Theta(\hat{\theta}, \nabla \psi_\rho(\hat{\theta}); \eta)\|] = \mathcal{O}\left(\sqrt{\frac{m \text{diam}(\Theta)}{N\rho^2}} + \frac{m}{\rho} \epsilon_v\right).$$

Setting  $\epsilon_v := \rho \epsilon m^{-1}$  and taking  $N \gtrsim m \text{diam}(\Theta) \rho^{-2} \epsilon^{-2}$  yields

$$\mathbb{E}[\|\mathcal{G}_\Theta(\hat{\theta}, \nabla \psi_\rho(\hat{\theta}); \eta)\|] = \mathcal{O}(\epsilon),$$

so  $\hat{\theta}$  is an  $(\epsilon, \rho, \eta)$ -generalized Goldstein stationary point of  $F_{\max}$ .

Each outer iteration of Algorithm 4 uses  $b_u$  two-point evaluations of the oracle  $\hat{\psi}$ . Each call to  $\hat{\psi}$  in turn runs PSGD-LMC with  $|I|$  parallel LMC chains of length  $n$ . Thus the total number of lower-level gradient evaluations is

$$N \times n \times (b_u L + b_u |I|).$$

Substituting the choices of  $N$ ,  $n$ ,  $L$ , and  $|I|$  from Lemma E.1 and the LMC mixing bound (Proposition 5.6), with the choice  $\epsilon_v = \rho \epsilon m^{-1}$ , gives

$$N \times n \times (b_u L + b_u |I|) = \mathcal{O} \left( \frac{d m^{9+8k} [k B^2 + \tilde{C}_f] \log(\epsilon^{-1})}{\epsilon^{8k+10} \rho^{8k+10}} \right),$$

which is the claimed complexity bound. □